Input and output of the central complex related to polarized light in the nervous system of the desert locust *Schistocerca gregaria*

Ein- und Ausgang des Zentralkomplexes
in Bezug auf polarisiertes Licht im Nervensystem der
Wüstenheuschrecke *Schistocerca gregaria*

Dissertation

zur Erlangung des Doktorgrades der Naturwissenschaften
(Dr. rer. nat.)

dem Fachbereich Biologie
der Philipps-Universität Marburg
vorgelegt von
Ulrike Träger
aus Grimma
Marburg/Lahn 2010

Vom Fachbereich Biologie der Philipps-Universität Marburg
als Dissertation am 28.10.2010 angenommen.

Erstgutachter: Prof. Dr. Uwe Homberg
Zweitgutachter: Prof. Dr. Roland Brandl

Tag der mündlichen Prüfung am: 29.11.2010

Das Titelbild zeigt ein "hopperband" der Art *Locustana pardalina*, aufgenommen auf der "Wolfkop"-Farm in der Karoo-Wüste bei Pofadder in Südafrika während meines Forschungsaufenthaltes im November 2008.

Inhaltsverzeichnis

Erklärung: Eigene Beiträge und veröffentlichte Teile der Arbeit

Laut §8, Absatz 3 der Promotionsordnung der Philipps-Universität Marburg (Fassung vom 12.4.2000) müssen bei den Teilen der Dissertation, die aus gemeinsamer Forschungsarbeit entstanden sind, "die individuellen Leistungen des Doktoranden deutlich abgrenzbar und bewertbar sein." Dies betrifft die Kapitel 1-3, und soll im Folgenden detailliert erläutert werden.

Kapitel 1: A novel type of microglomerular synaptic complex in the polarization vision pathway of the locust brain

- Durchführung aller Farbstoffinjektionen für Doppel-Fluoreszenz-Schnittserien inklusive Anfertigung aller immuncytochemischen Doppelmarkierungen (Vibratomschnitte).
- Auswertung der elektronenmikroskopischen Einzelschnitte inklusive Immunogold-Färbungen und Schnittserien aus mikrofotografischen Aufnahmen. Diese wurden von Robert Wagner mit technischer Unterstützung von Geza Thiess und von Bernhard Bausenwein angefertigt.
- Anfertigung aller dreidimensionalen Rekonstruktionen und Detailaufnahmen mittels Mikroskopkamera (5 von 5), sowie 75% aller Zeichnungen (3 von 4).
- Erstellung sämtlicher Abbildungen und Tabellen.
- Anfertigung des Manuskriptes und layout der fertigen Abbildungen in Zusammenarbeit (Korrektur) mit Prof. Dr. Uwe Homberg.
- Dieses Kapitel wurde in der vorliegenden Form im Journal of Comparative Neurology veröffentlicht. (Träger, U., Wagner, R. Bausenwein, B. & Homberg, U. (2008) A novel type of microglomerular synaptic complex in the polarization vision pathway of the locust brain. *J Comp Neurol, 506*:288-300.)

Kapitel 2: Polarization sensitive descending neurons in the locust: connecting the brain to thoracic ganglia

- Durchführung von 85% (22 von 26) der präsentierten intrazellulären Ableitungen.
- Umbau eines elektrophysiologischen Arbeitsstandes und Etablierung der routinemäßigen Ableitung vom Halskonnektiv.
- Auswertung und statistische Analyse aller elektrophysiologischen Daten.
- Anfertigung aller dargestellten Rekonstruktionen, sowie histochemische Aufbereitung einiger fluoreszenzmarkierter Präparate mittels konfokaler Mikroskopie.
- Anfertigung sämtlicher Abbildungen.
- Anfertigung des Manuskriptes sowie layout der fertigen Abbildungen in Zusammenarbeit (Korrektur) mit Prof. Dr. Uwe Homberg.
- Dieses Kapitel wurde in der vorliegenden Form am 12.07.2010 beim Journal of Neuroscience (JN-RM-3624-10) eingereicht und am 20.08.2010 zur Revision zugelassen.

<u>Kapitel 3:</u> Behavioral and electrophysiological evidence for a role of polarized light in optomotor responses of the desert locust *Schistocerca gregaria*

- Die Verhaltensexperimente an fixiert fliegenden Heuschrecken wurden von Bianca Backasch durchgeführt und ausgewertet sowie als Rohabbildung zur Verfügung gestellt. Die Schlussfolgerungen daraus diskutierten Prof. Dr. Uwe Homberg und ich.
- Die Analyse des Powersprektums (FFT) mittels eigens dafür angefertigtem MatLab-Programm wurde durchgeführt von Dr. Ronny Rosner.
- Durchführung von 62,5% (5 von 8) der präsentierten intrazellulären Ableitungen.
- Auswertung und statistische Analyse aller elektrophysiologischen Daten.
- Anfertigung aller zweidimensionalen Rekonstruktionen.
- Die dreidimensionalen Rekonstruktionen wurden angefertigt von Christoph Busche und als Rohabbildung von Basil el Jundi zusammengestellt.
- Anfertigung der elektrophysiologischen Abbildungen und endgültiges layout aller fertigen Abbildungen.
- Anfertigung des Manuskriptes in Zusammenarbeit (Korrektur) mit Prof. Dr. Uwe Homberg.
- Dieses Kapitel ist für die Einreichung beim Journal of Neurophysiology vorgesehen.

Die Abfassung der Dissertation in englischer Sprache wurde vom Dekan des Fachbereichs Biologie am 03.03.2010 genehmigt.

Zusammenfassung

Viele Tiere vollführen wahre Meisterleistungen, indem sie ein ausgeprägtes Migrationsverhalten über schier unvorstellbare Distanzen zeigen oder sich an für uns unsichtbaren Mustern, wie z.B. das Magnetfeld der Erde oder das Polarisationsmuster des blauen Himmels, orientieren (Frost & Mouritsen, 2006). Viele Insekten nutzen auf ihren teils ausgeprägten Wanderungen (wie auf dem Titelbild dieser Dissertationsschrift am Beispiel der südafrikanischen Heuschrecke *Locustana pardalina* zu sehen) das Polarisationsmuster zur Navigation. Dieses Muster entsteht durch an Luftmolekülen gestreutes Sonnenlicht. Direktes Sonnenlicht hingegen ist unpolarisiert und weist sämtliche Schwingungsrichtungen (*E*-Vektoren) auf. Das gestreute und somit polarisierte Licht hat nur noch eine einzige Schwingungsrichtung und ist in konzentrischen Kreisen um die Sonne ausgerichtet. Dieses Polarisationsmuster unterscheidet sich, abhängig vom Winkel zur Sonne, im Grad der Polarisation. Mit bis zu 75% ist der Polarisationsgrad im 90° Winkel zur Sonne am stärksten. Da das Polarisationsmuster direkt auf dem Sonnenstand beruht, unterliegt dieses Muster einer tageszeitlichen Veränderung, welche von den Tieren, die dieses Muster zur Navigation nutzen, kompensiert werden muss (Wehner & Labhart, 2006). In zahlreichen Verhaltensstudien konnte gezeigt werden, dass bereits ein kleiner Ausschnitt des blauen Himmels ohne sichtbare Sonne ausreicht, um für Bienen und Ameisen eine Navigationsgrundlage zu bilden. Aber nicht nur tagaktive Tiere nutzen diesen Himmelskompass, denn auch der nachtaktive Pillendreher *Scarabaeus zambesianus* macht sich das Polarisationsmuster des monderhellten Nachthimmels zunutze, um seine Dungkugel in direktem Weg von einem Dunghaufen zu entfernen (Dacke et al., 2003). Weiterhin konnte in Laborversuchen gezeigt werden, dass sich auch Fliegen (von Philipsborn & Labhart, 1990), Grillen (Brunner & Labhart, 1987) und Heuschrecken (Mappes & Homberg, 2004) an polarisiertem Licht orientieren können.

Labhart und Meyer (1999) zeigten, dass viele Insekten eine besondere Augenregion, die dorsale Randregion (engl. *dorsal rim area*, DRA), aufweisen, die sich in vielen Merkmalen vom Restauge unterscheidet (siehe auch Homberg & Paech, 2002). Zum einen sind die Rhabdome der Ommatidien der DRA im Wesentlichen kürzer und breiter als die aus dem Restauge und zum anderen weisen die Mikrovilliorientierungen der Retinulazellen einen Versatz von 90° zueinander auf. Neben weiteren Unterschieden in der Optik sind die Photorezeptoren der DRA aufgrund der oben genannten Eigenschaften für die Wahrnehmung von polarisiertem Licht prädestiniert.
Zur Aufklärung der neuronalen Verarbeitung bieten sich Heuschrecken aber auch Grillen aufgrund ihrer Größe als Modellorganismen an. Aufgeklärt durch Farbstoffinjektionen, erstreckt sich die Polarisations-Sehbahn (siehe Abb. 1, rot markiert) ausgehend von der DRA über die dorsalen Randregionen der ersten und zweiten visuellen Verarbeitungszentren Lamina und Medulla und weiter über die anteriore Lobula als drittes visuelles Zentrum bis hin zu einem räumlich stark begrenzten Areal, dem anterioren optischen Tuberkel (AOTu) (Homberg, 2004). Die Neurone dieses kleinen Hirnareals konnten außerordentlich gut mittels elektrophysiologischer Techniken untersucht werden (Pfeiffer et al., 2005; Kinoshita et al., 2007; Pfeiffer & Homberg, 2007). Die abgeleiteten Neurone weisen eine Modulation ihrer Aktionspotentialfrequenz auf und besitzen sogenannte Gegenpol-Eigenschaften. Das bedeutet, dass sie unter Stimulation mit rotierendem, von dorsal präsentiertem polarisierten Licht durch eine bestimmte *E*-Vektor-Orientierung (Φ_{max}) maximal erregt werden, während sie durch eine genau um 90° zu Φ_{max} versetzten *E*-Vektor-Orientierung maximal inhibiert werden. Die Neurone des AOTu verschalten zu spezialisierten Arealen, dem lateralen Dreieck und der medianen Olive, des lateralen akzessorischen Lobus (LAL). Von diesen Arealen erhalten tangentiale Zellen des Zentralkomplexes ihren Eingang und projizieren weiter zur unteren Einheit des Zentralkörpers (Vitzthum et al., 2002). Innerhalb des Zentralkomplexes, der aus der Protozerebralbrücke, oberer und unterer Einheit des Zentralkörpers sowie den paarigen Noduli besteht, konnten mindestens 13 weitere polarisationssensitive Neuronentypen nachgewiesen werden (Vitzthum et al., 2002; Heinze & Homberg, 2007, 2008, 2009; Heinze et al., 2009). Weiterhin konnte eine topographische Karte in Bezug auf die dorsalen *E*-Vektoren nachgewiesen werden. Die Polarotopie der Zellen entspricht einer geordneten Reihe

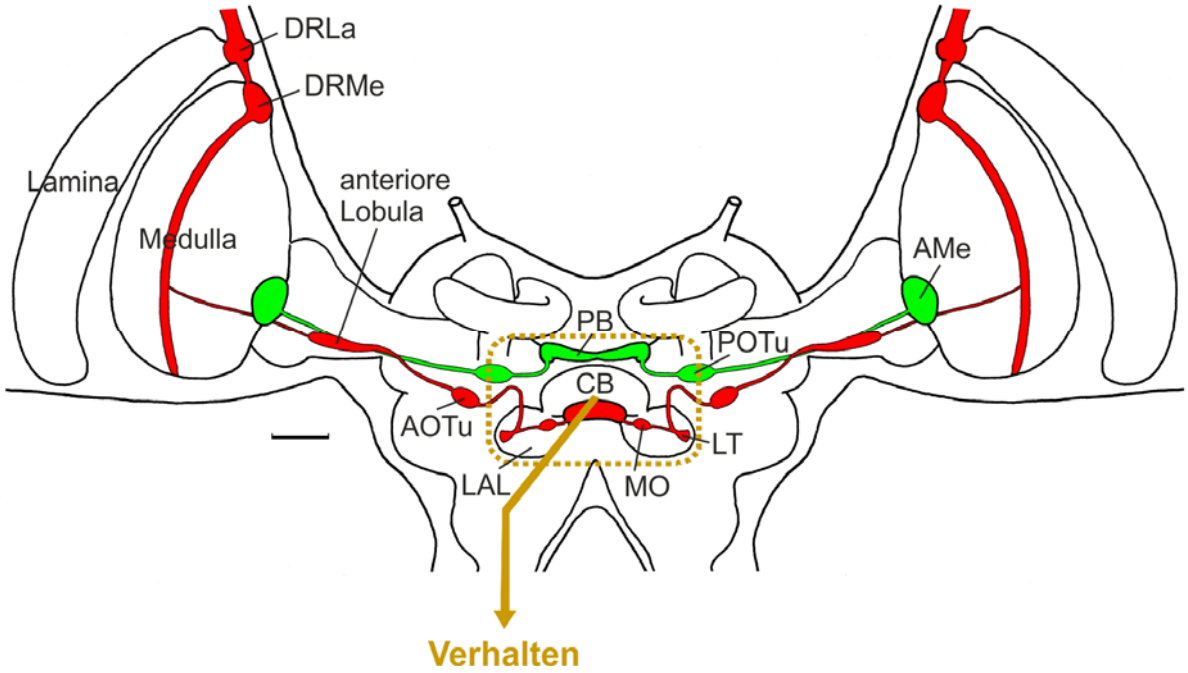

Abb. 1 Polarisations-Sehbahnen im Gehirn der Wüstenheuschrecke mit Andeutung der Verbindung zur Motorik in den Thorakalganglien, welche schließlich zum Verhalten des Tieres führt. In der Polarisationssehbahn (rot), ausgehend von den dorsalen Randregionen der Lamina und Medulla, projizieren Neurone der Medulla über die anteriore Lobula in den anterioren optischen Tuberkel (AOTu), welcher mittels verschiedener Neurone mit der medianen Olive (MO) und dem lateralen Dreieck (LT), beides Untereinheiten des lateralen akzessorischen Lobus (LAL), in Verbindung steht. Über den LAL erhält der Zentralkomplex, bestehend aus dem Zentralkörper (CB) und der Protozerebralbrücke (PB), polarisationssensitiven Eingang. Neurone einer zweiten Sehbahn (grün) verbinden die akzessorische Medulla (AMe) mit dem posterioren optischen Tuberkel (POTu) und schließlich mit der Protozerebralbrücke. Ausgehend vom Zentralkomplex erhalten absteigende Neurone die verarbeitete Polarisationsinformation und leiten diese an die Motorik weiter und beeinflussen somit das Verhalten des Tieres. Der Maßstabsbalken entspricht 200 µm (verändert nach Homberg et al., 2003).

von Kopfrichtungsneuronen, die die Orientierung des Tieres relativ zum Sonnenmeridian kodieren und somit eine Art internen Kompass darstellen könnten (Heinze & Homberg, 2008).

Über eine zweite Polarisations-Sehbahn (siehe Abb. 1, grüner Teil) könnte die wichtige Information über die Tageszeit integriert werden. Wie el Jundi und Homberg (2010) vorschlagen, könnte diese zweite Bahn über die akzessorische Medulla Zeitgeber-Information erhalten, da dieses Areal zumindest in Schaben, Grillen, Fliegen und Käfern als Sitz der inneren zirkadianen Uhr betrachtet wird (Helfrich-Förster et al., 1998), und diese Information über den posterioren optischen Tuberkel auf bekannte Zellen des Zentralkomplexes verschalten.

Auf welche Weise die im Zentralkomplex verarbeitete Information des polarisierten Lichtes an die Motorik übermittelt wird, die das Lauf- oder Flugverhalten des Tieres kontrolliert, ist bisher unbekannt. Sogenannte absteigende Neurone, die ihren Zellkörper sowie die Eingangsregionen innerhalb des Gehirns aufweisen, müssten diese verarbeitete Information an die Thorakalganglien weiterleiten. Bisher sind allerdings bei keinem der bisher untersuchten Tiere polarisationssensitive absteigende Neurone nachgewiesen worden, sodass sich dieses Thema besonders eignet untersucht zu werden. Daher stellen die absteigenden Neurone den Hauptteil der vorliegenden Dissertationsschrift dar und wurden mittels elektrophysiologischer Methoden untersucht. Hierzu führte ich, unter Hilfestellung von Dr. Klaus Hensler, die Methodik zur intrazellulären Ableitung direkt von den Halskonnektiven in unserem Labor ein. Diese Methodik ermöglicht es, von absteigenden Neuronen intakter, horizontal fixierter Tiere abzuleiten. Ich optimierte sie dahingehend, dass stabile Ableitungen über einen längeren Zeitraum und auch gute Anfärbungen, mittels Farbstoffinjektionen, möglich wurden. Somit konnte neben der Untersuchung der physiologischen Eigenschaften auch ein Vergleich aufgrund anatomischer Merkmale mit bereits beschriebenen absteigenden Neuronen angestrebt werden beziehungsweise neue Neurone beschrieben werden.

Die vorliegende Arbeit gliedert sich in drei Kapitel, deren Inhalt im Folgenden kurz beschrieben werden soll.

Kapitel 1: A novel type of microglomerular synaptic complex in the polarization vision pathway of the locust brain

Das erste Kapitel beschäftigt sich zunächst mit der Eingangsregion des Zentralkomplexes, dem lateralen akzessorischen Lobus (LAL). In einer anatomischen Arbeit wurde die Verbindung zwischen den aus dem anterioren optischen Tuberkel (AOTu) stammenden Neuronentypen (TuLAL) und den Tangentialneuronen (TL), die Signale an die untere Zentralkörpereinheit liefern, näher untersucht. Der AOTu besteht im Wesentlichen aus zwei Untereinheiten, von denen ausschließlich die untere mit polarisationssensitiven Neuronen assoziiert ist. Mittels Farbstoffinjektion direkt in diese untere Einheit des AOTu wurden Projektionen der beiden Neuronentypen TuLAL1a und 1b angefärbt. Während die Neuronen des Typs TuLAL1a ausschließlich im lateralen Dreieck und somit auf die Tangentialneurone der Typen TL1/2 verschalten, weisen die TuLAL1b Neurone in beiden Arealen, lateralem Dreieck und medianer Olive, Verzweigungen auf und könnten somit sowohl auf die TL1/2 als auch auf die TL3 Neurone verschalten. Das Besondere an dieser Verschaltung ist, dass das präsynaptische Neuron sowohl in der medianen Olive als auch im lateralen Dreieck eine Art becherförmige Endigung ausbildet, die in ihrem Inneren zahlreiche im wesentlichen γ-Aminobuttersäure (engl. *γ-aminobutyric acid*, GABA)-immunreaktive postsynaptische Endigungen aufweist. Es ist bereits nachgewiesen wurden, dass die TL2 und TL3 Neurone, nicht aber die TL1 Neurone, GABA-immunreaktiv sind (Homberg et al., 1999). Auf lichtmikroskopischer Ebene konnte gezeigt werden, dass sich die beiden Areale mediane Olive und laterales Dreieck durch den Isthmustrakt gut abgrenzen lassen und jeweils kleine Strukturen GABA-immunreaktiver Profile erkennen lassen, die regelmäßig durch unmarkierte Bereiche voneinander abgegrenzt sind. In Doppelfärbungen konnte weiterhin gezeigt werden, dass eben jene unmarkierten 'Lücken' von Endigungen der durch Druckinjektion angefärbten TuLAL1a/b Neurone gefüllt werden. Die Terminalen der Neurone umschließen direkt die kleinen GABA-immunreaktiven Strukturen und bilden mikroglomeruläre Einheiten (Abb. 2). Durch elektronenmikroskopische Untersuchung des LAL wurden direkte synaptische Kontakte der großen umschließenden Profile auf zahlreiche kleine eingeschlossene zumeist GABA-immunreaktive Profile nachgewiesen und somit die Polarität der Verschaltung bestätigt. Zur besseren Illustration wurde ein kleiner Mikroglomerulus dreidimensional rekonstruiert, um die mehr als 150 ausnahmslos dyadischen synaptischen Kontaktstellen in seinem Inneren besser darzustellen.
Im Vergleich mit anderen spezialisierten synaptischen Verschaltungen fällt eine bemerkenswerte Ähnlichkeit mit dem in Vertebraten vorkommenden Held'schen Calyx auf. Diese Riesensynapse ist Teil der Hörbahn, wobei das präsynaptische Profil becher- oder fingerförmig das Soma der postsynaptischen Zelle umschließt. Diese enge und feste Umklammerung ist eine Anpassung an eine starke und zeitlich präzise Signalübertragung, wodurch die Phaseninformation des auditorischen Signals bewahrt wird (Carr & Soares, 2002). Im Heuschreckengehirn sind diese hochspezialisierten synaptischen Verschaltungen Teil der Polarisations-Sehbahn und stellen auf der Ebe-

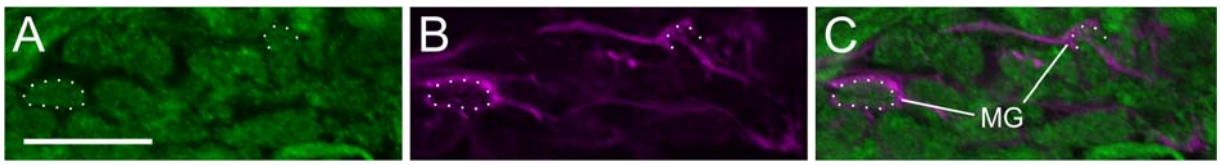

Abb. 2 Konfokalaufnahmen eines 1 µm dicken Teilbereiches der medianen Olive im lateralen akzessorischen Lobus. ***A,*** Mittels eines Antikörpers gegen GABA sind die GABA-immunreaktiven separierten Bereiche in grün (zwei Beispiele gepunktet umrandet) gut zu erkennen. Die Dextran/Cy3-markierten Endigungen einiger TuLAL-Neurone des anterioren optischen Tuberkels (magenta) sind in ***B*** dargestellt. ***C,*** Die Überlagerung der beiden Einzelabbildungen verdeutlicht die umfassende Struktur der TuLAL-Endigungen, welche die 'Lücken' füllt und mikroglomeruläre Einheiten (MG) bilden. Der Maßstabsbalken in A entspricht 20 µm und ist gleichermaßen für B und C gültig.

ne des LAL den Eingang in den Zentralkomplex dar. Aufgrund dieser Mikroglomeruli, deren synaptische Kontakte ausschließlich auf das Innere beschränkt sind und somit verbunden mit einer umgebenden Gliahülle eine Art 'Abschirmung' oder besser eine Diffusionsbarriere für die synaptischen Transmitter darstellen, scheint eine besonders starke und schnelle synaptische Verschaltung auf dieser Ebene der Polarisations-Sehbahn stattzufinden.

Die Studie umfasst erstmalig eine bis zur Ultrastruktur reichende Beschreibung einer hoch spezialisierten Schaltstelle zwischen Neuronen der Polarisations-Sehbahn, die den Eingang in den Zentralkomplex darstellen. Dennoch bleibt die Frage ungeklärt, auf welche Art und Weise die Weiterleitung über inhibitorische Neurone erfolgt. Dessen ungeachtet stellt diese mikroglomeruläre synaptische Verschaltung zweifelsfrei eine Art Schlüsselfunktion dar, indem sie eine zeitlich äußerst präzise Weiterleitung der Signale beider Hirnhemisphären in ein unpaariges Areal, die untere Einheit des Zentralkomplexes, bewirkt. Diese Schaltstelle ist damit aktiv an der Integration binokularer Eingänge beteiligt, welche möglicherweise eine entscheidende Voraussetzung für die Überführung von *E*-Vektorsignalen in ein räumliches Signal für die Kompass-Orientierung und Navigation darstellt.

<u>Kapitel 2:</u> Polarization sensitive descending neurons in the locust: connecting the brain to thoracic ganglia

Während sich das erste Kapitel mit dem Eingang in den Zentralkomplex beschäftigt, ist der Ausgang bzw. die Verschaltung auf die motorischen Zentren im Bauchmark zentrales Thema in Kapitel 2. Um gezielt von absteigenden Neuronen ableiten zu können, war es zunächst erforderlich, einen elektrophysiologischen Arbeitsstand dahingehend anzupassen, dass die Halskonnektive frei zugänglich waren. Die abgeleiteten Neurone wurden mittels dorsal rotierender *E*-Vektoren stimuliert und wiesen eine für polarisationssensitive Neurone typische Modulation der Aktionspotentialfrequenz mit eindeutiger Vorzugsrichtung (Φ_{max}) auf. Durch erfolgreiche Farbstoffinjektionen und verlässliche physiologische Eigenschaften war es möglich, 26 absteigende Neurone drei Zelltypen zuzuordnen. Während zwei dieser Zelltypen ausgehend vom Gehirn in die Thorakalganglien und möglicherweise direkt auf motorische Neurone projizieren, weist der dritte Typus keine Verbindungen mit dem Gehirn auf, sondern verbindet lediglich das Unterschlundganglion mit dem nachfolgenden Prothorakalganglion. Aufgrund morphologischer Ähnlichkeiten der einzelnen Ableitungen kann davon ausgegangen werden, dass es sich zumindest bei den beiden vom Gehirn ausgehenden Zelltypen um individuelle Neurone handelt.

Die absteigenden polarisationssensitiven Neurone des Gehirns (n = 10) weisen eine zeitliche Beziehung zwischen der Vorzugsrichtung und der Tageszeit auf, die erstmalig für das gesamte Tierreich geltend auf eine Zeitkompensation des Himmelskompasses hindeutet. Weiterhin schließen diese beiden Neuronen die Lücke zwischen den Verarbeitungszentren des Gehirns und der verhaltensauslösenden Motorik in den Thorakalganglien und stellen damit möglicherweise die letzte interneuronale Schaltstelle der Polarisationswahrnehmung und -verarbeitung dar. Aufgrund multimodaler Eigenschaften, wie z.B. die zusätzliche Reaktion dieser Neurone auf bewegte Stimuli, stellen diese Neurone eine Integrationsstelle für Bewegungssensitivität und *E*-Vektor-Detektion dar, welches in einer besonders starken Kodierung für Änderungen der Kopforientierung unter verschiedenen Himmels- und Bodenkontrasten resultieren könnte. Auf welche Art und Weise diese beiden Eingänge dabei exakt interagieren und sich möglicherweise gegenseitig ergänzen, kann erst durch gemeinsame Stimulation während einer Ableitung untersucht werden. Diese Studie beschreibt erstmalig polarisationssensitive absteigende Neurone und bietet ferner eine exzellente Ansatzmöglichkeit für weiterführende Versuche. Im Rahmen dieser Arbeit wurden bereits einige weitere Ansätze verfolgt.

Der dritte Zelltyp, der sich allenfalls in zwei einzelne Neurone unterteilen lässt sowie das Unterschlundganglion mit dem Prothorakalganglion verbindet, deckt ein äußerst breites (bis zu 180°) Sehfeld in lateraler Ausdehnung ab. Dieser Zelltyp wies keine zeitliche Beziehung zwischen

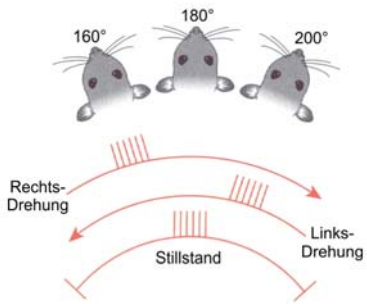

Abb. 3 Antwortverhalten eines hypothetischen antizipatorischen Kopfrichtungsneurons aus dem anterioren dorsalen thalamischen Nukleus. Die Aufgabe dieser Zelle ist es, der Ratte das baldige Erreichen der 180° Position des Kopfes zu signalisieren. Bei Annäherung von Links (Rechtsdrehung des Tieres) feuert die Zelle *links* von 180° (z. B. bei 160°) während sie bei Annäherung von Rechts (Linksdrehung) *rechts* von 180° (z. B. bei 200°) feuert. Bei Stillstand des Tieres feuert die Zelle genau bei 180° (verändert nach Carew, 2000).

der Tageszeit und dem *E*-Vektor-Tuning auf. In Kombination mit vorherigen Studien, in denen eine rhythmische Aktivität eines solchen Neurons während des Fluges nachgewiesen wurde sowie elektrische Stimulation dieser Zelle zu Kopfrollbewegungen führte (Hensler, 1989), vermute ich eine integrative Beteiligung der *E*-Vektor-Orientierung des polarisierten Lichtes an der Kontrolle der Kopforientierung infolge von Horizonterkennung. Auch diese völlig unerwartete polarisationssensitive Eigenschaft eines bekannten 'Flugsteuer'-Neurons bietet eine hervorragende Ausgangsposition für weiterführende Studien. Darüber hinaus konnten innerhalb dieser Studie keine Hinweise auf eine überlappende Färbung mittels Antisera gegen gängige Neurotransmitter gefunden werden, so dass auch auf dieser Ebene weitere Ansatzstellen vorhanden wären.

Zusätzlich wurde in dieser Studie das Navigationsprinzip von Vertebraten aufgegriffen, da sich alle absteigenden polarisationssensitiven Neurone gleichsam wie die sogenannten 'antizipatorischen Kopfrichtungsneurone' des anterioren dorsalen thalamischen Nukleus von Ratten verhalten, welche dem Tier bereits vor Erreichen einer bestimmten Kopfrichtung das baldige Eintreten dieses Ereignisses signalisieren (Abb. 3; Blair & Sharp, 1995; Taube & Basset, 2003). Dieses Navigationsprinzip eröffnet wiederum eine völlig neue Perspektive in Bezug auf die Interpretation der Funktionsweise polarisationssensitiver Neurone.

<u>Kapitel 3:</u> Behavioral and electrophysiological evidence for a role of polarized light in optomotor responses of the desert locust *Schistocerca gregaria*

Im Rahmen der Untersuchung der absteigenden Neurone kristallisierten sich auch einige Sonderfälle polarisationssensitiver Neurone heraus. Diese Neurone schienen zwischen Links- und Rechtsdrehungen des Polarisationsfilters unterscheiden zu können. Im Gehirn konnte ebenfalls von solchen Neuronen abgeleitet werden. Allen gemeinsam war die signifikante Antwort, mit einer deutlich bestimmbaren Vorzugsrichtung (Φ_{max}), auf eine der beiden Drehrichtungen des Polarisators, während die andere Drehrichtung zu einer gleichförmigen Antwort ohne erkennbare *E*-Vektor-Empfindlichkeit führte. Die untersuchten drehrichtungssensitiven Neurone des Heuschreckengehirns ähnelten bekannten bewegungssensitiven Zellen und scheinen deren physiologische Eigenschaften um die Wahrnehmung polarisierten Lichtes zu ergänzen.

Mit Verhaltensstudien wurde bestätigt, dass die Tiere die Drehrichtung eines dorsal rotierenden Polarisationsfilters erkennen und dem Stimulus folgen können. Dazu wurden Heuschrecken in einem Windkanal (siehe Abb. 4) fixiert und deren Flugverhalten, ausgelöst durch den frontalen Windstimulus, untersucht. Mittels eines Drehmomentmessers konnten die Drehkräfte der fixiert fliegenden Heuschrecken nach links bzw. nach rechts gemessen und über die Zeit graphisch aufgetragen werden. Daraus resultierte ein sägezahnförmiger Kurvenverlauf, der sich pro Drehrichtung signifikant zwischen den Kraftaufwendungen nach rechts bzw. nach links unterschied. Demnach folgen die Heuschrecken dem Stimulus aktiv, drehen sich dann bei maximaler Kraft in einer schnellen Rückstellbewegung entgegen der Drehrichtung des Polfilers, und folgen der Drehrichtung des Stimulus anschließend wieder. Dieses Verhalten ähnelt einem optokinetischen Nystagmus und tritt in ähnlicher Form auch bei der Bewegung eines schwarz-weißen Streifenmusters um das Tier herum auf (Schlieper, 1927; Varjú, 1975; Kien und Land; 1978; Barnes & Nalbach, 1993). Mittels dieser Studie konnte erstmals nachgewiesen werden, dass Heuschrecken in der Lage sind, die Bewegungsrichtung des rotierenden Polarisationsfilters zu erkennen und daraufhin eine optomotorische Reaktion zu zeigen. Da unbehandelte Tiere ein tendenziell ver-

gleichbares Verhalten zeigten wie Tiere, bei denen die Komplexaugen bis auf die dorsale Randregion mit schwarzer Farbe übermalt wurden, muss dieses bewegungssensitive polarisationsempfindliche Verhalten über die dorsale Randregion des Auges wahrgenommen werden.

Die neuronale Grundlage einer solchen optomotorischen Antwort könnte in der fächerförmigen Anordnung der Ommatidien der dorsalen Randregion begründet sein, die mit einer kreisförmigen lateralen Interaktion der nachgeschalteten Neurone einhergehen müsste. Dies könnte eine biologische Anpassung an die Wahrnehmung von rotationsbedingten Bewegungen um die Körperhochachse des Tieres herum darstellen. Die drehrichtungssensitiven polarisationsempfindlichen Neurone des Gehirns, wie auch die absteigenden drehrichtungssensitiven polarisationsempfindlichen Zellen stellen Neurone dar, deren vorgeschaltete Elemente zeitverzögerten Eingang von benachbarten Photorezeptoren der dorsalen Randregion erhalten haben. Dieses der Wahrnehmung von Bewegungsinformation zugrunde liegende Prinzip wird als 'Reichardt'-scher Bewegungsdetektor' bezeichnet. Diese drehrichtungssensitiven polarisationsempfindlichen Neurone offenbaren ein von der bisher untersuchten Polarisations-Sehbahn getrenntes System, das dem Polarisations-Sehsystem möglicherweise eine völlig neuartige Funktion auferlegt, die eng verbunden mit der Bewegungssensitivität Gierbewegungen der Heuschrecke kontrolliert und damit zur Flugbalance beträgt.

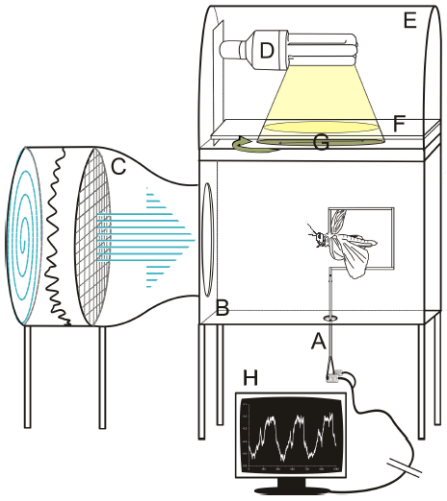

Abb. 4 Versuchsaufbau zur Untersuchung der Polarotaxis. Das über eine Halterung mit einem Drehmomentmesser (**A**) in der Flugkammer (**B**) fixierte Versuchstier wurde durch laminaren Luftstrom aus dem Windkanal (**C**) zum stationären Flug motiviert. Eine Lichtquelle (**D**), abgeschirmt von einer Abdeckung (**E**), projizierte durch einen Diffusor (**F**) gleichmäßig ausgeleuchtetes Licht durch einen drehbaren Polarisationsfilter (**G**). Der Pfeil neben dem Polarisationsfilter deutet eine Linksdrehung des Tieres in Bezug auf den präsentierten *E*-Vektor an. Durch Digitalisierungsschritte konnten die Drehmomente der Heuschrecke direkt beobachtet werden (**H**); (verändert nach Backasch, 2009).

Diese Studie liefert weiterhin einen Beitrag zur Aufklärung der Wahrnehmung individueller *E*-Vektoren, da bisher zwei Theorien in der Literatur diskutiert wurden. Nach der 'sukzessiven Methode' werden die polarisationssensitiven Photorezeptoren relativ zum *E*-Vektor ausgerichtet, um die vorherrschende Vorzugsrichtung am Himmel erkennen zu können. Nach der 'simultanen Methode' kann dagegen, ungeachtet der Körperstellung durch drei Photorezeptoren mit unterschiedlichem *E*-Vektor-Tuning die *E*-Vektorstellung am Himmel unmittelbar erkannt werden. Für letzteres spricht auch die orthogonal ausgerichtete Mikrovillianordnung der einzelnen Ommatidien in der dorsalen Randregion. Unsere Daten unterstützen indirekt die simultane Methode der *E*-Vektor-Erkennung durch permanenten Abgleich von mindestens drei unabhängigen Kanälen von *E*-Vektor-Analysatoren wie bereits 1972 von Kirschfeld vorgeschlagen. Die fächerförmige Anordnung der Photorezeptoren der dorsalen Randregion würde damit, anders als von Wehner (1989) angenommen nicht als ein peripherer sensorischer Filter fungieren, der das *E*-Vektormuster des blauen Himmel gemäß der sukzessiven Methode abgleicht, sondern zur Wahrnehmung horizontaler Rotationsrichtung dienen.

Literatur

Backasch, B. (2009) Untersuchungen zur Phototaxis und Polarotaxis fixiert fliegender Wüstenheuschrecken. Diplomarbeit, Philipps-Universität Marburg.

Barnes, W. & Nalbach, H. (1993) Eye movements in freely moving crabs: Their sensory basis and possible role in flow-field analysis. *Comp Biochem Physiol, 104A,* 675-693.

Blair, H. T. & Sharp, P. E. (1995) Anticipatory head direction signals in anterior thalamus: evidence for a thalamocortical circuit that integrates angular head motion to compute head direction. *J Neurosci, 15*, 6260-6270.

Brunner, D. & Labhart, T. (1987) Behavioural evidence for polarization vision in crickets. *Physiol Entomol, 12*, 1-10.

Carew, T. J. (2000) Spatial Navigation in Rats. *In:* Carew, T. J. *(ed.)* Behavioral Neurobiology: The Cellular Organization of Natural Behavior. *Sinauer Associates,* 377-413.

Carr, C. E. & Soares, D. (2002) Evolutionary convergence and shared computational principles in the auditory system. *Brain Behav Evol, 59*, 294-311.

Dacke, M., Nilsson, D., Scholtz, C., Byrne, M. & Warrant, E. (2003) Animal behaviour: insect orientation to polarized moonlight. *Nature, 424*, 33.

el Jundi, B. & Homberg, U. (2010) Evidence for the possible existence of a second polarization vision pathway in the locust brain. *J Insect Physiol, 56*, 971-979.

Frost, B. & Mouritsen, H. (2006) The neural mechanisms of long distance animal navigation. *Curr Opin Neurobiol, 16*, 481-488.

Hensler, K. (1989) Corrective flight steering in locusts: Convergence of extero- and proprioceptive inputs in descending deviation detectors. *In:* Singh, R. N. & Strausfeld, N. J. *(ed.)* Neurobiology of sensory systems. *Plenum Press, New York & London,* 531-554.

Heinze, S. & Homberg, U. (2007) Maplike representation of celestial *E*-vector orientations in the brain of an insect. *Science, 315*, 995-997.

Heinze, S. & Homberg, U. (2008) Neuroarchitecture of the central complex of the desert locust: Intrinsic and columnar neurons. *J Comp Neurol., 511*, 454-478.

Heinze, S. & Homberg, U. (2009) Linking the input to the output: new sets of neurons complement the polarization vision network in the locust central complex. *J Neurosci, 29*, 4911-4921.

Heinze, S., Gotthardt, S. & Homberg, U. (2009) Transformation of polarized light information in the central complex of the locust. *J Neurosci, 29*, 11783-11793.

Helfrich-Förster, C., Stengl, M. & Homberg, U. (1998) Organization of the circadian system in insects. *Chronobiol Int, 15*, 567-594.

Homberg, U. & Paech, A. (2002) Ultrastructure and orientation of ommatidia in the dorsal rim area of the locust compound eye. *Arthropod Struct Dev, 30*, 271-280.

Homberg, U. (2004) In search of the sky compass in the insect brain. *Naturwissenschaften, 91*, 199-208.

Homberg, U., Hofer, S., Pfeiffer, K. & Gebhardt, S. (2003) Organization and neural connections of the anterior optic tubercle in the brain of the locust, *Schistocerca gregaria. J Comp Neurol, 462*, 415-430.

Homberg, U., Vitzthum, H., Müller, M. & Binkle, U. (1999) Immunocytochemistry of GABA in the central complex of the locust *Schistocerca gregaria*: identification of immunoreactive neurons and colocalization with neuropeptides. *J Comp Neurol, 409*, 495-507.

Homberg, U., Hofer, S., Pfeiffer, K. & Gebhardt, S. (2003) Organization and neural connections of the anterior optic tubercle in the brain of the locust, *Schistocerca gregaria. J Comp Neurol, 462*, 415-430.

Kinoshita, M., Pfeiffer, K. & Homberg, U. (2007) Spectral properties of identified polarized-light sensitive interneurons in the brain of the desert locust *Schistocerca gregaria. J Exp Biol, 210*, 1350-1361.

Labhart, T. & Meyer, E. P. (1999) Detectors for polarized skylight in insects: a survey of ommatidial specializations in the dorsal rim area of the compound eye. *Microsc Res Tech, 47*, 368-379.

Mappes, M. & Homberg, U. (2004) Behavioral analysis of polarization vision in tethered flying locusts. *J Comp Physiol A, 190*, 61-68.

Pfeiffer, K. & Homberg, U. (2007) Coding of azimuthal directions via time-compensated combination of celestial compass cues. *Curr Biol, 17*, 960-965.

Pfeiffer, K., Kinoshita, M. & Homberg, U. (2005) Polarization-sensitive and light-sensitive neurons in two parallel pathways passing through the anterior optic tubercle in the locust brain. *J Neurophysiol, 94*, 3903-3915.

Schlieper, C. (1927) Farbensinn der Tiere und optomotorische Reaktionen. *Zeitschrift für vergleichende Physiologie, 6*, 453-472.

Taube, J. S. & Bassett, J. P. (2003) Persistent neural activity in head direction cells. *Cereb Cortex, 13*, 1162-1172.

Varjú, D. (1975) Stationary and dynamic responses during visual edge fixation by walking insects. *Nature, 255*, 330-332.

Vitzthum, H., Müller, M. & Homberg, U. (2002) Neurons of the central complex of the locust *Schistocerca gregaria* are sensitive to polarized light. *J Neurosci, 22*, 1114-1125.

von Philipsborn, A. & Labhart, T. (1990) A behavioural study of polarization vision in the fly, *Musca domestica. J Comp Physiol A, 167*, 737-743.

Wehner R. (1989) The hymenopteran skylight compass: Matched filtering and parallel coding. *J Exp Biol, 146,* 62-85.

Wehner, R. & Labhart, T. (2006) Polarisation vision. *In:* Warrant, E. & Nilsson, D. *(ed.)* Invertebrate Vision. *Cambridge University Press,* 291-348.

Introduction

Animal species from nearly all major taxa show migratory behavior, and some of these animals cover remarkable distances. Well studied examples are migratory birds like the arctic tern *Sterna paradisaea* that migrates from boreal and high Arctic breeding grounds to the Southern Ocean (Egevang et al., 2009). Insects also attain excellent achievements in annual migration as shown by the monarch butterfly *Danaus plexippus* which changes its habitat between eastern North America and central Mexico (Kyriacou, 2009). How can these animals perform such remarkable migrations? Which mechanisms underlie such a performance? Foraging ants and bees use navigational strategies similar to those of birds and mammals to reach a goal. To navigate through familiar terrain, all of these species use path integration and memories of visual landmarks (Collett & Collett, 2002). During path integration, an animal permanently updates a homing vector resulting from all angular and translational movements so that it can always take a direct path back to its starting point (Collett & Collett, 2000). To compute resulting novel routes out of several single homing flights, bees use a map-like navigation strategy that allows target-oriented decisions at any place and toward any intended location within the familiar terrain (Menzel et al., 2006). These mechanisms are used for near-range navigation, termed as 'homing', rather than for long-distance navigation tasks. Animals that navigate through unknown space are forced to use cues of a global nature, such as the geomagnetic field, the stars, and cues related to the position of the sun (Frost & Mouritsen, 2006). Like diverse marine animals, e.g. marine turtles, lobsters, and molluscs, the green sea-turtle *Chelonia mydas* has a magnetic map sense for navigation to specific targets (Cain et al., 2005; Lohmann et al., 2004). Many diurnal species use a time-compensated sun-compass, other sky compass cues like polarized light, or stars for steering toward distant targets (Wehner, 1984; Homberg, 2004; Frost & Mouritsen, 2006).

Swarming locusts

The desert locust *Schistocerca gregaria* performs extensive movements through North Africa and the Middle East and retains annual migratory directions. The flight directions of locust swarms largely correspond with wind directions (Uvarov, 1977). The hopper band, illustrated on the cover of this doctoral thesis, shows 2nd and 3rd instar larvae of the South African locust *Locustana pardalina*. These hoppers also marched with the wind, but against the sun through the farm land in the Karoo desert (own observations, 2008). Kennedy (1951) described that the locusts did not follow arbitrary shifts in wind directions, but tended to remain oriented toward the mean wind direction, indicating that other environmental features that are less variable than the wind itself, are important for the control of flight directions. In field studies, Kennedy (1945, 1951) demonstrated that marching hopper bands and flying migrants change their course predictably by reflecting the sun with a mirror, indicating that migratory directions also depend on a sun-compass-mechanism.

Polarized light

Naturally polarized light arises either from the scattering of sunlight within the atmosphere and hydrosphere, or from reflection of light by shiny, non-metallic, dielectric surfaces such as a body of water, vegetation, or the surface of an animal's body (Wehner & Labhart, 2006). Underneath the celestial hemisphere, a pattern of polarization spans the entire sky produced by scattering (Rayleigh scattering) of sunlight through gas molecules and particles of the Earth's atmosphere (Strutt, 1871; Coemans et al., 1994). The pattern of linearly polarized skylight consists of circles of electric field-vectors (*E*-vectors), the oscillation-direction of the scattered sunlight, which are concentrically arranged around the sun. Direct sunlight is unpolarized and has *E*-vectors oscillat-

ing in all possible planes. The celestial *E*-vector pattern is linked to the position of the sun and, therefore, changes with the diurnal and annual movement of the sun. The only constant feature is the solar and antisolar meridian, which forms a plane of symmetry across the sky. Depending on the viewing direction, the degree of polarization changes within the celestial hemisphere from zero near the sun to 75% in the zenith when the sun is close to the horizon and the air is clear and dry (Wehner & Labhart, 2006). Colored gradients along the sky arise as a result of atmospheric scattering (Coemans et al., 1994).

Especially insects use the polarized light pattern of the blue sky for navigation. The honeybee *Apis mellifera* uses the *E*-vector of polarized light to inform its hive mates about the location of a food source by performing the so-called tail-waggle dance (von Frisch, 1949). The polarization compass of the honeybee works even if only small patches of blue sky are visible (reviewed in Wehner & Labhart, 2006). The desert ant *Cataglyphis bicolor* (Wehner, 2003) as well as the monarch butterfly *Danaus plexippus* (Reppert et al., 2004) use the polarization pattern for navigation. However, usage of a sky compass based on polarized light is not restricted to diurnal insects. The African dung beetle *Scarabaeus zambesianus* uses the polarization of the moonlit sky to orientate itself by rolling a ball of dung away in a straight line (Dacke et al., 2003). Under laboratory conditions, the fly *Musca domestica* (von Philipsborn & Labhart, 1990), the cricket *Gryllus campestris* (Brunner & Labhart, 1987; Henze & Labhart, 2007), and the locust *Schistocerca gregaria* (Mappes & Homberg, 2004) show orientated behavior under polarized light. The polarization-sensitive photoreceptors of bees, ants, and flies are UV-sensitive, while those of crickets and locusts are sensitive to blue, and those of the cockchafer are sensitive to green light, indicating that the polarization compass is monochromatic (Labhart & Meyer, 1999; Horváth & Varjú, 2004).

Polarization vision pathways in the brain

Because of their large size, the cricket *Gryllus campestris* and the locust *Schistocerca gregaria* are well suited for studying the neuronal mechanisms underlying polarization vision. Both animals have a dorsal rim area (DRA) with fan-like arranged analyzer pairs suitable for the detection of sky polarization (Labhart & Meyer, 1999; Homberg & Paech, 2002). Each analyzer pair consists of two sets of retinula cells with orthogonally arranged microvillar orientations (Wehner & Labhart, 2006). In the DRA, the ommatidia differ considerably in size and shape from the ommatidia of the rest of the eye (non-DRA). The rhabdoms are shorter in length to reduce self-screening and have a larger cross-sectional area which increases sensitivity. Furthermore, the optics of the DRA ommatidia are degraded, whereas the visual field of the photoreceptors is increased (Labhart & Meyer, 1999; Homberg & Paech, 2002). Dextran injections revealed that the photoreceptors from the DRA project to dorsal rim areas in the lamina and medulla of the optic lobe (Homberg & Paech, 2002). In the cricket, the dorsal rim area of the medulla is connected via a commissural interneuron, termed POL1, with the medulla of the other hemisphere (Labhart & Petzold, 1993; Labhart & Meyer, 2002). The POL1 neuron was the first polarization-opponent neuron that was investigated electrophysiologically (Labhart, 1988). Under stimulation with polarized light this neuron is maximally excited by a particular *E*-vector orientation, termed Φ_{max}, and maximally inhibited by an *E*-vector orientation orthogonal to Φ_{max}.

Tracer injections in locusts revealed that neurons from the medulla project via the anterior optic tract through the outer lobe of the lobula into the lower unit of the anterior optic tubercle (AOTu) (Homberg et al., 2003). The AOTu has been studied intensively in the locust and provides input to four neuron types: LoTu1 and TuTu1 neurons that connect the anterior optic tubercles of both hemispheres, and TuLAL1a and 1b neurons that project to two small regions in the lateral accessory lobe (LAL), the lateral triangle and the median olive (Fig. 1; Pfeiffer et al., 2005; Kinoshita et al., 2007; Pfeiffer & Homberg, 2007). LoTu1 and TuTu1 show spectral differences in their response to unpolarized light stimuli (Kinoshita et al., 2007). While dorsally presented unpolarized blue light inhibited both neurons, laterally presented UV or green light re-

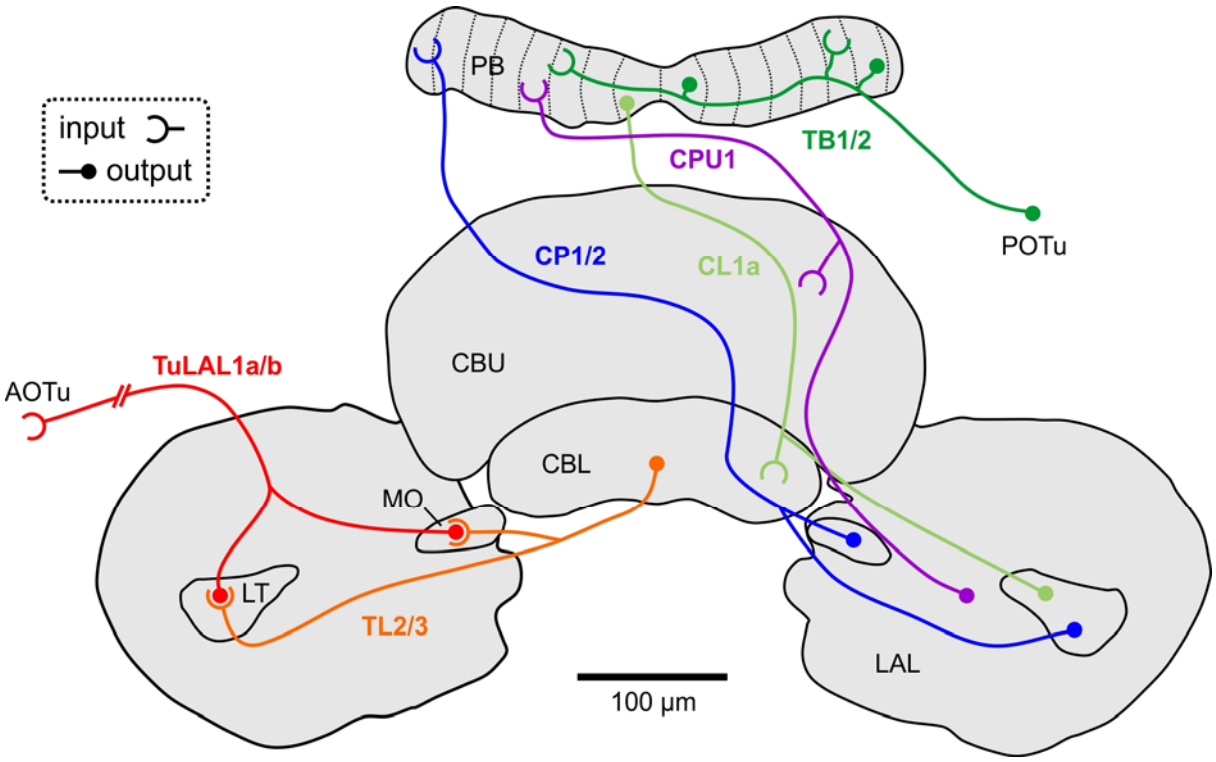

Fig. 1 Schematic illustration of the main parts of central complex showing the proposed neuronal connections between input neurons to, and intrinsic neurons in the central complex as part of the polarization vision pathway (modified from el Jundi et al., 2010; Heinze & Homberg, 2009). TuLAL1a/b neurons receive their input from the lower unit of the anterior optic tubercle (AOTu) and provide synaptic input to TL2/3 neurons with ramifications in the lateral triangle (LT) and/or median olive (MO) (Pfeiffer et al., 2005; Träger et al., 2008). TL2/3 neurons mediate polarization input into the central complex through axonal processes in the lower division of the central body (CBL). The CL1a neurons receive input in the CBL and project to the protocerebral bridge (PB). The 16 columns in the PB are connected with each other by the TB1/2 neurons that additionally provide polarization sensitive signals to the posterior optic tubercle (POTu) (Heinze & Homberg, 2007). The output of the PB is transmitted by CP1/2 and CPU1 neurons to various areas in the lateral accessory lobe (LAL). The CPU1 neurons additionally receive input from the upper division of the central body (CBU).

sulted in opponent responses. One subtype of the TuTu1 neurons was excited by UV and inhibited by green light, while the LoTu1 neurons showed the opposite response. These neurons are not only suited to code for the polarization pattern of the blue sky, but also for chromatic contrasts. Light with longer wavelengths, e.g. green light, dominates in the solar hemisphere, whereas light with short and long wavelengths in similar intensities exists in the antisolar hemisphere. Besides, the combination of information about the polarization pattern and the chromatic contrast enables the locust to compensate diurnal differences resulting from deviations in solar elevation (Pfeiffer & Homberg, 2007).

The LAL is the input structure into the central complex. The central complex consists of the protocerebral bridge (PB), the upper (CBU) and lower division of the central body (CBL), and the paired noduli (Müller et al., 1997; Heinze & Homberg, 2008) and contains at least 13 types of polarization-sensitive neurons which have been studied intensively (Fig. 1; Vitzthum et al., 2002; Heinze & Homberg, 2007, 2008, 2009; Heinze et al., 2009). Two main classes of polarization-sensitive neurons have been distinguished: Tangential neurons and columnar neurons. Physiological properties of all neuron types provide some indication of the direction of information flow through the central complex. A compass-like topographic representation of *E*-vectors, which is very well suited to encode for head orientation under the open sky, exists in the 16 columns of the PB (Williams, 1975; Heinze & Homberg, 2007). At the level of the input stage into the central complex three types of tangential neurons, TL1, TL2, and TL3, have been identified and send axonal projections to the CBL. TL2 neurons receive their input exclusively from the lateral triangle, whereas TL3 neurons have dendritic ramifications only in the median olive (Vitz-

thum et al., 2002). The LALs of both hemispheres are further connected with the PB via the columnar neurons CPU1 and CP1/2. Additionally, the PB receives input from the CBL via the columnar neurons of type CL1 and from the posterior optic tubercle (POTu) via the tangential neurons TB1/2 (Heinze et al., 2009). All of these neurons show polarization opponent responses to polarized light stimuli. Neurons at the input level (TL2/3) show the strongest response, measured by calculation of the relative response amplitude, compared to neurons at the output level (TB1/2, CPU1 and CP1/2). Following the information flow through the central complex, an expansion in receptive fields of the neuron types mentioned above has been observed. Owing to this high density of polarization-sensitive neurons, the central complex is considered as internal sky compass within the polarization vision pathway. How is this internal sky compass connected to the behavior of the animal that shows such a fascinating orientation to polarized light as described above? Heinze and Homberg (2009) described two neurons that might transmit output signals from the central complex to other brain areas.

Descending neurons

Commonly, descending neurons mediate highly processed signals from the brain to the motor centers of the thoracic ganglia. About 200 bilateral pairs of neurons descend from the brain of the cricket *Gryllus bimaculatus* to the thoracic ganglia (Staudacher, 1998). These descending neurons have wide arborizations in the posterior protocerebrum of the brain, but no ramifications in the optic lobe, the mushroom bodies, or the central body (Staudacher, 1998; Heinrich, 2002). In addition to arborizations in the posterior protocerebrum, they often have ramifications in the deutocerebrum. Their somata are arranged in clusters (n = 17) situated in the protocerebrum (10) including the pars intercerebralis (1), the deutocerebrum (5), and the tritocerebrum (1). Two main classes of descending neurons, with respect to the side of their somata, are distinguishable: The first type descends through the ipsilateral connective and the second descends, after crossing the midline within the brain or through the tritocerebral commissure, through the contralateral connective. In addition to neurons descending from the brain, about 150 neurons descend ipsi- or contralaterally from the suboesophageal ganglion (SOG). All of these 150 neurons have axons running through several thoracic ganglia, except one neuron type which terminates in the prothoracic ganglion (Kien et al., 1990).

Within the thoracic ganglia, descending neurons affect central rhythm-generating circuits, project to premotor interneurons or directly to motoneurons (Heinrich, 2002). As one of the first authors, Williams (1975) described some of the larger descending neurons in the desert locust. To date, only one descending neuron has been associated with a particular neurotransmitter. The tritocerebral dwarf (TCD) of the locust is immunoreactive with antisera to γ-amminobutyric acid (GABA), suggesting that it provides inhibitory signals to downstream neurons (Tyrer et al., 1988). The activity of descending neurons strongly depends on the ongoing activity of the animal (e.g. totally silenced, spontaneous behavior, or behavior upon other sensory stimulation), and most descending neurons respond to more than one stimulus modality and are preferentially activated by a specific combination of stimuli. Hence, functional studies are complicated (Kien, 1976; Rowell & Reichert, 1986; Heinrich, 2002). In spite of these difficulties, some descending neurons were successfully investigated, including neurons that mediate escape behavior (Bacon & Strausfeld, 1986), control different stridulatory motor patterns (Hedwig & Heinrich, 1997), or initiate pheromon-mediated behavior in the male silkworm moth *Bombyx mori* (Mishima & Kanzaki, 1999).

In the locust *Schistocerca gregaria*, descending neurons have been studied intensively. One example, the DCMD-neuron, mediates escape response to approaching objects or looming stimuli (Rind and Simmons, 1999; Santer et al., 2006), others, termed 'deviation detector neurons', respond to deviations from the normal flight posture mediated by visual and wind cues (e.g. Rowell

& Reichert, 1986; Hensler, 1992). In contrast, nothing is known at present about polarization-sensitive descending neurons, neither in the locust nor in any other animal.

Time-compensation

As mentioned above, the locust *Schistocerca gregaria* is able to maintain constant migratory directions independent of changing wind directions (Kennedy, 1945, 1951). In order to do so, the locust needs a time-compensated sky compass. All animals that navigate with respect to celestial cues need to change their navigational angles relative to the position of the sun over the course of the day. Behavioral data showed that the internal sun compass of honeybees, ants, and monarch butterflies is time-compensated (Lindauer, 1960; Wehner, 1992; Mouritsen & Frost, 2002). How this time-compensation is achieved is unknown. Neither the neurons of the AOTu nor the central-complex neurons provide evidence for time-compensation in *E*-vector signaling. At least at the level of descending neurons, time-compensation should be included because the integration of daytime information with information about position of the sun is indispensable. The anatomical localization in the brain where this putative integration is achieved is presently unknown. Recently, el Jundi and Homberg (2010) provided evidence that possibly a second polarization vision pathway in the locust brain connects the accessory medulla with the POTu and, thus, to the known neurons from the central complex. Like the TuTu1 neurons from the AOTu, intertubercle neurons connect both posterior optic tubercles.

The accessory medulla is considered as the site of the internal circadian clock in cockroaches, crickets, flies, and beetles (Helfrich-Förster et al., 1998). So far, direct evidence for its role as an internal clock in locusts is lacking, but close relationship to the cockroach and anatomical similarities suggest a role as an internal clock in the locust, too.

Optomotor responses

The behavior of the animal is influenced by the neurons described above. To investigate the locomotor or flight behavior, researchers study the behavior of an animal in wind tunnels or arenas with different stimuli around the tethered or freely moving animal like a striped drum or rotating filters from above or underneath. During locomotion, a continuous flow of image motion moves across the observer's retina. Animals use control mechanisms, 'optomotor responses', to stabilize this optic flow. Such an optomotor response is turning in the direction of the motion to maintain a straight course (Kirschfeld, 1997; Srinivasan et al., 1999; Srinivasan & Zhang, 2000; Egelhaaf, 2006; Borst et al., 2010). Many behavioral studies have focused on optomotor responses of insects elicited by moving black-and-white patterns (e.g. Götz, 1972; Egelhaaf & Borst, 1993; Rind, 2002). Like the polarization vision system, the motion detecting system that mediates optomotor responses, is color-blind (Schlieper, 1927; Srinivasan, 1985; Schaerer & Neumeyer, 1996; Yamaguchi et al., 2008). Similar to black-and-white patterns, patterns consisting of *E*-vector contrast can also elicit optomotor responses as described by crabs, honeybees, flies, backswimmers, or waterstriders (Horváth & Varjú, 2006; Wehner & Labhart, 2006; Glantz, 2008).

Scope of this work

Until now, nothing is known about descending polarization-sensitive neurons in any animal, and, furthermore, there has not been any evidence for time-compensated neurons within the internal sun compass. The major scope of this doctoral thesis was to characterize and identify descending neurons signaling polarized light information to thoracic motor centers that finally influence the behavior of the animal. To achieve that goal, I introduced (with support of Dr. Klaus Hensler)

the technique of recording from neck-connectives to our laboratory and performed routine and stable recordings from descending neurons. Based on anatomical and physiological properties, I characterized two neuron types whose *E*-vector tuning changes linearly depending on daytime and, additionally, one neuron type that connects only the SOG to the prothoracic ganglion. Moreover, I found some descending neurons that curiously respond only to one rotation direction of dorsally presented polarized light. Compared with findings from behavioral studies of tethered flying locusts, these direction-sensitive descending neurons could be involved in performing optomotor responses. Furthermore, I had a closer look at the input stage into the central complex. Within the LAL a highly specialized synaptic contact of the polarization vision pathway was analyzed in detail. This synaptic contact is the only confirmed connection between neurons of the polarization vision system.

References

Bacon, J. P. & Strausfeld, N. J. (1986) The dipteran 'giant fibre' pathway: Neurons and signals *J Comp Physiol A, 158*, 529-548.

Borst, A., Haag, J. & Reiff, D. F. (2010) Fly motion vision. *Annu Rev Neurosci, 33*, 49-70.

Brunner, D. & Labhart, T. (1987) Behavioural evidence for polarization vision in crickets. *Physiol Entomol, 12*, 1-10.

Cain, S. D., Boles, L. C., Wang, J. H. & Lohmann, K. J. (2005) Magnetic orientation and navigation in marine turtles, lobsters, and molluscs: Concepts and conundrums. *Integr Comp Biol, 45*, 539-546.

Coemans, M. A., Vos Hzn, J. J. V. & Nuboer, J. F. (1994) The relation between celestial colour gradients and the position of the sun, with regard to the sun compass. *Vision Res, 34*, 1461-1470.

Collett, T. S. & Collett, M. (2000) Path integration in insects. *Curr Opin Neurobiol, 10*, 757-762.

Collett, T. S. & Collett, M. (2002) Memory use in insect visual navigation. *Nat Rev Neurosci, 3*, 542-552.

Dacke, M., Nilsson, D., Scholtz, C., Byrne, M. & Warrant, E. (2003) Animal behaviour: insect orientation to polarized moonlight. *Nature, 424*, 33.

Egelhaaf, M. (2006) Invertebrate vision. *In:* Warrant, E. & Nilsson, D. *(ed.)* The neural computation of visual motion information *Cambridge University Press,* 399-461.

Egelhaaf, M. & Borst, A. (1993) Motion computation and visual orientation in flies. *Comp Biochem Physiol Comp Physiol, 104*, 659-673.

Egevang, C., Stenhouse, I. J., Phillips, R. A., Petersen, A., Fox, J. W. & Silk, J. R. D. (2010) Tracking of Arctic terns *Sterna paradisaea* reveals longest animal migration. *Proc Natl Acad Sci U S A, 107*, 2078-2081.

el Jundi, B. & Homberg, U. (2010) Evidence for the possible existence of a second polarization vision pathway in the locust brain. *J Insect Physiol, 56*, 971-979.

el Jundi, B., Heinze, S., Lenschow, C., Kurylas, A., Rohlfing, T. & Homberg, U. (2010) The Locust Standard Brain: A 3D Standard of the Central Complex as a Platform for Neural Network Analysis. *Front Syst Neurosci, 3*, Article 21.

Frost, B. & Mouritsen, H. (2006) The neural mechanisms of long distance animal navigation. *Curr Opin Neurobiol., 16*, 481-488.

Glantz, R. M. (2008) Polarization vision in crayfish motion detectors. *J Comp Physiol A Neuroethol Sens Neural Behav Physiol, 194*, 565-575.

Götz, K. G. (1972) Processing of cues from the moving environment in the *Drosophila* navigation system. VII. Visual Control of Orientation Patterns. *In:* Wehner, R. *(ed.)* Information Processing in the visual system of arthropods. *Springer-Verlag Berlin Heidelberg New York,* 255-263.

Hedwig, B. & Heinrich, R. (1997) Identified descending brain neurons control different stridulatory motor patterns in an acridid grasshopper. *J Comp Physiol A, 180*, 285-294.

Heinrich, R. (2002) Impact of descending brain neurons on the control of stridulation, walking, and flight in orthoptera. *Microsc Res Tech, 56*, 292-301.

Heinze, S. & Homberg, U. (2007) Maplike representation of celestial *E*-vector orientations in the brain of an insect. *Science, 315*, 995-997.

Heinze, S. & Homberg, U. (2008) Neuroarchitecture of the central complex of the desert locust: Intrinsic and columnar neurons. *J Comp Neurol, 511*, 454-478.

Heinze, S. & Homberg, U. (2009) Linking the input to the output: new sets of neurons complement the polarization vision network in the locust central complex. *J Neurosci, 29*, 4911-4921.

Heinze, S., Gotthardt, S. & Homberg, U. (2009) Transformation of polarized light information in the central complex of the locust. *J Neurosci, 29*, 11783-11793.

Helfrich-Förster, C., Stengl, M. & Homberg, U. (1998) Organization of the circadian system in insects. *Chronobiol Int, 15*, 567-594.

Hensler, K. (1992) Neuronal co-processing of course deviation and head movements in locusts. *J Comp Physiol A, 171*, 257-271.

Henze, M. & Labhart, T. (2007) Haze, clouds and limited sky visibility: polarotactic orientation of crickets under difficult stimulus conditions. *J Exp Biol, 210*, 3266-3276.

Homberg, U. (2004) In search of the sky compass in the insect brain. *Naturwissenschaften, 91*, 199-208.

Homberg, U. & Paech, A. (2002) Ultrastructure and orientation of ommatidia in the dorsal rim area of the locust compound eye. *Arthropod Struct Dev, 30*, 271-280.

Homberg, U., Hofer, S., Pfeiffer, K. & Gebhardt, S. (2003) Organization and neural connections of the anterior optic tubercle in the brain of the locust, *Schistocerca gregaria*. *J Comp Neurol, 462*, 415-430.

Horváth, G. & Varjú, D. (2004) Polarized light in animal vision - Polarization patterns in nature. *Springer Verlag Berlin Heidelberg*.

Kennedy, J. S. (1945) Observations on the mass migration of desert locust hoppers. *Trans R Entomol Soc Lond,* 95, 247-262.

Kennedy, J. S. (1951) The migration of the desert locust (*Schistocerca gregaria* FORSK.) I. The behaviour of swarms. II: A theory of long-range migrations. *Philos Trans R Soc Ser B,* 163-290.

Kien, J. (1976) Arousal changes in the locust optomotor system. *J Insect Physiol, 22*, 393-396.

Kien, J., Fletcher, W. A., Altman, J. S., Ramirez, J. & Roth, U. (1990) Organization of intersegmental interneurons in the suboesophageal ganglion of *Schistocerca gregaria* (Forksal) and *Locusta migratoria* migratorioides (Reiche & Fairmaire) (Acrididae, Orthoptera). *Int J Insect Morphol & Embryol, 19*, 35-60.

Kinoshita, M., Pfeiffer, K. & Homberg, U. (2007) Spectral properties of identified polarized-light sensitive interneurons in the brain of the desert locust *Schistocerca gregaria*. *J Exp Biol, 210*, 1350-1361.

Kirschfeld, K. (1997) Course control and tracking: orientation through image stabilization. *EXS, 84*, 67-93.

Kyriacou, C. P. (2009) Clocks, cryptochromes and Monarch migrations. *J Biol, 8*, 55.

Labhart, T. (1988) Polarization-opponent interneurons in the insect visual system *Nature, 331*, 435-437.

Labhart, T. & Meyer, E. P. (1999) Detectors for polarized skylight in insects: a survey of ommatidial specializations in the dorsal rim area of the compound eye. *Microsc Res Tech, 47*, 368-379.

Labhart, T. & Meyer, E. P. (2002) Neural mechanisms in insect navigation: polarization compass and odometer. *Curr Opin Neurobiol, 12*, 707-714.

Labhart, T. & Petzold, J. (1993) Processing of polarized light information in the visual system of crickets. *In:* Wiese, K., Gribakin, F. G., Popov, A. V. & Renninger, G. (*ed.*) Sensory systems of arthropods. *Birkhäuser, Basel*, 158-169.

Lindauer, M. (1960) Time-compensated sun orientation in bees. *Cold Spring Harbor Symposia on Quantitative Biology*, *25*, 371-377.

Lohmann, K. J., Lohmann, C. M. F., Ehrhart, L. M., Bagley, D. A. & Swing, T. (2004) Animal behaviour: geomagnetic map used in sea-turtle navigation. *Nature, 428*, 909-910.

Mappes, M. & Homberg, U. (2004) Behavioral analysis of polarization vision in tethered flying locusts. *J Comp Physiol A, 190*, 61-68.

Menzel, R., Marco, R. J. D. & Greggers, U. (2006) Spatial memory, navigation and dance behaviour in *Apis mellifera*. *J Comp Physiol A Neuroethol Sens Neural Behav Physiol, 192*, 889-903.

Mishima, T. & Kanzaki, R. (1999) Physiological and morphological characterization of olfactory descending interneurons of the male silkworm moth, *Bombyx mori*. *J Comp Physiol A, 184*, 143-160.

Müller, M., Homberg, U. & Kühn, A. (1997) Neuroarchitecture of the lower division of the central body in the brain of the locust (*Schistocerca gregaria*). *Cell Tissue Res, 288*, 159-176.

Pfeiffer, K. & Homberg, U. (2007) Coding of azimuthal directions via time-compensated combination of celestial compass cues. *Curr Biol, 17*, 960-965.

Pfeiffer, K., Kinoshita, M. & Homberg, U. (2005) Polarization-sensitive and light-sensitive neurons in two parallel pathways passing through the anterior optic tubercle in the locust brain. *J Neurophysiol, 94*, 3903-3915.

Reppert, S. M., Zhu, H. & White, R. H. (2004) Polarized light helps monarch butterflies navigate. *Curr Biol, 14*, 155-158.

Rind, F. C. (2002) Motion detectors in the locust visual system: From biology to robot sensors. *Microsc Res Tech, 56*, 256-269.

Rind, F. C. & Simmons, P. J. (1999) Seeing what is coming: building collision-sensitive neurones. *Trends Neurosci, 22*, 215-220.

Rowell, C. H. & Reichert, H. (1986) Three descending interneurons reporting deviation from course in the locust. II. Physiology. *J Comp Physiol A, 158*, 775-794.

Santer, R. D., Rind, F. C., Stafford, R. & Simmons, P. J. (2006) Role of an identified looming-sensitive neuron in triggering a flying locust's escape. *J Neurophysiol, 95*, 3391-3400.

Schaerer, S. & Neumeyer, C. (1996) Motion detection in goldfish investigated with the optomotor response is "color blind". *Vision Res, 36*, 4025-4034.

Schlieper, C. (1927) Farbensinn der Tiere und optomotorische Reaktionen. *Z Vergl Phys, 6*, 453-472.

Srinivasan, M. V. (1985) Shouldn't directional movement detection necessarily be "colour-blind"? *Vision Res, 25*, 997-1000.

Srinivasan, M. V. & Zhang, S. W. (2000) Visual navigation in flying insects. *Int Rev Neurobiol, 44*, 67-92.

Srinivasan, M. V., Poteser, M. & Kral, K. (1999) Motion detection in insect orientation and navigation. *Vision Res, 39*, 2749-2766.

Staudacher, E. (1998) Distribution and morphology of descending brain neurons in the cricket *Gryllus bimaculatus*. *Cell Tissue Res, 294*, 187-202.

Strutt, J. W. (1871) On the light from the sky, its polarization and colour. *Philos Mag, 41,* 107-120.

Träger, U., Wagner, R., Bausenwein, B. & Homberg, U. (2008) A novel type of microglomerular synaptic complex in the polarization vision pathway of the locust brain. *J Comp Neurol, 506*, 288-300.

Tyrer, N. M., Pozza, M. F., Humbel, U., Peters, B. H. & Bacon, J. P. (1988) The tritocerebral commissure 'dwarf' (TCD): a major GABA-immunoreactive descending interneuron in the locust. *J Comp Physiol A, 164*, 141-150.

Uvarov, S. B. (1977) Grasshoppers and Locusts - a handbook of general acridology. Volume 2 *Centre for overseas pest research - London*.

von Frisch, K. (1949) Die Polarisation des Himmelslichtes als orientierender Faktor bei den Tänzen der Bienen. *Experientia*, *5*, 142-148.

von Philipsborn, A. & Labhart, T. (1990) A behavioural study of polarization vision in the fly, *Musca domestica*. *J Comp Physiol A, 167*, 737-743.

Vitzthum, H., Müller, M. & Homberg, U. (2002) Neurons of the central complex of the locust *Schistocerca gregaria* are sensitive to polarized light. *J Neurosci, 22*, 1114-1125.

Wehner, R. (1984) Astronavigation in insects. *Annu Rev Entomol, 29*, 277-298.

Wehner, R. (1992) Arthropods. *In:* Papi, F. (*ed.*) Animal Homing. *Chapman and Hall, London*, 45-145.

Wehner, R. (2003) Desert ant navigation: how miniature brains solve complex tasks. *J Comp Physiol A Neuroethol Sens Neural Behav Physiol, 189*, 579-588.

Wehner, R. & Labhart, T. (2006) Polarisation vision. *In:* Warrant, E. & Nilsson, D. *(ed.)* Invertebrate Vision. *Cambridge University Press,* 291-348.

Williams, J. L. D. (1975) Anatomical studies of the insect central nervous system: A ground-plan of the midbrain and an introduction to the central complex in the locust, *Schistocerca gregaria* (Orthoptera). *J Zool, Lond, 176*, 67-86.

Yamaguchi, S., Wolf, R., Desplan, C. & Heisenberg, M. (2008) Motion vision is independent of color in *Drosophila. Proc Natl Acad Sci U S A, 105*, 4910-4915.

A Novel Type of Microglomerular Synaptic Complex in the Polarization Vision Pathway of the Locust Brain

THE JOURNAL OF COMPARATIVE NEUROLOGY 506:288–300 (2008)

A Novel Type of Microglomerular Synaptic Complex in the Polarization Vision Pathway of the Locust Brain

ULRIKE TRÄGER,[1] ROBERT WAGNER,[2] BERNHARD BAUSENWEIN,[2] AND UWE HOMBERG[1]*

[1]Fachbereich Biologie, Tierphysiologie, Philipps Universität Marburg, D-35032 Marburg, Germany

[2]Institut für Zoologie, Universität Regensburg, D-93040 Regensburg, Germany

ABSTRACT

The lateral accessory lobes (LALs) are prominent integration centers in the insect brain. In the desert locust *Schistocerca gregaria*, they are connected with the anterior optic tubercles (AOTus), with the central complex, and with the ventral nerve cord. Two subcompartments of the LALs, the lateral triangle and the median olive, are easily recognized by their prominent granular texture. Both areas are part of the polarization vision pathway in the locust brain; they receive input from projection neurons of the AOTu and are the site of presumed dendritic arborizations of tangential neurons of the lower division of the central body. Both types of neuron are sensitive to polarized light and most likely play a role in sky compass navigation of the locust. We show here that neurons from the AOTu and tangential neurons of the central body form large microglomerular contacts in the median olive and lateral triangle. Presynaptic elements from the AOTu end in small numbers of large cup-shaped terminals. These cups enclose many small γ-aminobutyric acid (GABA)-immunoreactive (-ir) profiles from tangential neurons of the lower division of the central body. Each cup-shaped profile makes numerous (>150) dyadic output synapses with the small postsynaptic GABA-ir profiles. No synaptic connections were found between the small core profiles. The microglomerular organization of the median olive and lateral triangle is unlike that of any other synaptic microglomeruli reported for the insect brain. It might provide precise spike timing information possibly used to extract spatial information by comparison of binocular inputs in the central complex. J. Comp. Neurol. 506:288–300, 2008.

Indexing terms: sky compass navigation; synaptic transmission; microglomeruli; GABA; insect brain; *Schistocerca gregaria*

For spatial orientation, many insects rely on landmarks or a vector integration strategy based on a sky compass (for review see Wehner, 2003; Menzel et al., 2006). In addition to direct sunlight, many insects can detect the polarization pattern of the blue sky and use it as a compass cue. In these species, a particular region of the compound eye, the dorsal rim area, is specialized for polarization vision (Labhart and Meyer, 1999; Homberg and Paech, 2002). Central processing of polarized light signals has been studied in the field cricket *Gryllus campestris* (Labhart and Meyer, 2002; Wehner, 2003) and in the desert locust *Schistocerca gregaria* (Homberg, 2004). In both species, polarization-sensitive (POL) interneurons have been discovered in the central body (Vitzthum et al., 2002; Sakura and Labhart, 2005; Heinze and Homberg, 2007), a neuropil in the median protocerebrum involved in visual pattern recognition, spatial orientation, right-left maneuvering, and other aspects of motor control (Strauss, 2002; Homberg, 2004; Liu et al., 2006).

Grant sponsor: Deutsche Forschungsgemeinschaft; Grant number: HO 950/16-1 and 14-3.

*Correspondence to: Uwe Homberg, Fachbereich Biologie, Tierphysiologie, Universität Marburg, D-35032 Marburg, Germany.
E-mail: homberg@staff.uni-marburg.de

Received 25 April 2007; Revised 20 July 2007; Accepted 22 August 2007
DOI 10.1002/cne.21512
Published online in Wiley InterScience (www.interscience.wiley.com).

The Journal of Comparative Neurology. DOI 10.1002/cne

In locusts, the polarization-vision pathway from the dorsal rim area of the compound eye to the central body has been analyzed (Homberg et al., 2003). Photoreceptors of the dorsal rim area project to dorsal rim areas in the lamina and medulla. Second-order neurons continue from the medulla through the anterior lobe of the lobula to the lower unit of the anterior optic tubercle (AOTu) in the median protocerebrum. Third-order neurons project from the AOTu through the tubercle-accessory lobe tract to two small areas in the lateral accessory lobe (LAL), termed *median olive* and *lateral triangle*. Finally, tangential neurons with dendritic ramifications in the median olive and lateral triangle arborize in particular layers of the lower division of the central body (Müller et al., 1997; see Fig. 1A). All neurons recorded from the lower unit of the AOTu are sensitive to polarized light, including two types of neuron, termed *TuLAL1a* (see Fig. 1D) and *TuLAL1b* (see Fig. 1E), that provide the connection to the median olive and lateral triangle (Pfeiffer et al., 2005). Likewise, three types of tangential neuron (TL1–TL3) that project from the lateral triangle (TL1, TL2; see Fig. 1B) and/or the median olive (TL3; see Fig. 1C) to the lower division of the central body are polarization sensitive (Vitzthum et al., 2002). TL2 and TL3 types of tangential neuron are, furthermore, immunoreactive with antisera against γ-aminobutyric acid (GABA; Homberg et al., 1999).

Neuronal terminals in the median olive and lateral triangle have unusually large knob-like or compact bushy appearances that have also been recognized in other insect species such as the fly *Drosophila melanogaster* (Hanesch et al., 1989), the sphinx moth *Manduca sexta* (Homberg et al., 1990), and the cricket *Gryllus bimaculatus* (Sakura and Labhart, 2005). To determine whether AOTu neurons in the locust make direct contacts with central-body neurons in the lateral triangle and median olive, we have analyzed these areas at the light microscopic and ultrastructural level. We show that neurons from the AOTu form extremely large presynaptic terminals of calycal shape that encompass numerous postsynaptic profiles of GABA-immunoreactive (-ir) tangential neurons of the central body. These contacts are a novel type of microglomerular synaptic complex and suggest particularly strong synaptic contacts with fast and reliable signal transmission in both areas of the polarization vision pathway of the locust.

MATERIALS AND METHODS

Animals

Experiments were performed on adult locusts, *Schistocerca gregaria*, obtained from crowded colonies at the Universities of Marburg and Regensburg. Animals were reared under 12L:12D photoperiod, at about 60% relative humidity and a temperature of 28°C during the day and 24°C during the night. Experiments were performed on sexually mature adult males and females.

Single-cell dye fills

Neurons were stained by iontophoretic injection of 4% Neurobiotin (Vector Laboratories, Burlingame, CA) in 1 M KCl with a constant depolarizing current (3 nA) for 1–7 minutes. Fixation, tissue embedding and sectioning, and immunostaining protocol have been described by Pfeiffer et al. (2005).

Dextran injections

Dextran injections were performed in 20 animals of both sexes. Locusts were immobilized by cooling for 20–30 minutes and decapitated. After dissection, brains were fixed with minute pins in a Sylgard dish containing locust saline (hypotonic, pH 6.8; Clements and May, 1974). The neurilemma was removed between the antennal lobes and calyces of the mushroom body. Dextran-biotin (lysine-fixable, 3,000 MW; Molecular Probes, Eugene, OR) was used as tracer. Dextran solution [10% in 0.1 M sodium phosphate buffer, pH 7.4, with 10% blue food dye (FD + C blue No. 1; McCormick, Baltimore, MD)] was pressure injected through borosilicate glass capillaries (1.5 mm OD, with filament; Clark Electromedical Instruments, Pangbourne, United Kingdom). Injected volumes varied from 56 pl to 28 nl as calculated from visually controlled injections into mineral oil prior to and after each experiment. After dextran application, brains were kept for 90 minutes at room temperature and were then processed as described below.

Double-labeling experiments

The dextran-injected brains were double-labeled with an antiserum against GABA (No. 9/24; provided by Dr. T.G. Kingan). The antiserum was raised in rabbit against GABA-glutaraldehyde-keyhole limpet hemocyanin (KLH). It has been affinity-purified against KLH as described by Hoskins et al. (1986). On brain section of *M. sexta*, immunostaining was abolished after preadsorption with 24 nM GABA-glutaraldehyde-KLH but was undiminished following preadsorption with similar concentrations of KLH or other amino acid-protein conjugates (Hoskins et al., 1986). In locusts, preadsorption with 15 nM GABA-glutaraldehyde-bovine serum albumin (BSA) conjugate abolished immunostaining (Homberg et al., 1999).

For double labeling, brains were fixed overnight in a solution prepared freshly by mixing one part (by volume) 25% glutaraldehyde and three parts saturated picric acid and adding acetic acid to a final concentration of 1% (Boer et al., 1979). Fixed brains were rinsed in sodium phosphate buffer. They were subsequently embedded in gelatin/albumin (4.8% gelatin and 12% ovalbumin in demineralized water) and postfixed in 8% formalin in sodium phosphate buffer (0.1 M, pH 7.4). Brains were sectioned with a vibrating-blade microtome (VT 1000S; Leica, Wetzlar, Germany) in the frontal plane at 30 μm thickness. The sections were treated for 10 minutes with sodium borohydride (0.1% in sodium phosphate buffer, 0.1 M, pH 7.4; Sigma-Aldrich, Steinheim, Germany) to reduce background fluorescence resulting from glutaraldehyde fixation. The sections were washed in Tris-buffered saline (TBS; 0.1 M Tris-HCl/0.3 M NaCl, pH 7.4) containing 0.1% Triton X-100 (TrX; Sigma, Deisenhofen, Germany). They were preincubated in TBS with 0.5% TrX and 5% normal donkey serum (NDS; Dako, Hamburg, Germany). The anti-GABA antiserum was diluted at 1:2,000 in TBS containing 0.5% TrX and 1% NDS and was applied to the sections for 18 hours. After rinsing in TBS containing 0.1% TrX, secondary antiserum, Cy2-conjugated donkey anti-rabbit IgG (Dianova, Hamburg, Germany; 1:300) and Cy3-conjugated streptavidin (Dianova; 1:1,000) were applied for at least 5 hours. Afterward, the sections were thoroughly washed in TBS containing 0.1% TrX. They were mounted on chromalum/gelatin-coated microscope

The Journal of Comparative Neurology. DOI 10.1002/cne

slides, dehydrated through a graded series of aqueous ethanol solutions, cleared in xylene, and embedded in Entellan (Merck, Darmstadt, Germany) under coverslips.

Electron microscopy

For routine electron microscopy, dissected brains were fixed overnight in freshly prepared fixative containing 4% paraformaldehyde/5% glutaraldehyde in sodium cacodylate buffer (0.2 M, pH 7.2; Osborne, 1980). After rinsing in sodium cacodylate buffer, brains were postfixed in osmium tetroxide (1% in sodium cacodylate buffer) for 1 hour, dehydrated in an ethanol series, and embedded in Epon 812 (Serva, Heidelberg, Germany) or Durcupan ACM (Fluka, Buchs, Switzerland). Ultrathin sections (~70 nm in thickness, gray to silver interference colors) were cut frontally on an ultramicrotome (Ultracut E; Reichert, Vienna, Austria) and collected on copper slot grids coated with pioloform (Plano, Marburg, Germany). Sections were contrasted with 2% uranyl acetate (15 minutes) followed by lead citrate (5 minutes; Venable and Coggeshall, 1965).

Immunogold labeling was performed with a polyclonal antiserum against GABA (No. 4TB; provided by Dr. H. Dircksen). The antiserum was raised in rabbits against GABA-glutaraldehyde-protein conjugates using an immunization technique modified from that of Seguela et al. (1984). In successive booster injections, GABA-glutaraldehyde-BSA, GABA-glutaraldehyde-hemoglobin, and GABA-glutaraldehyde-poly-L-lysine were injected into the rabbit. The antiserum has been used by Homberg et al. (1999) to label GABA-immunostained neurons of the locust central complex. Immunostaining in locust brain sections was abolished after preadsorption of the antiserum with GABA-glutaraldehyde complex (20 μM), but was only slightly reduced following preadsorption with 20 μM glutamate-glutaraldehyde complex (Homberg et al., 1999).

For immunogold labeling (postembedding staining), ultrathin sections from Durcupan-embedded brains were collected on coated nickel slot grids. Ultrathin sections were incubated for 1 hour on drops of a 25% aqueous solution of sodium metaperiodate. After thorough washing with distilled water, grids were incubated on phosphate-buffered saline (PBS; 0.01 M sodium phosphate buffer, 0.15 M NaCl, pH 7.4) containing 0.01% TrX for 15 minutes and subsequently for 30 minutes in incubation buffer (0.01 M sodium phosphate buffer, pH 7.4, containing 0.5 M NaCl, 0.75% fish gelatin, 0.1% ovalbumin, and 0.01% Tween 20). The sections were exposed to the anti-GABA antiserum at 1:1,500 in incubation buffer for 3 days at 4°C and were afterward washed thoroughly in PBS. Finally, the grids were transferred for 4 hours at room temperature to a solution of 10-nm gold-labeled goat anti-rabbit antibody (Auro Probe EM GAR G10; Amersham, Braunschweig, Germany) diluted 1:30 in incubation buffer. Preparations were then washed in PBS and distilled water and were contrasted with uranyl acetate (8 minutes) and lead citrate (2–3 minutes). In control experiments, substitution of the primary antibody solution with incubation buffer resulted in complete loss of immunolabeling. Preadsorption of the GABA antiserum with 20 μM GABA-glutaraldehyde conjugate, prepared as described by Ottersen et al. (1996), abolished immunostaining.

Statistical analysis of immunogold labeling

The mean labeling density of gold particles over selected profiles was determined in five or six consecutive ultrathin sections and compared against gold particle levels in other, presumably unlabeled profiles (Watson, 1988; Watson et al., 2000). Profiles were accepted as GABA immunolabeled if they had a significantly higher gold particle concentration than unmarked reference profiles (two-sided Student's t-test, $P < 0.05$). The statistical analysis was performed in SPSS 11.5 for Windows.

Image processing

Fluorescent preparations were viewed and imaged with a confocal laser scan microscope (Leica TCS SP2). Serial optical sections (usually at intervals of 0.2 μm) of labeled neurons were scanned at 1,024 × 1,024 pixel resolution by using a ×63 objective (HCX PL APO ×63/1.32 OIL PH 3CS; Leica, Bensheim, Germany) and saved as three-dimensional stacks. Contrast and brightness of selected images were optimized using Adobe Photoshop 7.0 software. Ultrathin sections were examined and photographed with a transmission electron microscope (EM10C; Zeiss, Oberkochen, Germany). Photomicrographs (Agfa Scientia EM film) from selected sections were scanned at 2,400 dpi (Scanjet 7400c; Hewlett Packard, Palo Alto, CA) and processed further in Adobe Photoshop 7.0 and Corel Draw 12. The reconstructed neurons (see Fig. 1B–E) were drawn from serial frontal sections by using a Zeiss microscope with camera lucida attachment. The photomicrographs for Figure 1F–J were made with a Zeiss Axioskop compound microscope equipped with a ProgRes C12plus digital camera (Jenoptic, Jena, Germany). Images were adjusted for brightness and contrast in Adobe Photoshop 7.0.

Three-dimensional reconstruction of a microglomerulus

For three-dimensional (3D) reconstruction of a microglomerulus, a series of 41 ultrathin sections (thickness 70 nm) through a small microglomerulus was used. The outlines of neuronal profiles and synaptic contacts were digitally stored in a digitizer tablet (Wacom, Krefeld, Germany). Further processing was performed in Amira 3.1 and 4.0 (Indeed-Visual Concepts, Berlin, Germany). The digital images were aligned with the "Align slices" tool. In each optical section, contours of pre- and postsynaptic profiles and of synapses were demarcated by hand (i.e., image segmentation). Pixels within contours enclosing the same profile in consecutive sections were given a randomly chosen color as described previously by Smid et al. (2003). This resulted in a 3D array of voxels that were labeled as "presynaptic," "postsynaptic," or "synapse." A 3D surface model of the microglomerulus was obtained by surface rendering. It showed surfaces of the microglomerulus viewed from any position, and individual profiles could be removed or made transparent to visualize underlying structures.

RESULTS

Light-microscopic analysis of the median olive and lateral triangle

The median olive and lateral triangle are conspicuous areas in the LAL of the locust brain. Both structures are

The Journal of Comparative Neurology. DOI 10.1002/cne

TABLE 1. Number of Innervated Glomeruli per Neuron Type[1]

Neuron type	n	No. of innervated glomeruli/ neuron (means ± SD)	
		LT	MO
TuLAL1a	9	8.7 ± 2.8	—
TuLAL1b	9	3.2 ± 1.6	4.7 ± 1.4
TL2	10	7.2 ± 1.8	—
TL3	9	1.7 ± 0.6	3.1 ± 1.3

[1]MO, median olive; LT, lateral triangle.

bordered by bundles of fibers of the isthmus tracts that connect the LAL to the central body and separate both areas from the surrounding neuropil. The lateral triangle is innervated by TuLAL1a neurons from the lower unit of the AOTu and by two types of tangential neuron (TL1, TL2) with projections to the lower division of the central body (Müller et al., 1997; Pfeiffer et al., 2005). TuLAL1a neurons have irregular varicose endings with fine filiform extensions in the lateral triangle (Fig. 1F). These large irregular terminals are more pronounced in some neurons than in others (Fig. 1D). TL2 neurons have densely clustered terminal processes in the lateral triangle (Fig. 1G), whereas TL1 neurons distribute their processes widely and uniformly throughout the lateral triangle (Müller et al., 1997). The median olive is innervated by TuLAL1b neurons with dendrites in the anterior lobe of the lobula and lower unit of the AOTu and by TL3 tangential neurons of the lower division of the central body (Müller et al., 1997; Pfeiffer et al., 2005). TuLAL1b neurons end in small numbers of large spheroidal terminals in the lateral triangle and median olive or in the median olive alone (Fig. 1H,I). TL3 tangential neurons have a few tightly clustered, bushy processes in the median olive and, more rarely, in the lateral triangle (Fig. 1J). The mean number of bushy or spheroidal terminals, calculated for each cell type, ranged from 1.7 ± 0.6 (mean ± SD) for TL3 neurons in the lateral triangle to 8.7 ± 2.8 (mean ± SD) for TuLAL1a neurons in the lateral triangle (Table 1).

Anterograde tracing of TuLAL1 neurons by dextran-biotin injection into the lower unit of the AOTu combined with GABA immunostaining of TL2/3 neurons showed that terminals from the AOTu neurons form large microglomerular contacts with processes from tangential neurons of the central body. These microglomeruli were observed in the median olive and in the lateral triangle. In both areas, projection neurons from the AOTu formed large cup-shaped shells that enclosed concentrations of GABA-ir profiles (Fig. 2). Axons from the AOTu commonly had several large cup-like endings that, judged by light microscopy, had a size of 10 μm or more. GABA immunostaining was concentrated in the core of the microglomeruli and had a dense and granular appearance. Confocal images showed that this microglomerular organization is prevalent throughout the median olive and in large parts of the lateral triangle (Fig. 2). In both areas, GABA immunostaining was arranged in small patches that were regularly separated from each other by unstained areas. These consisted of the cup-shaped terminals from TuLAL1 neurons (Fig. 2). In the median olive, microglomeruli usually had an ovoid shape (Fig. 2A), whereas, in the lateral triangle, they were more irregular, including fine extensions of the dextran-stained shells into the GABA-ir cores of the microglomeruli (Fig. 2D).

Electron microscopic analysis

For ultrastructural analysis of the median olive and lateral triangle, embedded brains were trimmed to the region of the LAL. Ultrathin sections containing the median olive and lateral triangle were inspected for synaptic contacts and microcircuits. In both areas, large cup-shaped profiles that enclosed many small profiles were the predominant structures (Figs. 3, 4). In certain planes of section, the large outer shell profiles formed a nearly closed ring around the central small profiles (Fig. 3A,B). These microglomeruli were uniformly distributed. They were arranged directly next to each other or were adjacent to other, e.g., axonal profiles. The lateral triangle consisted of 150–200 and the median olive of 40–50 microglomeruli. Microglomeruli in the median olive had diameters from 5.6 to 19.4 μm, with a mean diameter of 11.85 ± 3.66 μm (±SD, n = 31 from four animals); they were slightly but significantly larger (t-test, $P < 0.05$) than microglomeruli in the lateral triangle (ranging from 5.7 to 15.4 μm, mean diameter 9.48 ± 2.72, n = 21 from three animals). In some cases, single profiles forming the peripheral shell could be traced to participate in additional microglomeruli (Fig. 3C). The outer borders of the microglomeruli toward surrounding neuropil were lined with a thin glial sheath (Fig. 3C).

Ultrastructure of microglomeruli

Microglomerular complexes in the lateral triangle and median olive had a similar and characteristic ultrastructural appearance and composition of organelles (Figs. 3, 4). The outer cup-shaped profiles were densely packed with small clear vesicles and contained, in addition, larger round, dense-core vesicles of various sizes (Fig. 4). The numerous small profiles enclosed by the large cup-shaped terminal had diameters of 0.2–1.8 μm (Fig. 4A). These profiles were often filled with mitochondria and contained only small numbers of clear and dense-core vesicles. No synaptic contacts were found between the small profiles. Instead, multiple synapses made by the large shell profile onto the enclosed small profiles were a particularly prominent feature of the microglomeruli. In average-sized microglomeruli (Figs. 3A, 4A; diameter 10 μm), up to 30 synapses, arranged in a regular array along the membrane facing the neuropil of the microglomerulus, were present in a single section. These synapses occurred exclusively at the inner side of the large shell profiles onto the small profiles. Examination of serial sections showed that all synapses were dyadic, with one presynaptic element, the large profile, and two opposing postsynaptic elements, consisting of small profiles (Fig. 4B). The contacts showed all ultrastructural criteria of chemical synapses (Strausfeld, 1976; Watson and Schürmann, 2002): 1) a presynaptic bar, electron-dense specializations associated with the presynaptic membrane, 2) numerous clear vesicles accumulated around the presynaptic bar, 3) an expanded synaptic cleft filled with electron-dense material, and 4) additional electron-dense material on the cytosolic side of the membrane of the postsynaptic profile (Fig. 4B).

For a three-dimensional reconstruction, 41 consecutive sections through a small microglomerulus (diameter 4 μm) were imported into the software Amira and processed for a surface view (Fig. 5). The reconstructed large profile showed the characteristic cup-shaped form. The cavity

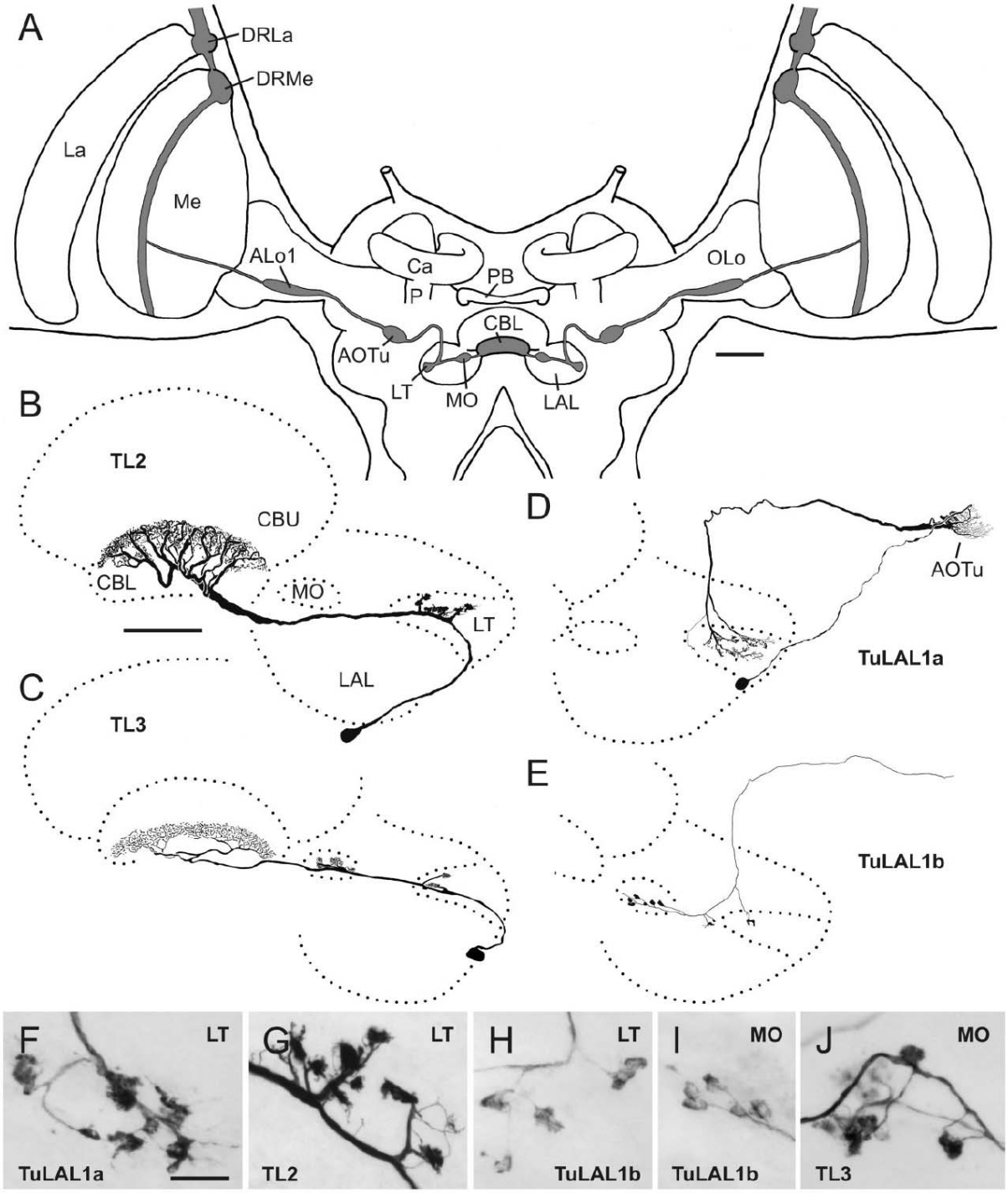

Fig. 1. **A:** Schematic diagram of the polarization vision pathway in the brain of the locust *Schistocerca gregaria*. Polarization-sensitive photoreceptors of the dorsal rim area of the compound eye project to dorsal rim areas in the lamina and medulla (DRLa, DRMe). First-order interneurons with dendritic ramifications in the DRMe and tangential arborizations in the medulla (Me) send axonal processes to the ventralmost layer of the anterior lobe of the lobula (ALo1) and to the lower unit of the anterior optic tubercle (AOTu). Second-order interneurons, termed *TuLAL1a* and *TuLAL1b*, connect the AOTu with the median olive (MO) and lateral triangle (LT) of the lateral accessory lobe (LAL). Third-order interneurons with ramifications in the LT (type TL2) or MO (type TL3) provide input to the lower division of the central body (CBL). Ca, P, calyx and pedunculus of the mushroom body; La, lamina; PB, protocerebral bridge. Modified from Homberg et al. (2003). **B–E:** Reconstructed morphologies of a TL2 neuron (B), a TL3 neuron (C), a TuLAL1a neuron (D), and the central projections of a TuLAL1b neuron (E). CBU, upper division of the central body. **F–J:** Terminals of these cell types in the LT (F–H) and in the MO (I,J). Single cell dye fills in B–J were generously provided by M. Kinoshita (D–F,H,I), H. Vitzthum (C,J), S. Gebhardt (B), and S. Gotthardt (G). Scale bars = 200 μm in A; 100 μm in B (applies to B–E); 25 μm in F (applies to F–J).

The Journal of Comparative Neurology. DOI 10.1002/cne

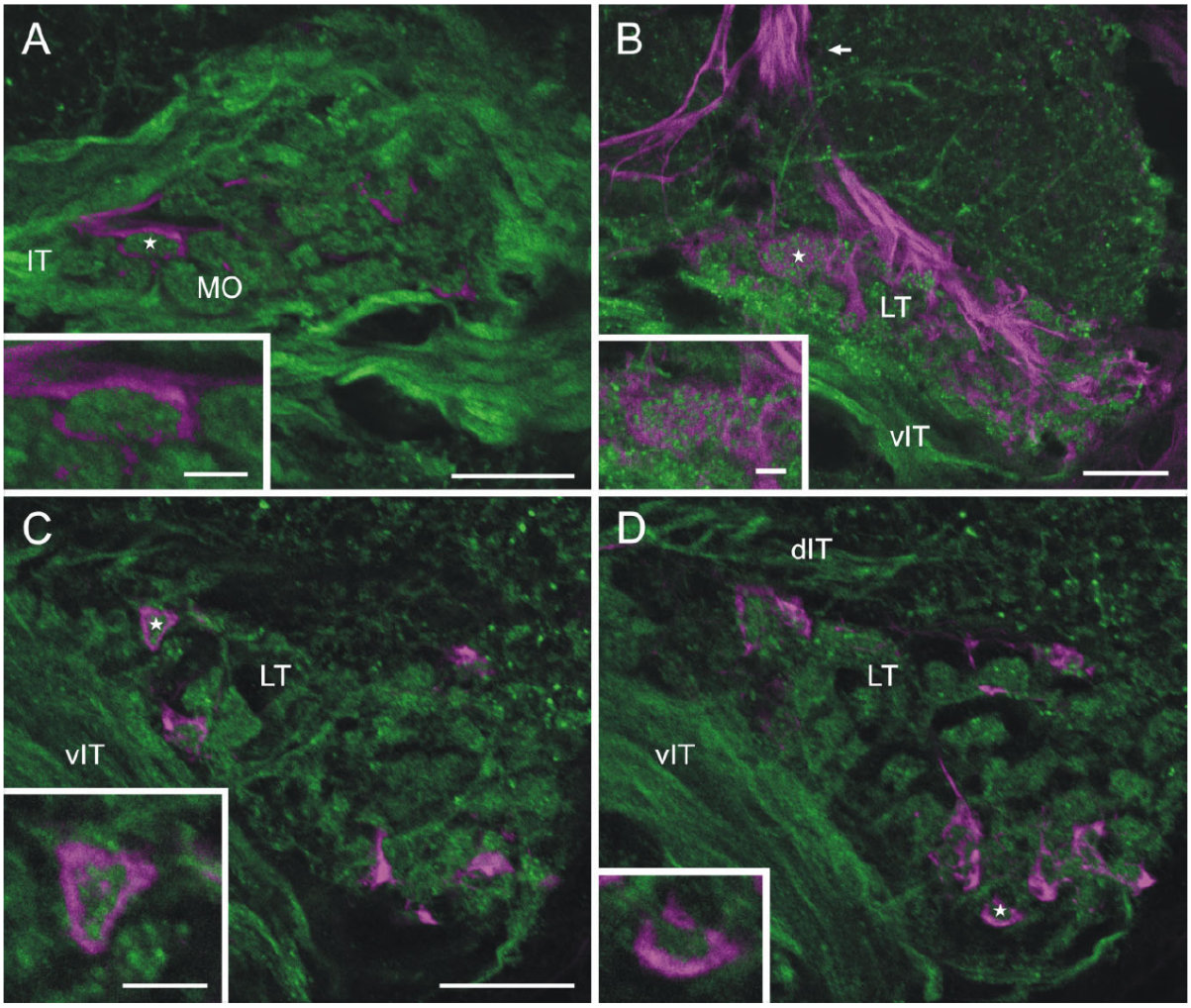

Fig. 2. Confocal laser images (single optical sections) obtained from vibratome sections through the median olive (MO, in A) and the lateral triangle (LT, in B–D) of the lateral accessory lobe. Dextran/Cy3-stained projections from the lower unit of the anterior optic tubercle are shown in magenta, and GABA immunostaining is shown in green. **Insets** show individual microglomeruli from the sections (asterisks). **A:** Terminals of TuLAL neurons from the anterior optic tubercle (magenta) encircle granular concentrations of GABA immunostaining in several microglomeruli. GABA-ir fibers of the isthmus tract (IT) encompass the MO. **B:** TuLAL neurons from the anterior optic tubercle (arrow, magenta) project to the LT and form outer shells of microglomeruli that are filled with granular GABA-ir terminals. **C,D:** Single optical sections through the LT from the same preparation, z-distance 1.4 μm. In contrast to microglomeruli in the MO, those in the LT (asterisks) have an irregular shape, and processes from the dextran-filled outer shell partially invade the GABA-ir core of the microglomeruli. Dorsal (dIT) and ventral (vIT) bundles of GABA-ir fibers of the isthmus tract demarcate the boundaries of the LT. Scale bars = 20 μm in A,B; 20 μm in C (applies to C,D); 5 μm in insets.

was filled by numerous small profiles. These neurons extended fine processes into the cup and had synaptic contacts only with the inner side of the large cup-shaped terminal. Therefore, the microglomerulus is a spatially circumscribed structure with an expanded contact surface between the large profile of one neuron and the small profiles of the enclosed postsynaptic neurons. More than 150 synapses were counted for the large profile (Fig. 5B). Tracing through consecutive sections revealed that the synaptic contacts had elongated shapes with a length of 140–490 nm and a width of about 100 nm. No synaptic contacts were found among large profiles or between the small profiles. Reconstruction of individual small processes within the microglomerulus was not possible, but inspection of selected sections from a different glomerulus shows that small profiles arborize within the glomerulus and have multiple synaptic contacts with the large cup profiles (Fig. 6B,C).

GABA immunostaining

At the light microscopic level, core terminals of microglomeruli and axonal fibers in the isthmus tract showed

The Journal of Comparative Neurology. DOI 10.1002/cne

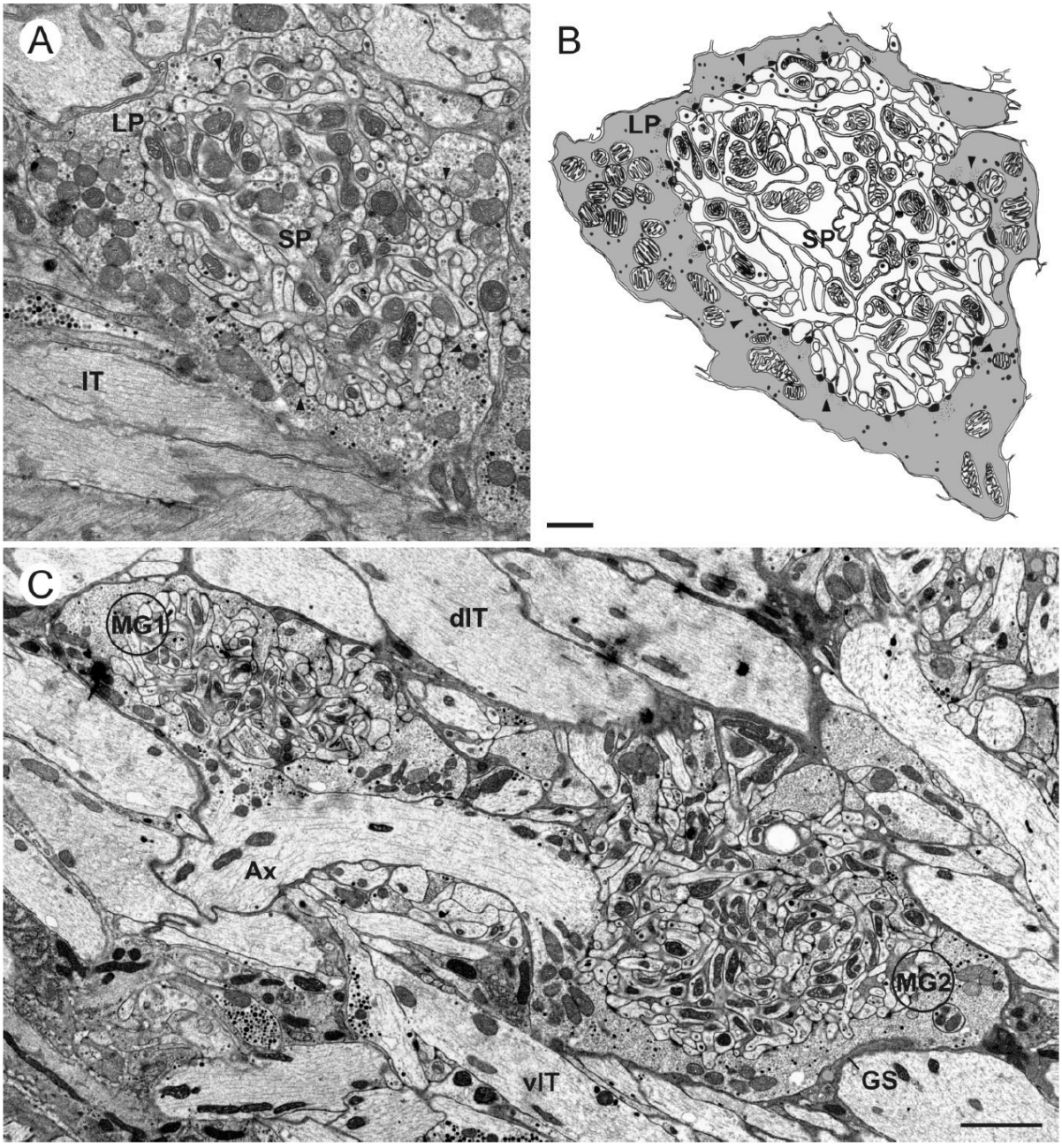

Fig. 3. Electron micrographs showing microglomeruli in the median olive (A,B) and in the lateral triangle (C) of the lateral accessory lobe. **A:** Microglomerulus consisting of a large profile (LP) that almost completely encloses numerous small profiles (SP). Numerous synaptic contacts exist between the large outer profile and the small core profiles (arrowheads). IT, isthmus tract. **B:** Drawing of the microglomerulus in A showing outlines of profiles and synaptic contacts (arrowheads). The large profile is shown in light gray. **C:** Two microglomeruli (MG1 and MG2) from the median tip of the lateral triangle. Both microglomeruli are directly bordered by axonal profiles of the dorsal (dIT) and ventral (vIT) bundle of the isthmus tract. The large outer shell profiles of MG1 and MG2 originate from the same axon (Ax). GS, glial sheath. Scale bars = 1 μm in B (applies to A,B); 3 μm in C.

GABA immunostaining (Fig. 2). At the ultrastructural level, many fibers of the isthmus tract were GABA-ir (Fig. 6), but assessment of GABA labeling in the large vs. small profiles was not always obvious, probably because of the large differences in profile size. Therefore, the concentrations of gold particles were compared with statistical tests.

The Journal of Comparative Neurology. DOI 10.1002/cne

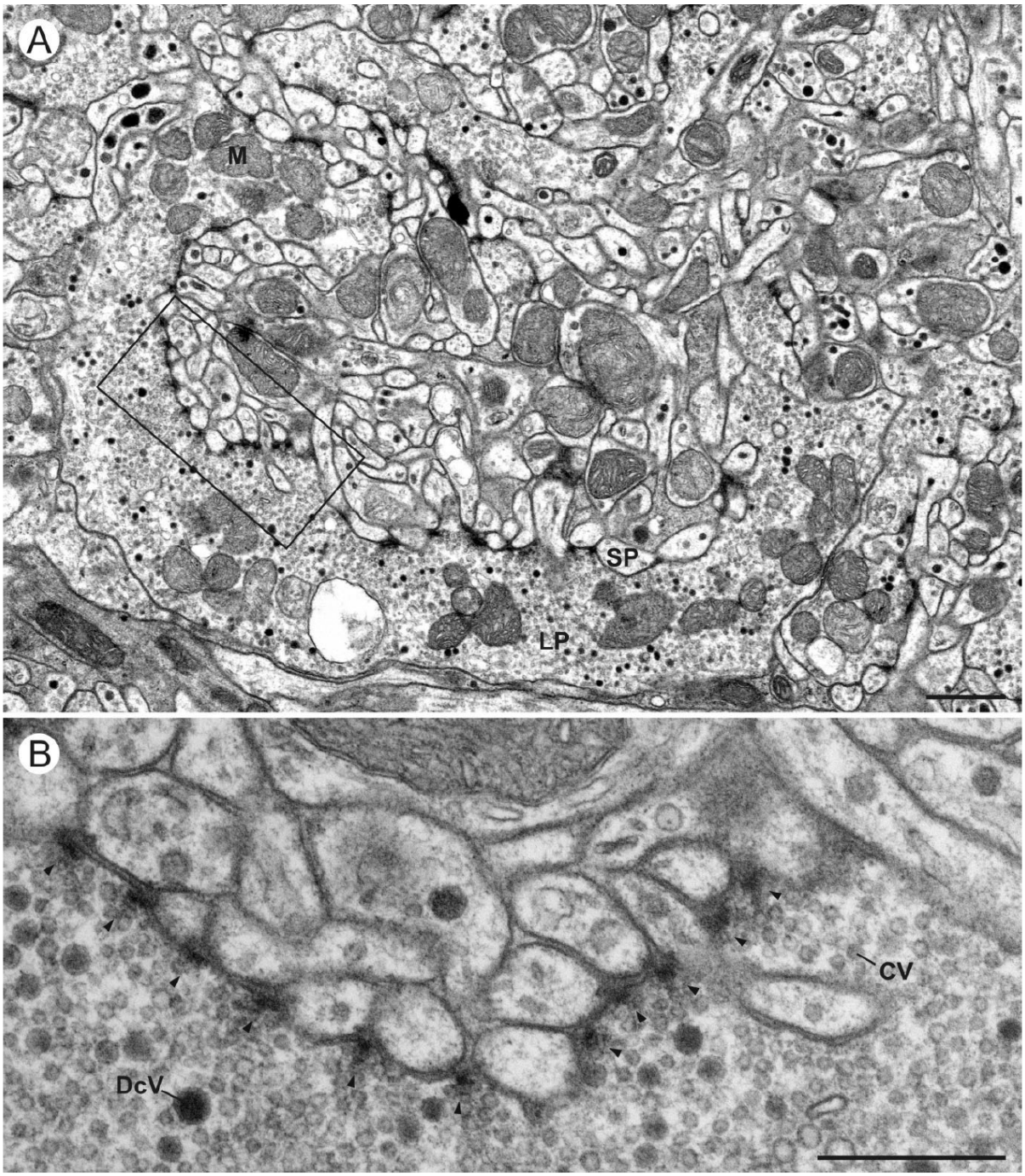

Fig. 4. Electron micrographs from a frontal section through the central region of the lateral triangle. **A:** Microglomerulus comprising a large peripheral profile (LP) that is presynaptic to numerous enclosed small profiles (SP). Along the inside membrane of the cup-shaped profile, 28 dyadic synapses onto small core profiles are present. M, mitochondrion. **B:** High-magnification view of the boxed area in A. Note chain-like alignment of dyadic synapses (arrowheads). The large profile contains numerous clear vesicles (CV) and scattered dense core vesicles (DcV) of different sizes. Scale bars = 1 μm in A; 0.5 μm in B.

The Journal of Comparative Neurology. DOI 10.1002/cne

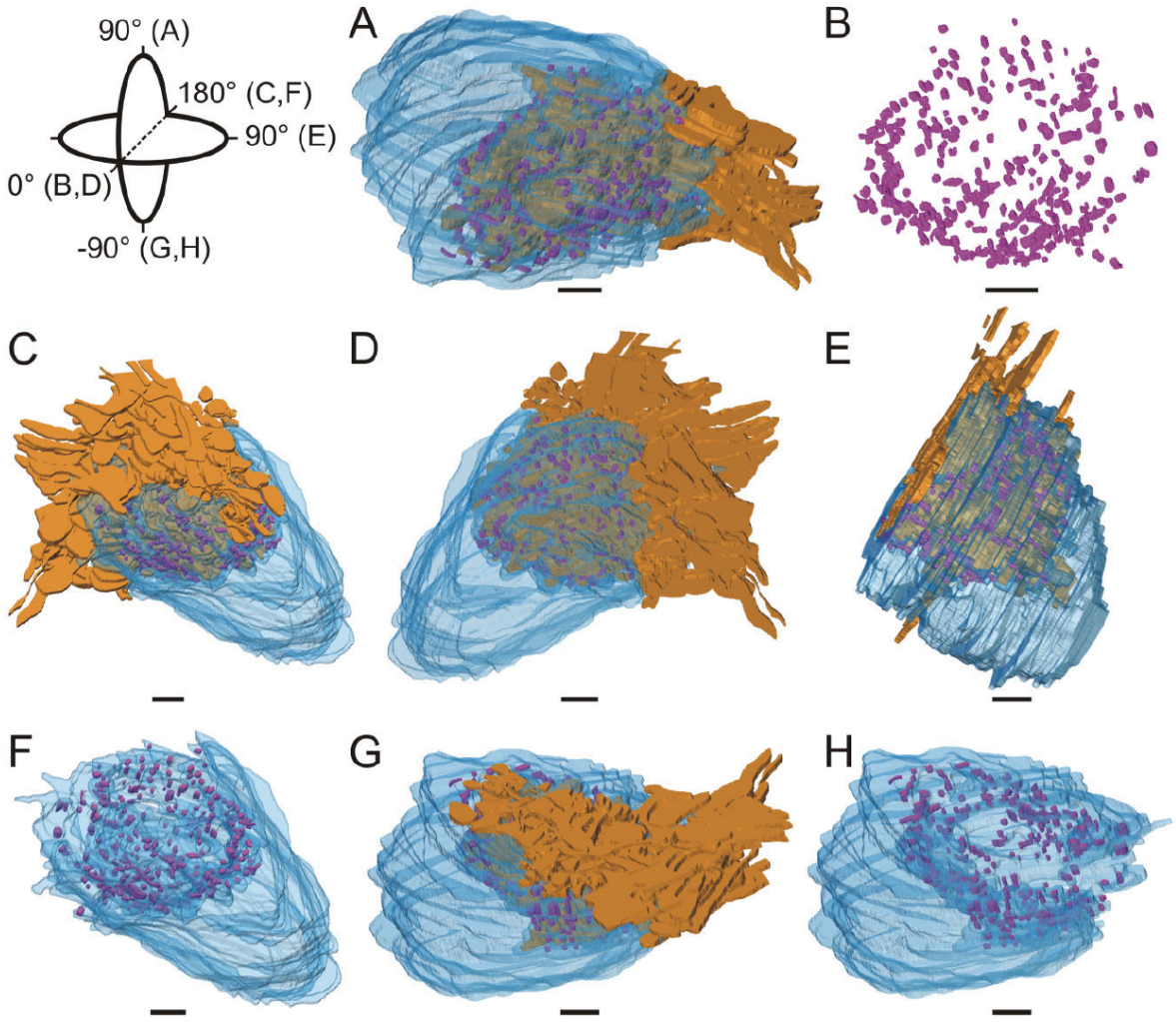

Fig. 5. **A–H:** Surface views from different directions of the three-dimensional reconstruction of a small microglomerulus of the lateral triangle. The presynaptic element (transparent blue) encloses numerous small postsynaptic profiles (orange). It forms a cup-like structure with 153 synapses (purple) distributed over its inner face. Orientations of the different views relative to B and D (0°) are indicated in the left upper corner. A: Rotation by 90° upward; C,F: 180°; E: 90° to the right; G,H: 90° downward. Scale bars = 500 nm.

Profiles were classified as GABA-ir if they displayed levels of immunogold labeling in several (five or six) consecutive ultrathin sections that were significantly higher than background levels (determined as level of immunogold labeling in an obviously unlabeled large axonal fiber in the vicinity of the lateral triangle). Sixteen profiles (four large outer profiles and 12 small core profiles) from two microglomeruli were analyzed (Fig. 6). Gold particle levels in the four large profiles (3.4 ± 1.6 particles/μm^2; mean ± SD) were not significantly different from background level (2.7 ± 0.8 particles/μm^2). Among the small profiles, nine profiles had levels of labeling ranging from 23.3 ± 8.8 particles/μm^2 to 31.8 ± 7.7 particles/μm^2. Their gold particle levels were significantly higher than control levels and the levels of the large cup profiles (two-sided Student's *t*-test, $P \leq 0.01$). Four of these small profiles had direct synaptic contacts with the large profiles. To determine whether some small profiles were not GABA-ir, three additional small profiles were selected for their apparently low gold particle densities. Gold particle levels in these profiles ranged from 9.9 ± 7.8 particles/μm^2 (SP5 in Fig. 6) to 12.5 ± 11.7 particles/μm^2 and were not significantly different from background levels (*t*-test). One of these profiles had direct synaptic contacts with a large profile. The direct neighborhood of nonmarked and marked profiles, such as GABA-positive small and GABA-negative large profiles (Fig. 6) as well as GABA-positive fibers of the isthmus tract and GABA-negative large profiles, confirms the specificity of the immunogold labeling. The gold particles did not bind preferentially on vesicles or synapses but were distributed uniformly over the profiles. Some affinity of the gold particles for mitochondria was noticed.

The Journal of Comparative Neurology. DOI 10.1002/cne

DISCUSSION

Structure and components of microglomeruli in the lateral triangle and median olive

We have characterized a novel type of microglomerular synaptic complex in the brain of an insect, the locust *Schistocerca gregaria*. These microglomeruli were found in the median olive and in the lateral triangle of the LAL, two synaptic areas of the polarization vision pathway of the locust brain. Each microglomerulus consists of a single large cup-like presynaptic terminal that forms numerous dyadic synapses with small enclosed profiles. The large presynaptic terminals are formed by TuLAL1a and TuLAL1b projection neurons from the lower division of the AOTu (Homberg et al., 2003; Pfeiffer et al., 2005), and the small postsynaptic profiles in the center of the microglomeruli originate from TL2 and TL3 tangential neurons of the lower division of the central body (Müller et al., 1997; Vitzthum et al., 2002). In the median olive and lateral triangle, TL2 and TL3 neurons have characteristic knob-like dendritic endings, which at high magnification consist of dense tangles of very fine processes. Each tangential neuron gives rise to several of these bushes of thin processes, which correspond to the microglomerular domains of the small processes at the electron microscopic level.

Homberg et al. (1999) estimated the total number of GABA-ir tangential neurons of the central body at about 100. These comprise TL2 and TL3 tangential neurons of the lower division and two or three TU1 and about 10 TU2 tangential neurons of the upper division of the central body, as judged from counts of their main axonal fibers in the central body (Homberg et al., 1999). The large majority of these neurons, probably about 90, are, therefore, TL2 and TL3 neurons. Given the mean numbers of microglomeruli invaded by these neurons (Table 1) and the total numbers of microglomeruli in the lateral triangle (150–200) and median olive (40–50), it follows that on average each microglomerulus is invaded by only two or three TL neurons (lateral triangle 2.1–2.8 neurons, median olive 2.5–3.1 neurons per microglomerulus). In each microglomerulus, the dense dendritic bushes of these neurons are likely to intermingle and receive common multiple synaptic input from the shell profile of a TuLAL neuron. If the assumptions made above are correct, the connections between TuLAL neurons and TL neurons within a microglomerulus would be divergent, but, because each TL neuron invades several microglomeruli, it might also receive convergent input from more than one TuLAL neuron.

Although most of the small microglomerular core profiles were GABA-ir, several small profiles showed low gold particle concentrations that were statistically not different from background levels. These profiles are, therefore, likely to originate from GABA-negative cell types different from TL2 or TL3. In addition to the cell types studied here, at least five other types of neuron ramify in the median olive or lateral triangle. These are GABA-negative TL1 neurons with fine dendritic ramifications in the lateral triangle (Müller et al., 1997), serotonin-ir neurons with ramifications in the median olive (Homberg, 1991), and three types of columnar neuron of the central complex that invade the median olive (type CP1; Vitzthum et al., 2002) or lateral triangle (types CL1 and CP2; Müller et al., 1997; Vitzthum et al., 2002). Whether these neurons participate in the microglomeruli is presently unclear. At least the terminals of the columnar neurons are bleb-like, suggesting that they are presynaptic (Müller et al., 1997; Vitzthum et al., 2002) and, therefore, probably do not take part in the microglomerular circuits described here.

Comparison with other species

Several observations suggest that the microglomerular complexes reported for the locust are also present in the LAL of other insects. Homologues of the locust TL neurons have been identified in the cricket *Gryllus bimaculatus* (Sakura and Labhart, 2005) and in the fruit fly *Drosophila melanogaster* (R-neurons; Hanesch et al., 1989). In both species, these neurons have, as in the locust, small, exceptionally compact bushes of thin fibers in areas lateral to the central body. In *D. melanogaster*, each R-neuron gives rise to only a single bush of fine fibers, and, as in the locust, these neurons are GABA-ir (Hanesch et al., 1989). In the fly and the cricket, the presynaptic elements providing input to the bushy terminals have not been identified, but neurons from the AOTu projecting to a small region of the LAL have been revealed in the sphinx moth *Manduca sexta* through immunolabeling for FMRFamide (Homberg et al., 1990). The projections completely overlap with a subfield of terminals of GABA-ir tangential neurons of the lower division of the central body. The contact zone in the LAL is characterized by large bulging terminals that might well correspond to the microglomerular organization in the locust. Finally, Kreissl and Bicker (1989) reported a cluster of somata stained for acetylcholinesterase in the brain of the honeybee ventrally to the central body, a position that is usually free of neuronal somata. Judged from their position, these large round condensations of staining might be synaptic contacts homologous to the microglomeruli reported here.

Microglomerular structures have been reported from other areas of the insect brain and have been analyzed particularly well in the calyces of the mushroom body (Trujillo-Cenóz and Melamed, 1962; Schürmann, 1974; ant: Steiger, 1967; Lamparter et al., 1969; cricket: Frambach et al., 2004; honeybee: Ganeshina and Menzel, 2001; fruit fly: Yasuyama et al., 2002). Calycal microglomeruli are much smaller than the ones reported here; they are about 2–7 μm in the calyx of *D. melanogaster* (Yasuyama et al., 2002), 2–3 μm in *Apis mellifera* (Ganeshina and Menzel, 2001), 2–8 μm in *Gryllus bimaculatus* (Frambach et al., 2004), and 2–3 μm in *Formica rufa* (Steiger, 1967). They consist of a large central bouton, the presynaptic element, encircled by postsynaptic profiles of putative Kenyon cell dendrites (Yasuyama et al., 2002). Although the LAL microglomeruli of the locust are larger than calycal microglomeruli, both synaptic complexes share a single large presynaptic profile that makes synaptic contacts with many small postsynaptic elements.

Microglomerular structures are not unique to the insect nervous system. In vertebrates, especially the calyx of Held (Held, 1893; Sätzler et al., 2002; Schneggenburger and Forsythe, 2006) and the endbulb of Held (Ryugo et al., 1996; Schneggenburger and Forsythe, 2006) share particular features with the microglomeruli described here. The calyx and endbulb of Held are giant synapses in the mammalian auditory pathway. They are composed of a large cup- or claw-like presynaptic element that makes multiple synaptic contacts with the cell body of a principal neuron of the medial nucleus of the trapezoid body (MNTB; calyx

The Journal of Comparative Neurology. DOI 10.1002/cne

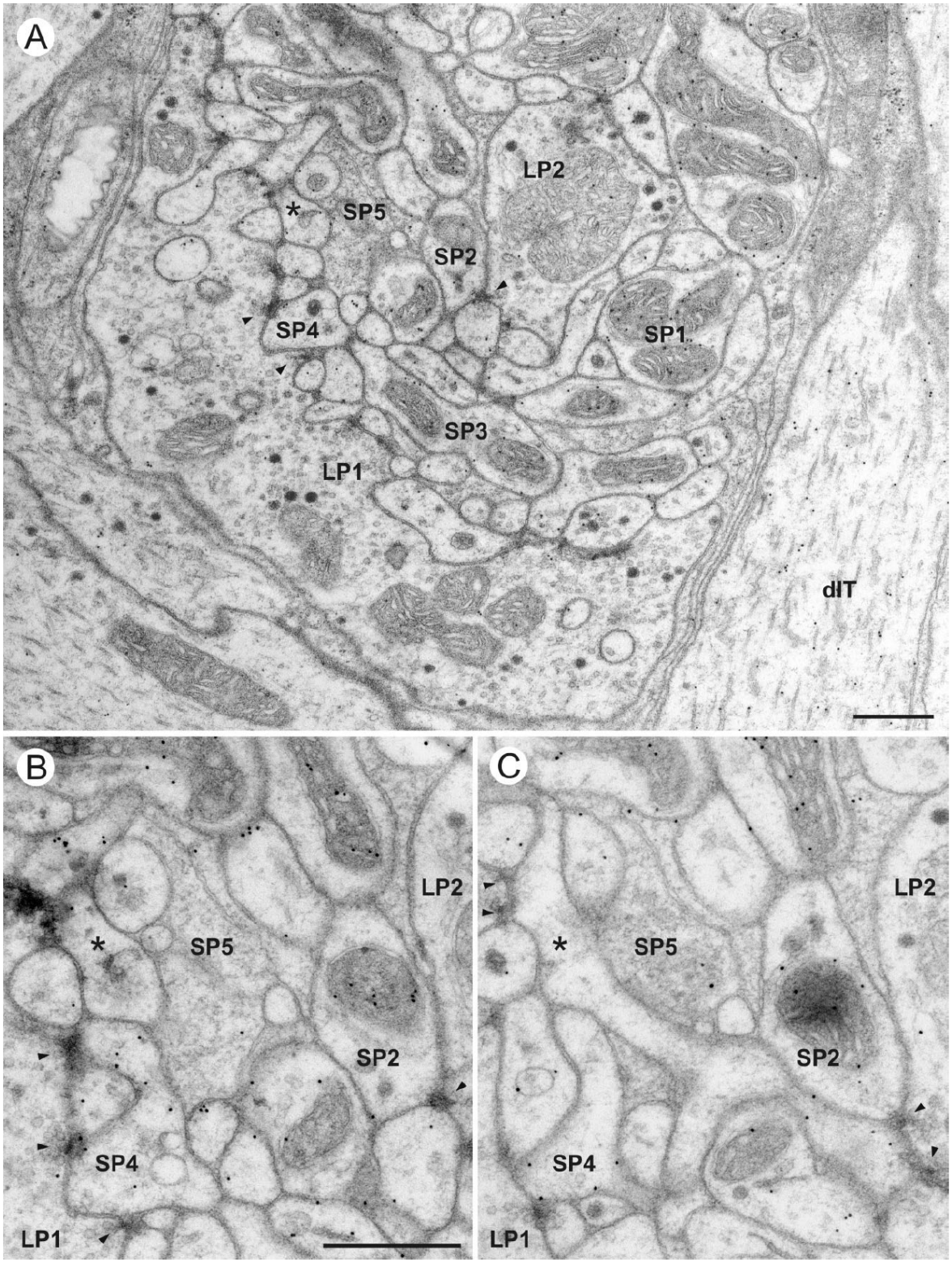

Figure 6

The Journal of Comparative Neurology. DOI 10.1002/cne

of Held) and with a bushy cell of the anterior ventral cochlear nucleus (aVCN; endbulb of Held; Sätzler et al., 2002; Schneggenburger and Forsythe, 2006). The presynaptic profile, called the *calyx*, is a complex nerve terminal forming a cup with fingerlike stalks that envelopes approximately one-half of a single cell body. In total, 550 synaptic release sites have been counted in a 3D reconstruction of an entire calyx of Held (Sätzler et al., 2002). Although the connectivity in the calyx of Held is 1:1, a slightly divergent connection (1:2 to 1:3) is more likely in the locust microglomerular complex. The calyx reconstructed by Sätzler et al. (2002) has a spatial expanse of about 18 × 22 μm and is, thus, slightly larger than the largest locust microglomeruli.

Functional implications

The microglomerular contacts in the LAL are part of the polarization vision system of the locust. Polarized light is detected by photoreceptor cells in the dorsal rim area of the compound eye. Signals are transmitted by neurons of the AOTu (TuLAL neurons) to tangential neurons (TL neurons) of the central body. The large presynaptic element of each microglomerulus has more than 100 synaptic release sites onto the enclosed dendritic bushes of probably two or three TL neurons. In addition, the presynaptic terminal provides a shield, i.e., a diffusion barrier, because the synapses are located exclusively at the inner side of the cup. The shielding effect might be enhanced by the glial sheath around the outer side of the large profile. Taken together, these features are likely to provide for particularly strong and fast synaptic transmission at this stage of the polarization vision pathway.

Physiological characterizations of the calyx of Held showed that a single action potential in the presynaptic cell rapidly leads to depolarization of the postsynaptic MNTB neuron to threshold through the release of hundreds of quanta that trigger a large excitatory postsynaptic current (Schneggenburger and Forsythe, 2006). The same functional principle may also hold for the LAL microglomeruli. The presynaptic action potential of a single TuLAL neuron may suffice to depolarize the postsynaptic TL neuron to near threshold, because the TL neuron receives input through only a small number of microglomerular connections (Table 1). The exclusively dyadic synapses may further strengthen the signal, because a single presynaptic contact simultaneously contacts two postsynaptic profiles. Thus, the large size of the presynaptic terminals together with the large number of active zones in the locust LAL, as in the MNTB of the cat (Schneggenburger and Forsythe, 2006), is likely to provide for strong and rapid signaling and preserves the timing information of the sensory signal.

In vertebrates, the evolution of endbulb terminals such as the calyx of Held has been regarded as an adaptation to high temporal accuracy of transmission, in particular to preserve phase information of the auditory signal, which allows right-left computation of spike timing for sound localization (Carr and Soares, 2002). Likewise, the LAL microglomeruli may ensure synaptic transmission with a high safety factor. Similar to the position of the calyx of Held at the input stage to binaural coding in the auditory system, the LAL microglomeruli occur at the transition from monocular neurons in the AOTu (Pfeiffer et al., 2005) to binocular columnar neurons in the central complex (S. Heinze and U. Homberg, unpublished). TL2 and TL3 neurons can be regarded as input elements to the network of polarization-sensitive neurons of the central complex. Heinze and Homberg (2007) showed that a compass-like linear map of *E*-vector tunings covering 2 × 180° underlies the 16-fold columnar organization of the central complex, but how this map arises is still unclear. It is tempting to speculate that small phase differences in *E*-vector signaling by TL neurons from the right and left LAL contribute to create this map or are used to monitor right-left turns of the animal for a path integration mechanism. Maintenance of precise phase information by narrow *E*-vector tuning characteristics (Vitzthum et al., 2002; Sakura and Labhart, 2005) could be provided by the microglomerular synaptic contacts in the LAL and may be an important prerequisite to translate minute differences in binocular inputs into a spatial signal for compass orientation and navigation.

Fig. 6. GABA immunolabeling of a microglomerulus of the lateral triangle. Postembedding immunogold technique. Mean densities of immunogold labeling were analyzed in seven profiles over five consecutive sections (section 2 in **A**, enlarged areas of section 3 in **B**, and section 5 in **C**), including two large presynaptic profiles (LP1, LP2) and five small profiles. Two small profiles (SP2 and SP4) have direct synaptic contact (arrowheads in A) with LP1 or LP2, and three others have no direct contacts (SP1, SP3, and SP5). Densities of gold particles (means ± standard deviation) are 3.3 ± 0.3 particles/μm² in LP1 and 2.9 ± 1.5 particles/μm² in LP2, which does not differ significantly from background levels (2.7 ± 0.8 particles/μm²). Four of the small profiles (SP1–4) have gold particle levels that are about seven times the level in the large profiles (SP1 31.8 ± 7.7, SP2 25.3 ± 7.5, SP3 24.4 ± 8.5, SP4 21.2 ± 8.9 particles/μm²). The small profile SP5 differs from the other small profiles by having a slightly higher electron density. Its gold particle level (9.9 ± 7.8 particles/μm²) is smaller than the levels of the other small profiles and is not significantly different from background levels. The adjacent fiber of the dorsal bundle of the isthmus tract (dIT) has a gold particle level (13.3 ± 3.4 particles/μm²) that is significantly higher than background levels. Asterisks in A–C indicate a small profile with bifurcations and at least four synaptic contacts with large profiles (arrowheads in C). Scale bars = 0.5 μm in A; 0.5 μm in B (applies to B,C).

ACKNOWLEDGMENTS

We thank Drs. T.G. Kingan and H. Dircksen for the donation of GABA antisera. We are grateful to Sascha Gotthardt, Stefan Gebhardt, and Drs. Michiyo Kinoshita and Harm Vitzthum for access to their Neurobiotin-stained preparations and their generous permission to use these preparations for Figure 1B–J; to Sandra Söhler for help with the pressure injection equipment; to Bianca Backasch for advice on statistics; and to Stanley Heinze and Angela Kurylas for assistance with confocal microscopy and introduction to Amira. We are particularly grateful to Geza Thiess for technical assistance with the ultrastructural studies.

LITERATURE CITED

Boer HH, Schot LPC, Roubos EW, ter Maat A, Lodder JC, Reichelt D, Swaab DF. 1979. ACTH-like immunoreactivity in two electronically coupled giant neurons in the pond snail *Lymnea stagnalis*. Cell Tissue Res 202:231–240.

Carr CE, Soares D. 2002. Evolutionary convergence and shared computational principles in the auditory system. Brain Behav Evol 59:294–311.

Clements AN, May TE. 1974. Studies on locust neuromuscular physiology in relation to glutamic acid. J Exp Biol 60:673–705.

Frambach I, Rössler W, Winkler M, Schürmann F. 2004. F-actin at identified synapses in the mushroom body neuropil of the insect brain. J Comp Neurol 475:303–314.

Ganeshina O, Menzel R. 2001. GABA-immunoreactive neurons in the mushroom bodies of the honeybee: an electron microscopic study. J Comp Neurol 437:335–349.

Hanesch U, Fischbach KF, Heisenberg M. 1989. Neural architecture of the central complex in *Drosophila melanogaster*. Cell Tissue Res 457:343–366.

Heinze S, Homberg U. 2007. Maplike representation of celestial *E*-vector orientations in the brain of an insect. Science 315:995–997.

Held H. 1893. Die zentrale Gehörleitung. Arch Anat Physiol Anat Abt 17:201–248.

Homberg U. 1991. Neuroarchitecture of the central complex in the brain of the locust *Schistocerca gregaria* and *S. americana* as revealed by serotonin immunocytochemistry. J Comp Neurol 303:245–254.

Homberg U. 2004. In search of the sky compass in the insect brain. Naturwissenschaften 91:199–208.

Homberg U, Paech A. 2002. Ultrastructure and orientation of ommatidia in the dorsal rim area of the locust compound eye. Arthropod Struct Dev 30:271–280.

Homberg U, Kingan TG, Hildebrand JG. 1990. Distribution of FMRFamide-like immunoreactivity in the brain and suboesophageal ganglion of the sphinx moth *Manduca sexta* and colocalization with SCP_B-, BPP-, and GABA-like immunoreactivity. Cell Tissue Res 259: 401–419.

Homberg U, Vitzthum H, Müller M, Binkle U. 1999. Immunocytochemistry of GABA in the central complex of the locust *Schistocerca gregaria*: identification of immunoreactive neurons and colocalization with neuropeptides. J Comp Neurol 409:495–507.

Homberg U, Hofer S, Pfeiffer K, Gebhardt S. 2003. Organization and neural connections of the anterior optic tubercle in the brain of the locust, *Schistocerca gregaria*. J Comp Neurol 462:415–430.

Hoskins SG, Homberg U, Kingan TG, Christensen TA, Hildebrand JG. 1986. Immunocytochemistry of GABA in the antennal lobes of the sphinx moth *Manduca sexta*. Cell Tissue Res 244:243–252.

Kreissl S, Bicker G. 1989. Histochemistry of acetylcholinesterase and immunocytochemistry of an acetylcholine receptor-like antigen in the brain of the honeybee. J Comp Neurol 286:71–84.

Labhart T, Meyer EP. 1999. Detectors for polarized skylight in insects: a survey of ommatidial specializations in the dorsal rim area of the compound eye. Microsc Res Techniq 47:368–379.

Labhart T, Meyer EP. 2002. Neural mechanisms in insect navigation: polarization compass and odometer. Curr Opin Neurobiol 12:707–714.

Lamparter HE, Steiger U, Sandri C, Akert K. 1969. Zum Feinbau der Synapsen im Zentralnervensystem der Insekten. Z Zellforsch 99:435–442.

Liu G, Seiler H, Wen A, Zars T, Ito K, Wolf R, Heisenberg M, Liu L. 2006. Distinct memory traces for two visual features in the *Drosophila* brain. Nature 439:551–556.

Menzel R, De Marco RJ, Greggers U. 2006. Spatial memory, navigation and dance behaviour in *Apis mellifera*. J Comp Physiol A192:889–903.

Müller M, Homberg U, Kühn A. 1997. Neuroarchitecture of the lower division of the central body in the brain of the locust *Schistocerca gregaria*. Cell Tissue Res 288:159–176.

Osborne MP. 1980. Electron microscopic methods for nervous tissues. In: Strausfeld NJ, Miller TA, editors. Neuroanatomical techniques—insect nervous system. Berlin: Springer, p 205–239.

Ottersen OP, Laake JH, Reichelt W, Haug FM, Torp R. 1996. Ischemic disruption of glutamate homeostasis in brain: quantitative immunocytochemical analyses. J Chem Neuroanat 12:1–14.

Pfeiffer K, Kinoshita M, Homberg U. 2005. Polarization-sensitive and light-sensitive neurons in two parallel pathways passing through the anterior optic tubercle in the locust brain. J Neurophysiol 94:3903–3915.

Ryugo DK, Wu MM, Pongstaporn T. 1996. Activity-related features of synapse morphology: a study of endbulbs of Held. J Comp Neurol 365:141–158.

Sakura M, Labhart T. 2005. Polarization-sensitive neurons in the central complex of the cricket, *Gryllus bimaculatus*. In: Krieglstein K, Zimmermann H, editors. Neuroforum 2005 Suppl. Heidelberg: Spektrum, p 154B.

Sätzler K, Söhl LF, Bollmann JH, Borst JGG, Frotscher M, Sakmann B, Lübke JHR. 2002. Three-dimensional reconstruction of a calyx of Held and its postsynaptic principal neuron in the medial nucleus of the trapezoid body. J Neurosci 22:10567–10579.

Schneggenburger R, Forsythe ID. 2006. The calyx of Held. Cell Tissue Res 326:311–337.

Schürmann FW. 1974. Bemerkungen zur Funktion der Corpora pedunculata im Gehirn der Insekten aus morphologischer Sicht. Exp Brain Res 19:406–432.

Seguela P, Geffard M, Buijs RM, Le Moal M. 1984. Antibodies against γ-aminobutyric acid: specificity studies and immunocytochemical results. Proc Natl Acad Sci U S A 81:3888–3892.

Smid HM, Bleeker MA, van Loon JJ, Vet LE. 2003. Three-dimensional organization of the glomeruli in the antennal lobe of the parasitoid wasps *Cotesia glomerata* and *C. rubecula*. Cell Tissue Res 312:237–248.

Steiger U. 1967. Über den Feinbau des Neuropils im Corpus pedunculatum der Waldameise—Elektronenoptische Untersuchungen. Z Zellforsch 81:511–536.

Strausfeld NJ. 1976. Atlas of an insect brain. Berlin: Springer.

Strauss R. 2002. The central complex and the genetic dissection of locomotor behaviour. Curr Opin Neurobiol 12:633–638.

Trujillo-Cenóz O, Melamed J. 1962. Electron microscope observation on the calyces of the insect brain. J Ultrastruct Res 7:389–398.

Venable JH, Coggeshall R. 1965. A simplified lead citrate stain for use in electron microscopy. J Cell Biol 25:407–408.

Vitzthum H, Müller M, Homberg U. 2002. Neurons of the central complex of the locust *Schistocerca gregaria* are sensitive to polarized light. J Neurosci 22:1114–1125.

Watson AHD. 1988. Antibodies against GABA and glutamate label neurons with morphologically distinct synaptic vesicles in the locust central nervous system. J Neurosci 26:33–44.

Watson AHD, Schürmann F-W. 2002. Synaptic structure, distribution, and circuitry in the central nervous system of the locust and related insects. Microsc Res Techniq 56:210–226.

Watson AHD, Bévengut M, Pearlstein E, Cattaert D. 2000. GABA and glutamate-like immunoreactivity at synapses on depressor motorneurones of the leg of the crayfish, *Procambarus clarkii*. J Comp Neurol 422:510–520.

Wehner R. 2003. Desert ant navigation: how miniature brains solve complex tasks. J Comp Physiol A189:579–588.

Yasuyama K, Meinertzhagen IA, Schürmann F-W. 2002. Synaptic organisation of the mushroom body calyx in *Drosophila melanogaster*. J Comp Neurol 445:211–226.

Polarization Sensitive Descending Neurons in the Locust: Connecting the Brain to Thoracic Ganglia

Behavioral/Systems/Cognitive

Polarization-sensitive descending neurons in the locust: connecting the brain to thoracic ganglia.

Ulrike Träger and Uwe Homberg*

Fachbereich Biologie, Tierphysiologie, Philipps-Universität Marburg, D-35032 Marburg, Germany

Many animal species, in particular insects, exploit the *E*-vector pattern of the blue sky for sun compass navigation. Like other insects, locusts detect dorsal polarized light via photoreceptors in a specialized dorsal rim area of the compound eye. Polarized light information is transmitted through several processing stages to the central complex, a brain area showing a compass-like topographic representation of celestial *E*-vectors. To investigate how polarized light information is transmitted to thoracic motor circuits, we studied the responses of locust descending neurons to polarized light. Three sets of polarization-sensitive descending neurons were characterized through intracellular recordings from axonal fibers in the neck connectives combined with single cell dye injections. Two descending neurons from the brain, one with ipsilaterally and the second, with contralaterally descending axon are likely to bridge the gap between polarization-sensitive neurons in the brain and thoracic motor centers. In both neurons, *E*-vector tuning changed linearly with daytime suggesting that they signal time-compensated spatial directions, an important prerequisite for navigation using celestial signals. The third type connects the suboesophageal ganglion (SOG) with the prothoracic ganglion. It showed no evidence for time-compensation in *E*-vector tuning, and might play a role in flight stabilization and control of head movements.

Introduction

Many insects, crustaceans, arachnids, and representatives of several vertebrate taxa are able to detect the polarization pattern of the blue sky and use it, in addition to direct sunlight, for navigational tasks (Horváth and Varjú, 2004; Wehner and Labhart, 2006). At the neuronal level, polarization vision pathways in the brain have been studied most extensively in locusts and crickets (Labhart and Meyer, 2002; Homberg, 2004). In these insects, the central complex is a major processing stage for polarized light (Vitzthum et al., 2002; Heinze and Homberg, 2007, 2009; Sakura et al., 2008; Heinze et al., 2009). Heinze and Homberg (2009) showed that polarization-sensitive (POL-) neurons connect the central complex to the lateral accessory lobes and the posterior protocerebrum, brain areas that are innervated by intersegmental neurons (Williams, 1975; Strausfeld and Seyan, 1985; Okada et al., 2003). Although polarization-mediated behavior in insects has been studied extensively (bees and ants: Wehner and Rossel, 1985; Wehner, 2003; crickets: Brunner and Labhart, 1987; Henze and Labhart, 2007; flies: von Philipsborn and Labhart, 1990; beetles: Dacke et al., 2003; locusts: Mappes and Homberg, 2004; butterflies: Reppert et al., 2004), the anatomical and functional connections from POL-neurons in the brain to thoracic motor centers have not been explored in any species.

Descending neurons mediate behaviorally relevant signals from the brain to motor circuits in the thoracic ganglia. They activate or modify thoracic networks or control specific parameters of a behavior depending on stimulus conditions. Previous studies on descending visual neurons have analyzed looming-sensitive neurons mediating escape (Rind et al., 2008; Yamawaki and Toh, 2009; Fotowat et al., 2009), deviation detector neurons controlling flight balance (Griss and Rowell, 1986; Rowell and Reichert, 1986; Hensler, 1988; Hensler and Rowell, 1990; Hensler, 1992), neurons coding for selfmotion (Wertz et al., 2008, 2009a, b), target-selective neurons mediating prey detection (Olberg, 1986; Frye and Olberg, 1995), and figure detecting neurons involved in flower recognition (Sprayberry, 2009).

The polarization pattern of the blue sky is fixed to the position of the sun and, therefore, changes during the day as the sun moves across the sky. Animals that use the sun or polarization pattern for navigation have to compensate that shift, based on daytime information and knowledge of the local solar ephemeris function. In flies, cockroaches and bugs, master circadian clocks have been associated with the accessory medulla in the optic lobe (Helfrich-Förster et al., 1998; Homberg et al., 2003; Vafopoulou et al., 2010). In contrast, Merlin et al. (2009) found circadian clocks in

We are grateful to Dr. Klaus Hensler for technical advice on neck connective recordings. We thank Dr. Keram Pfeiffer for providing Spike2-scripts for data analysis, Dr. Stanley Heinze and Basil el Jundi for contributing physiological data on four descending neurons, and Drs. Eve Marder, Hans Agricola, and Heinrich Dircksen for the donation of antisera. We are grateful to Sebastian Richter and Manfred Peil for constructing the stimulation devices and control equipment and to Karl Heinz Herklotz and Martina Kern for raising desert locusts. This work was supported by DFG grant HO 950/18-1.

Correspondence should be addressed to Uwe Homberg, Fachbereich Biologie, Tierphysiologie, Universität Marburg, D-35032 Marburg, Germany. E-mail: homberg@staff.uni-marburg.de.

the antennae of the monarch butterfly and suggested a role in time compensation for navigation.

The present study employed intracellular recordings to identify and characterize polarization-sensitive descending neurons in the desert locust. Three types of POL-neurons were characterized. Two of these cell types show evidence for time-compensation in *E*-vector tuning. The data close the gap between processing of polarization information in the brain and behavioral output mediated by thoracic motor centers.

Materials and Methods

Preparation of animals. Locusts (*Schistocerca gregaria*) raised under 12L:12D photoperiod, 50% relative humidity, and a temperature cycle of 28°C during the night and 35°C during the day were taken from crowded colonies at the University of Marburg. Adult animals of both sexes were used 1-3 weeks after imaginal moult. They were anesthetized by cooling for 15-30 min and waxed onto a metal holder in horizontal position. In some cases the tibiae of the hind legs were cut off. A 3×5 mm window was cut dorsally into the pronotum. After removal of gut, tracheal air sacs, fat bodies, and the tissue membrane between gut and ventral body cavity the neck connectives between suboesophageal- and prothoracic ganglia were exposed. Using a glass hook the neck connectives were manipulated into two grooves of a rectangular platform (1×2 mm) made of platinum. The connectives were submersed in locust saline at all times to prevent desiccation (Clements and May, 1974).

Electrophysiology. For intracellular recordings, microelectrodes (resistance 10-50 MΩ) were drawn from borosilicate capillaries (0.75 mm inner diameter, 1.5 mm outer diameter; Hilgenberg, Malsfeld, Germany) using a Flaming/Brown horizontal puller (P-97, Sutter, Novato, CA). Their tips were either filled with a 3% aqueous solution of fluorescent dextran (Alexa 488 or 647; 10 000 MW, anionic, fixable; Invitrogen, Karlsruhe, Germany) or with 4% Neurobiotin (Vector Laboratories, Burlingame, UK) in 1 M KCl and backed up with 1 M KCl. Intracellular signals were amplified (10×) with a custom-made amplifier and monitored with an audio-monitor and a digital oscilloscope (Hameg HM 305; Hameg, Frankfurt/Main, Germany). After sampling at a rate of 10 kHz with a Digidata 1322A (Molecular Devices, Sunnyvale, CA, USA), signals were stored on a personal computer using PClamp9 software (Molecular Devices). Some recordings were digitally high pass filtered to compensate for shifts in baseline. After recording, the tracer was injected iontophoretically into the cell with constant hyperpolarizing current (2-10 nA for 1-36 min, dextran) or constant depolarizing current (2-7 nA for 1-65 min, Neurobiotin).

Visual stimulation. For visual stimulation a xenon arc (XBO 150 W) was used as light source. It was connected via a light guide (Schölly, Denzlingen, Germany; spectral range 400-800 nm) to a perimeter (50 cm in diameter) placed around the animal. Either a linear polarizer (HN38S, Polaroid, Cambridge, MA) or a neutral density filter of equal transmission to present unpolarized light was moved into the light path (irradiance: 105 μW/cm^2, angular size: 3°). The polarizer was rotated via custom build hard- and software by 360° counterclockwise or clockwise at speeds between 15°/s and 60°/s. An *E*-vector orientation parallel to the longitudinal axis of the animal was defined as 0°. To investigate the receptive field size of the recorded neurons, the polarizer was presented from different elevations along the right-left-meridian, covering a range from 0° elevation on either side of the animal up to 90° elevation (zenith).

In addition, a moving grating was presented in front of the locust. The grating consisted of a piece of cardboard with alternating black and white bars (cardboard 7×18 cm; alternating stripes 7×1 cm). It was moved by hand at a distance of about 5 cm in front of the animal from right to left and vice versa.

Data analysis. Sampled spike trains were stored on a computer and evaluated using Spike2 software (Cambridge Electronic Design, UK) with implemented, custom designed scripts. Action potentials were detected with threshold based event detection. By using a gliding average algorithm at a bin size of 1 s, the detected events could be visualized as mean frequency. Mean background activities during darkness were obtained from counts of spikes in a defined time interval (usually 12 s) before and between visual stimuli. Neuronal responses to polarized light were analyzed using Oriana 2.02a (Kovach Computing Services, Anglesey, UK) for circular statistics and Origin 6.0 (Microcal, Northhampton, CA) for curve fitting. Events within each 360° rotation of the polarizer were assigned a corresponding *E*-vector angle to quantify responses to polarized light. A list of these angles was exported for each *E*-vector rotation and all individual and combined rotations of each neuron were tested statistically for polarization sensitivity. If the distribution of these angles during *E*-vector rotation was significantly different from randomness (Rayleigh-test for axial data), a neuron was rated polarization-sensitive. The mean angle of the distribution was defined as the Φ_{max}-value of that neuron. Differences in Φ_{max}-values of clockwise and counterclockwise rotations were statistically analyzed with Student's *t*-test for paired samples using SPSS software (version 11.5; significance level, 0.05), after the data were tested for normal distribution using the Kolmogorov-Smirnov test (significance level, 0.05).

To calculate the amplitude of frequency modulation and thus the strength of a polarized-light response (response amplitude = *R*), each filter rotation was divided into 20° bins. The spiking frequency within each bin was calculated, as well as the mean frequency over all bins. The summed, absolute difference between the mean frequency and the individual frequencies was defined as the *R* value of that polarized-light response. *R* values derived from rotations at different rotation velocities were directly comparable, owing to the usage of frequencies (impulses per second) rather than spike counts per bin (Labhart, 1996; Pfeiffer, 2006).

For evaluation of receptive fields, the *R* values of polarized-light responses to a rotating polarizer presented from different elevations were calculated. For each neuron, these *R* values were normalized with respect to the largest value, i.e., the center of the receptive field, and finally plotted against the elevation. The mean receptive field of a neuron type was established by averaging the means of all recorded neurons at each elevation.

For estimation of daytime relations, the preferred *E*-vector orientations were plotted against time of recording. Linear regression and correlation analysis were performed in Origin 6.0 software. The correlation coefficient (R_{cor}) was calculated, and the significance of the regression was tested with Student's *t*-test against a regression line with a slope of zero (significance level, 0.05). Circular activity plots of the polarization-sensitive neurons, receptive field plots, a plot showing elevation-dependent differences in Φ_{max}, distribution of Φ_{max} plots and the plot showing relation between Φ_{max} and daytime were created in Origin 6.0 (Microcal, Northhampton, CA).

Histology. After recording, the thoracic cavity was rinsed with locust saline and the window in the pronotum was sealed with a piece of tissue. The locust was incubated over night in a moist chamber by 4°C to allow diffusion of the tracer. On the next day the brain and ventral nerve cord without the free abdominal ganglia were dissected out and fixed in a mixture of 4% paraformaldehyde, 0.25% glutaraldehyde and 2% saturated picric acid (in 0.1 M phosphate buffer) over night at 4°C. Ganglia were processed as whole mounts. They were rinsed 4 × 15 min in PBS, dehydrated through an increasing ethanol series (25%, 50%, 70%, 90%, 95%, 100%; 15 min each), transfered to a 1:1 mixture of ethanol and methylsalicylate for 15 min and, finally, cleared in methylsalicylate for at least 45 min. When Neurobiotin was injected into the neurons, ganglia were incubated with Cy3-conjugated Streptavidin (Dianova, Hamburg, Germany; 1:1000) for three days at 4°C in PBT (PBS, including 0.5% Triton X-100) followed by rinsing with PBT (3 × 10 min) and PBS (6 × 30 min). Ganglia were finally mounted in Permount (Fisher Scientific, Pittsburgh, PA) between two coverslips. Adhesive strips were used as spacers to avoid compressions. Neurons were scanned with a confocal microscope (Leica TCS-SP2) equipped with a 10× oil immersion objective (HC PL APO 10×/0.4 Imm Corr CS) at minimal pinhole size and intervals of 4 μm. Reconstructions based on the data stacks were performed using Adobe Photoshop CS2.

To acquire higher morphological resolution of Neurobiotin-injected neurons, some ganglia were rehydrated and embedded in albumin-gelatin (4.8% gelatin and 12% ovalbumin in demineralized water) for sectioning. Embedded ganglia were postfixed in 8% formaldehyde (in 0.1 M phosphate buffer) overnight at 4°C. Using a vibrating blade microtome (VT 1200S; Leica, Wetzlar, Germany)

the ganglia were sectioned in thick sections (130 µm thickness; for details see Heinze and Homberg, 2008). These preparations were scanned at high resolution (40× or 63× objective, HCX PL Apo 40×/1.25 oil or HCX PL Apo 63×/1.32 oil) and are shown as maximum intensity projections or as single optical sections. All images were optimized for contrast and brightness and described corresponding to the body axis.

The rehydrated preparations were used for immunfluorescent colabeling with antibodies against γ-aminobutyric acid (GABA), serotonin, locustatachykinin II, A-type allatostatin, RFamide, or pigment-dispersing hormone, and against synapsin. For the detailed protocol and specificity of synapsin and serotonin immunostaining see Heinze and Homberg (2008). The anti-GABA antibody (NT-108, Protos Biotech Corp., New York, USA) was raised in guinea pig. It was used at a dilution of 1:500. The anti-locustatachykinin II (Lom-TK II) antiserum (K1-50820091) was donated by Dr. Hans Agricola (University of Jena, Germany) and was used at a dilution of 1:30.000. Its specificity on *S. gregaria* brain sections has been characterized by Vitzthum and Homberg (1998). For staining of neurons containing A-type allatostatins (AST-A), an antiserum against *Diploptera punctata* allatostatin 7 (Dip-Ast7) was used. The antiserum was a gift from Dr. Hans Agricola and was used at a dilution of 1:15.000. Competitive enzyme-linked immunosorbent assays showed that the serum cross-reacts with other members of the A-type allatostatin family of peptides with a common Y/FXFGLamide C-terminus (Vitzthum et al., 1996). The anti-FMRFamide antiserum (#671, used at 1:4.000) was generated against synthetic FMRFamide conjugated to thyroglobulin (Marder et al., 1987) and was generously supplied by Dr. Eve Marder (Brandeis University, Waltham, USA). Specificity tests by radio-immunoassay showed cross-reactivity of the antiserum with various C-terminally extended -MRFamides and -LRFamides (Marder et al., 1987). The anti-pigment-dispersing hormone (PDH) serum (no. 3B3, used at dilutions of 1:20.000) was raised in rabbit against conjugates of synthetic *Uca pugilator/Cancer magister* β-PDH and bovine thyroglobulin. Its specificity was demonstrated by Dircksen et al. (1987) and Homberg et al. (1991).

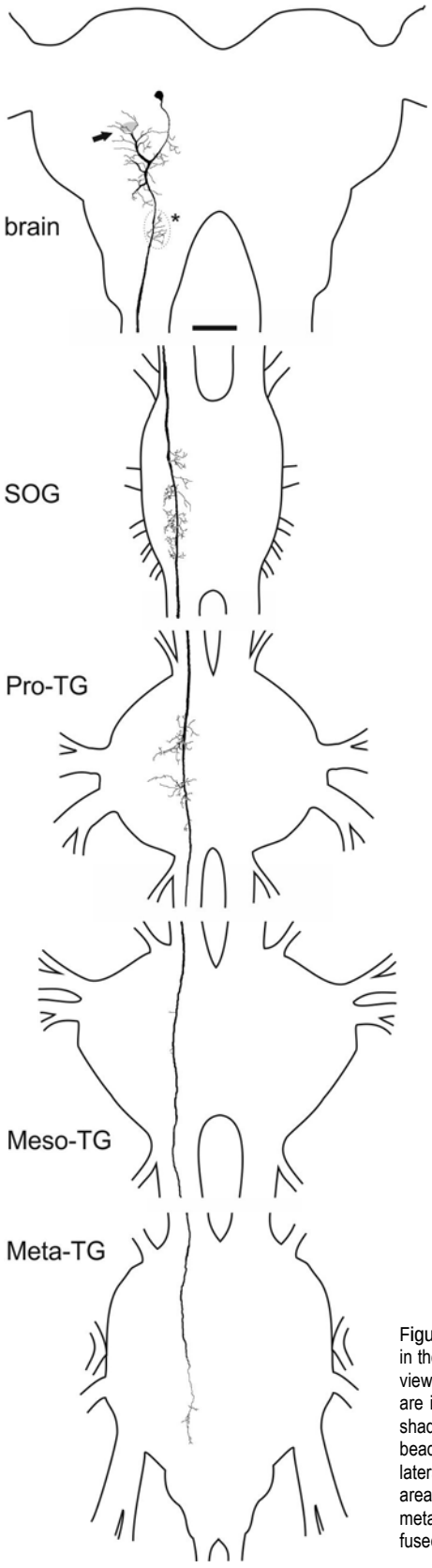

Figure 1. Morphology of the ipsilaterally descending brain neuron. Reconstruction of arborizations in the brain (posterior view), suboesophageal ganglion (SOG) and the three thoracic ganglia (dorsal view). Arborizations in all ganglia are confined to the ipsilateral hemispheres. Dendritic ramifications are in the posterior protocerebrum at the level of the posterior optic tubercle (arrow; POTu, gray-shaded). The antennal mechanosensory and motor center (dotted line, asterisk) is invaded by beaded arborizations. An axonal fiber descends through the SOG with ramifications extending laterally and medially around the axon. In the prothoracic ganglion (Pro-TG), two characteristic areas of ramification extend laterally. The axon passes through the mesothoracic (Meso-TG) and metathoracic ganglion (Meta-TG) with only sparse sidebranches and could not be traced beyond the fused first abdominal ganglion. Scale bar: 200 µm.

Results

Descending POL-neurons in the locust nervous system

Through intracellular recordings combined with dye fills we identified three types of descending POL-neurons in the nervous system of the desert locust. In total, 26 intracellular recordings were obtained from axons in the neck connectives or from neuronal processes in the posterior protocerebrum of the brain. Dye injections were successful in 17 neurons, belonging to three morphological types. Nine neurons that could not be stained were assigned to the three types based on their physiological response properties. Two of the three neuron types had descending axons from the brain, one descended through the ipsilateral and the other through the contralateral connective. The third type had no arborizations in the brain but was a contralaterally descending neuron from the suboesophageal ganglion (SOG). In some preparations, more than one cell was stained. In these cases, one of the neurons, interpreted as the recorded cell, was stained more intensely, whereas others appeared less strongly fluorescent. The most likely reason for these colabelings is dye leakage through injury of neighboring axons.

The responses of the descending neurons to polarized light were highly variable. In some recordings

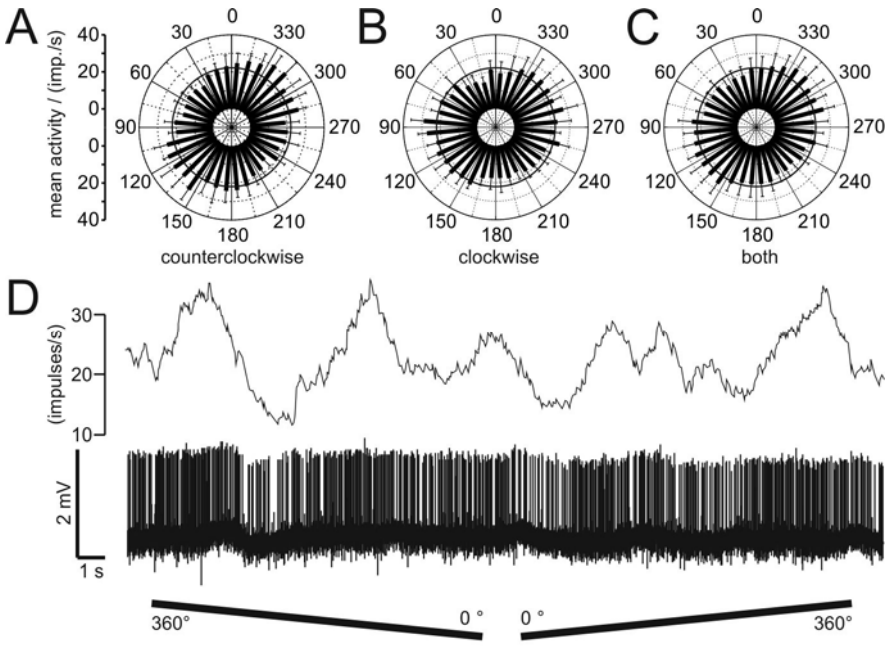

Figure 2. Responses of an ipsilaterally descending neuron to polarized light. *A-C,* Circular diagrams of mean frequencies of action potentials plotted against *E*-vector orientation during dorsal stimulation with a rotating polarizer. Background activity is indicated by a black circle within each plot. *A,* During counterclockwise rotations of the polarizer, *E*-vector tuning (Φ_{max}) was at 142° (n = 7, error bars = SD, bin size 10°, $p = 1.9 \times 10^{-12}$). *B,* The preferred *E*-vector orientation during clockwise rotations (n = 7, error bars = SD, bin size 10°, $p = 2.2 \times 10^{-8}$) had a Φ_{max} of 111° and differed significantly from Φ_{max} during counterclockwise rotations (n = 7, $p = 0.009$; students *t*-test for paired probes). *C,* Circular diagram from equal numbers (n =14) of clockwise and counterclockwise rotations revealed a Φ_{max} of 128° (error bars = SD, bin size 10°, $p < 10^{-12}$). *D,* Spike train (lower trace) and mean spiking frequency (upper trace, gliding average with bin size of 1 s) from the same neuron as in A-C during a counterclockwise (360° - 0°) and a clockwise (0° - 360°) rotation of the polarizer.

the responsiveness varied in relation to arousal of the animal, which has also been observed by Kien (1976) and Rowell and Reichert (1986) in locust visual interneurons. Two spontaneous types of arousal changes could be distinguished. The first type is characterized by spontaneous activity bursts of the animal correlated with high spiking frequency of the recorded neuron; a previously quiescent animal suddenly began a series of vigorous movements which quickly subsided leaving the animal as quiet as before. The second type is characterized by spontaneous activity changes of the recorded cell without observable movements of the animal. In some cases the arousal changes were correlated with the presented stimuli but in most cases the ongoing activity changes of the neuron were apparently independent of visual input. These arousal changes made it difficult to evaluate the responses to the presented visual stimuli because the neurons were either highly responsive or unresponsive. *E*-vector rotations that were accompanied by spontaneous activity bursts of type one were not included in the analysis. The level of responsiveness of a preparation could change spontaneously over periods of minutes in either direction. Rowell and Reichert (1986) reported that the visual responses of the DNC descending neuron were especially prone to such fluctuations.

Ipsilaterally descending brain neurons

Stable recordings from ipsilaterally descending POL-neurons were obtained in six experiments with successful staining in three cases. The morphologies of the stained neurons were indistinguishable, suggesting that all recordings were from the same neuron. Their somata were located near the posterior brain surface medio-ventrally from the calyces of the mushroom body (Fig. 1). Fine and, therefore, probably dendritic arborizations were concentrated in the posterior protocerebrum near but not within the posterior optic tubercle (see supplemental Fig. 1A,B; available at www.jneurosci.org as supplemental material) and close to the posterior surface of the brain. Beaded and, therefore, probably output ramifications occurred in the antennal mechanosensory and motor center (see supplemental Fig. 1C). An axonal fiber descended through the ipsilateral connective into the SOG and all thoracic ganglia and terminated with a few small sidebranches in the metathoracic ganglion (Meta-TG). Arborizations in the SOG and prothroacic ganglion had bleb-like and, therefore, presumably presynaptic endings in dorsal parts of the ganglia. All arborizations were restricted to the ipsilateral hemispheres of the ganglia.

The ipsilaterally descending neurons (n = 6) had highly variable background activity ranging from less than 1 spike per second up to 47 impulses per second (mean ± SD; 17.8 ± 16.7 impulses per second). All neurons showed polarization opponency (Fig. 2), i.e. they were maximally excited by a particular *E*-vector (Φ_{max}) and were maximally inhibited by an *E*-vector perpendicular to Φ_{max}. Corresponding to the large variation in background activity, the activity during stimulation with polarized light was also highly variable ($R = 78.2 \pm 40.7$). The preferred *E*-vector orientations (Φ_{max}) were 14°, 149° and 176° (not shown) and 128° (Fig. 2C) for four neurons with somata in the left brain hemisphere and 36° and 70° for two neurons with somata in the right brain hemisphere (not shown). The receptive field to polarized light stimuli, measured in one recording, extended over a range of 180° along the right-left meridian (not shown). One neuron, recorded in the left hemisphere was tested for motion sensitivity. The neuron was highly excited by the grating moving from right to left in front of the animal but remained silent during movement in the opposite direction (supplemental Fig. 2A).

Contralaterally descending brain neurons

Four contralaterally descending POL-neurons were recorded and stained. Again the morphologies of the neurons were indistinguishable, suggesting that recordings were from the same neuron. Their cell bodies were located in the posterior median pars intercerebralis at the level of the central body (Fig. 3). Protocerebral ramifications were concentrated in the posterior protocerebrum near the posterior surface of the neuropil. The main axonal fiber crossed the midline and descended through the contralateral connective to the SOG, all thoracic ganglia, and to the free abdominal ganglia, but their projections in the abdominal ganglia could not be revealed. Terminals in the SOG and Pro-TG had a bleb-like structure, suggesting output sites, and beaded endings were also found in the contralateral antennal mechanosensory and motor center in the brain. One neuron was recorded from the left connective and had its soma in the right brain hemisphere. The other three neurons were recorded from the input regions in the left brain hemisphere and descended through the right connective.

Responses of the contralaterally descending neurons (n = 4) to polarized light were weak compared with those of the ipsilaterally descending neurons and did not show strong fluctuations. The background activity varied between 0.6 and 16 impulses per second (9.5 ± 8 imp/s; n = 3). Preferred *E*-vector orientations (Φ_{max}) were at 70°, 87° and 102° (not shown) for the three neurons descending through the right connective and 130° (Fig. 4C) for the fourth neuron descending through the left connective. Motion stimuli were tested in one recording. The neuron showed strong responses with activation to moving black and white bars in front of the animal from left to right and vice versa (supplemental Fig. 2B). The motion response showed considerable adaptation.

SOG neurons

Neurons descending from the SOG were recorded in 16 experiments. Ten of these neurons were labeled. The somata of the stained neurons were located anterior-laterally in the labial neuromere. Their arborizations in the SOG were restricted to a small tree lateral to the ipsilateral dorsal intermediate tract and blebbed contralateral branches leaving the axon and arborizing in the labial neuromere dorsal and lateral to the dorsal intermediate and ventral lateral tract. Neurons of this type had been described by Kien et al. (1990) as a cluster of three neurons. Their cell bodies, arborizations and axons lie closely together at the labial-maxillary junction in the SOG, and at least one, but more likely two, of the axons terminate in the Pro-TG (Kien et al., 1990). The descending POL-neurons stained here (Fig. 5) shared all morphological features within the SOG with the neurons described by Kien et al. (1990). All neurons ramified with beaded endings in a narrow area of the contralateral Pro-TG close to the dorsal neuropil surface.

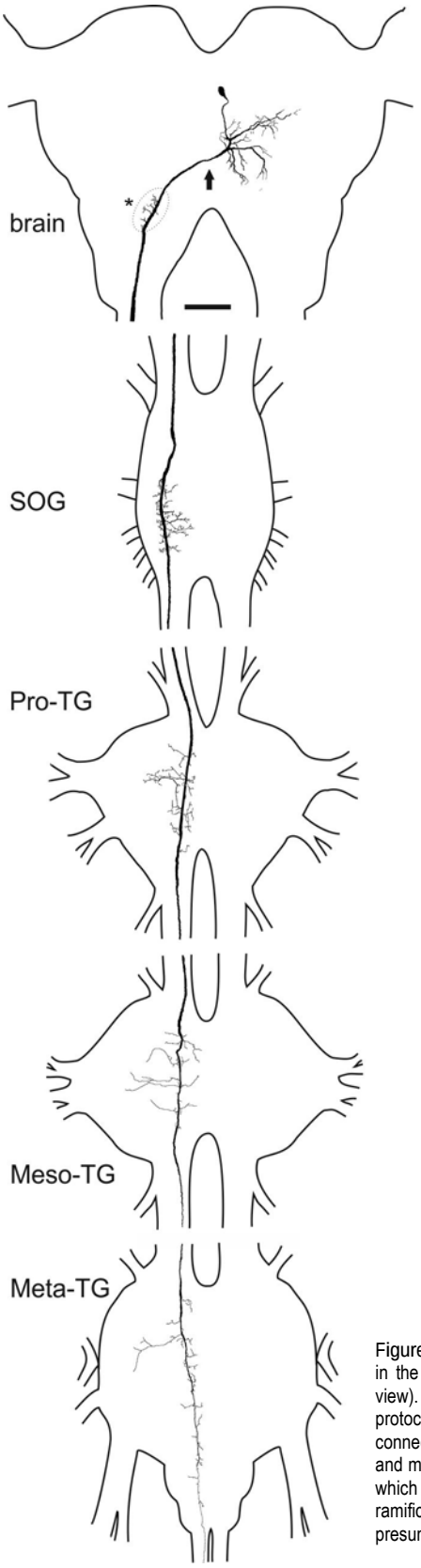

Figure 3. Morphology of the contralaterally descending brain neuron. Reconstruction of arborizations in the brain (posterior view), suboesophageal ganglion (SOG) and the three thoracic ganglia (dorsal view). The neuron has its soma and presumably dendritic arborizations in the ipsilateral posterior median protocerbrum. The axon crosses the midline of the brain (arrow) and descends through the contralateral connective. Presumably presynaptic endings with beaded terminals are in the antennal mechanosensory and motor center (asterisk). The neuron descends through the SOG, thoracic ganglia and sends a fiber, which could not be traced further, into the connective toward the free unfused abdominal ganglia. All ramifications in the ventral nerve cord are confined to the contralateral hemisphere and have beaded, presumably presynaptic terminals in dorsal aspects of the ganglia. Scale bar: 200 µm.

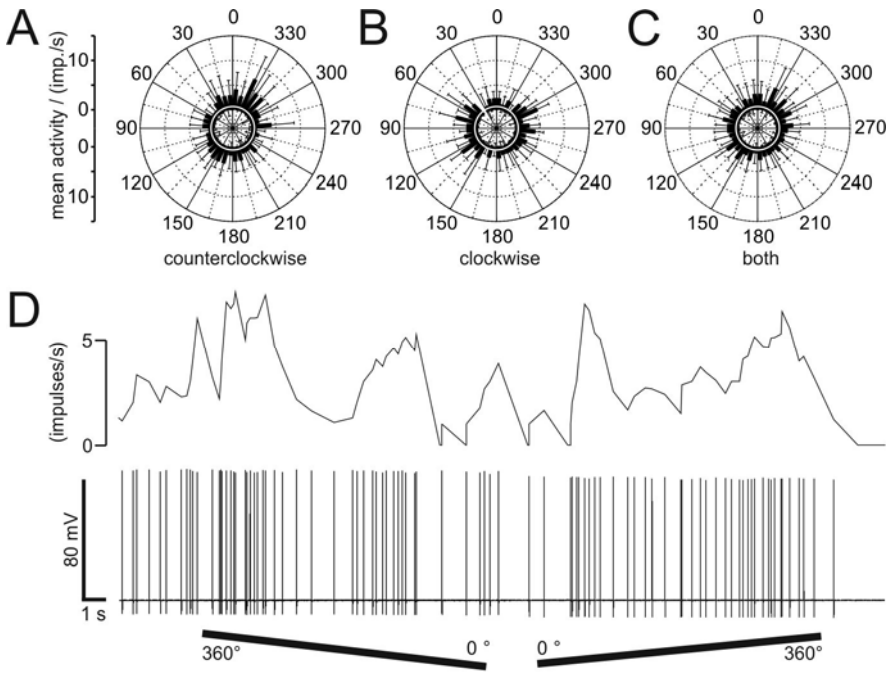

Figure 4. Responses of a contralaterally descending neuron to polarized light. *A-C,* Circular diagrams of mean frequencies of action potentials of the neuron against *E*-vector orientation during dorsal stimulation with a rotating polarizer. Each rotation-direction is shown separately. Background activity is indicated by a white circle within each plot. *A,* During counterclockwise rotations of the polarizer, the neuron had a preferred *E*-vector orientation (Φ_{max}) of 157° (n = 5, error bars = SD, bin size 10°, $p = 7.38 \times 10^{-4}$). *B,* The preferred *E*-vector orientation during clockwise rotations (n = 5, error bars = SD, bin size 10°, $p = 5.74 \times 10^{-4}$) had a Φ_{max} of 103°, and differed significantly from Φ_{max} during counterclockwise rotations (n = 5, $p = 0.002$; students *t*-test for paired probes). *C,* Circular diagram from equal numbers (n = 10) of clockwise and counterclockwise rotations revealed a Φ_{max} of 130° (error bars = SD, bin size 10°, $p = 0.005$). *D,* Spike train (lower trace) and mean spiking frequency (upper trace, gliding average with bin size of 1 s) of the same neuron during a counterclockwise (360° - 0°) and a clockwise (0° - 360°) rotation of the polarizer.

The descending SOG neurons responded with polarization opponency to dorsally presented polarized light. The neurons had a mean background activity of 4.9 ± 3.5 impulses per second (n = 15). Most SOG neurons showed strong modulation during stimulation with a rotating polarizer. They were activated up to peak frequencies of 20.2 ± 8.3 impulses per second at Φ_{max} and were usually totally silenced at Φ_{min} (Fig. 6). Φ_{max} values ranged from 3° to 137° and covered three-quarters of the total possible range of *E*-vectors (Fig. 8C). The Φ_{max} distribution appeared to be clustered around 42° and 116° but was not significantly different from randomness (Rao's spacing test, $p > 0.1$). Eight neurons were tested for motion-sensitivity but showed only weak bidirectional responses to the moving grating (supplemental Fig. 2C). The bilateral size of the receptive field to polarization stimuli was tested in ten recordings (Fig. 7A). The response strength to laterally presented polarized light (0° lateral expansion) was as strong as the response to zenithal stimulation (90°), and all neurons were polarization sensitive over the tested range of 180° along the right-left meridian (Fig. 7B). In these neurons Φ_{max} increased significantly when moving the polarizer from ipsilateral positions to positions in the contralateral hemisphere ($R_{cor} = 0.53$, *t* test against the slope of zero: p = 0.00453; Fig. 7C).

Five Neurobiotin-stained SOG neurons were tested for colabelling with antisera against FMRF-amide, serotonin, Lom-TK II, AST-A and GABA but none of these substances could be demonstrated in the SOG neurons (supplemental Fig. 3).

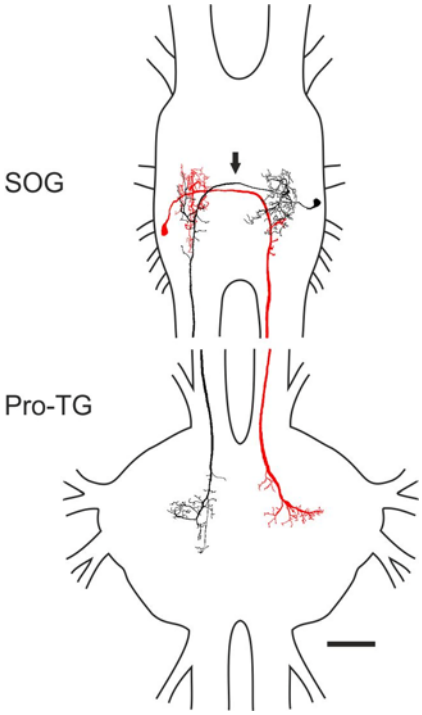

Figure 5. Morphology of two descending neurons from the SOG, horizontal superimposed reconstructions (dorsal view). The red neuron is mirrored. Both neurons differ slightly in morphology. They have their somata and presumably dendritic arborizations in posterior parts in the ipsilateral hemisphere of the SOG. Axons cross the midline (arrow), give rise to presumably presynaptic endings with bleb-like structures that partly overlap with the input region of the contralateral homologue and descend through the contralateral connective. The neurons have axonal beaded ramifications that differ slightly between the two cells in a narrow dorsal part of the prothoracic ganglion (Pro-TG). Scale bar: 200 µm.

Distribution and daytime dependence of Φ_{max} orientations

Judged by the striking morphological similarity in all stained preparations, the ipsi- and contralaterally descending POL-neurons from the brain probably exist only once per hemisphere. Φ_{max} values calculated from the different recordings from descending

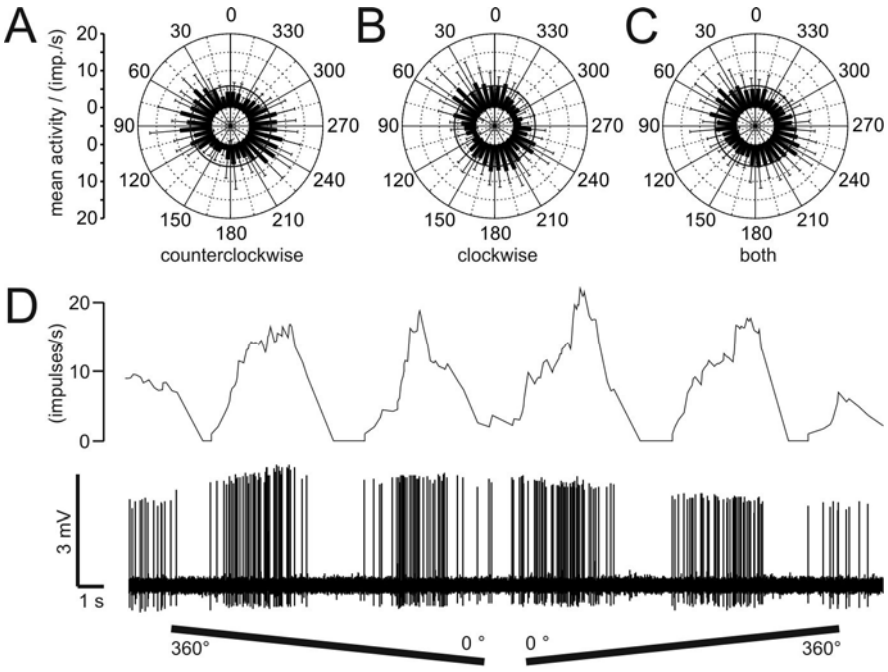

Figure 6. Responses of an SOG descending neuron to polarized light. *A-C,* Circular diagrams of mean frequencies of action potentials of the neuron against *E*-vector orientation during dorsal stimulation with a rotating polarizer. Each rotation-direction is shown separately. Background activity is indicated by a black circle within each plot. *A,* During counterclockwise rotations of the polarizer, the neuron had a preferred *E*-vector orientation (Φ_{max}) of 70° (n = 11, error bars = SD, bin size 10°, $p < 10^{-12}$). *B,* The preferred *E*-vector orientation (Φ_{max}) during clockwise rotations (n = 11, error bars = SD, bin size 10°, $p < 10^{-12}$) was at 27° and differed significantly from Φ_{max} during counterclockwise rotations (n = 11, $p < 0.001$; students *t*-test for paired probes). *C,* Circular diagram from equal numbers (n = 22) of clockwise and counterclockwise rotations revealed a Φ_{max} of 50° (error bars = SD, bin size 10°, $p < 10^{-12}$). *D,* Spike train (lower trace) and mean spiking frequency (upper trace, gliding average with bin size of 1 s) of the same neuron during a counterclockwise (360° - 0°) and a clockwise (0° - 360°) rotation of the polarizer.

brain neurons covered the full 180° range of possible *E*-vectors (not shown; Rao's spacing test, p > 0.95). When neurons with axons in the left (Fig. 8A) and right connective (Fig. 8B) were plotted separately, Φ_{max} distributions appeared to be clustered around 154° (Fig. 8A, left connective) resp. 74° (Fig. 8B, right connective) but in both cases, the distributions were not significantly different from randomness (Rao's spacing test, $p > 0.1$). Likewise, when Φ_{max} orientations from ipsilaterally and contralaterally descending neurons were analyzed separately, the distributions were not significantly different from randomness (Rao's spacing test, $p > 0.1$; not shown). In common, all cell types showed higher Φ_{max} values during counterclockwise rotations of the polarizer than during clockwise rotations (Figs. 2A,B; 4A,B; 6A,B). The $\Delta\Phi_{max}$ values of both brain neurons (mean ± SD: 37.6° ± 12.2°; n = 8) differed significantly from the $\Delta\Phi_{max}$ values of the SOG neurons (48.4° ± 7.4°; n = 15; p = 0.014; oneway-ANOVA).

All recordings were performed between 9:00 A.M. and 6:00 P.M. (CET). Figure 9 shows the Φ_{max} values of all recordings in relation to the time of recording. A linear correlation exists between the time of recording and *E*-vector tuning (Φ_{max}) for the descending neurons from the brain if considered as a functional unit of ipsilaterally and contralaterally descending POL-neurons (R_{cor} = -0.9, *t* test against the slope of zero; p = 0.00039; Fig. 9A). The slope of the regression line indicates a shift in Φ_{max} tuning of 21.5° per hour, covering 516° in 24 hours. No correlation between daytime and *E*-vector tuning was found in the SOG neurons (R_{cor} = 0.11, p = 0.97; Fig. 9B).

Discussion

We have characterized three types of descending

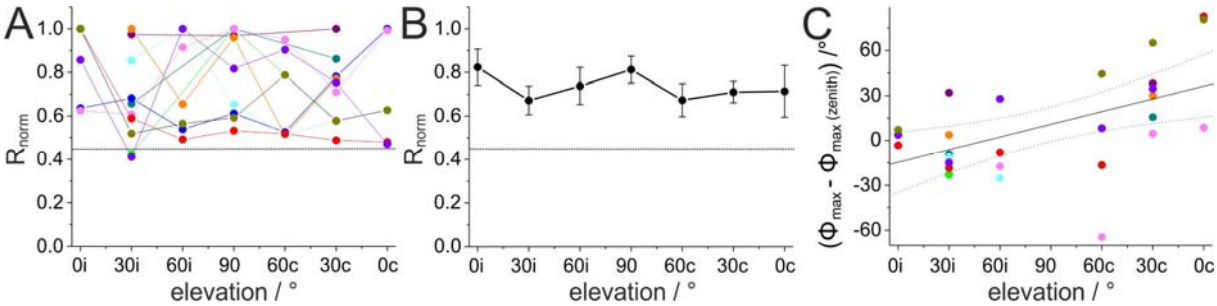

Figure 7. Receptive field properties of the descending SOG neurons when stimulated with polarized light. *A,* Response amplitudes from individual recordings, distinguished by different colors, plotted against elevation of polarized-light stimulus. Elevation is plotted with respect to the location of the soma and was sampled along the right-left meridian with respect to the locust. Values were normalized to the largest *R* value of each neuron (i.e. the receptive field center). Data points are connected by lines for better visibility. Dotted line indicates background variability for the neuron type, which has been renormalized with respect to the mean receptive field center. *B,* Average receptive field for the examined SOG neurons. Dotted line, background variability. Values are means ± SE. *C,* Deviations of Φ_{max} values at different elevations from zenithal Φ_{max} values. Differences in Φ_{max} values are plotted against the elevation. A significant correlation was observed (R_{cor} = 0.53, p = 0.00453). Colors of data points correspond to the colors in *A*.

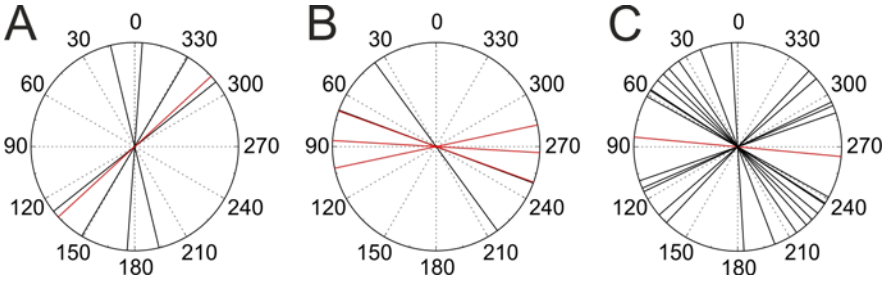

Figure 8. Distribution of Φ_{max} values in the three types of descending neuron. *A*, Φ_{max} values from brain POL-neurons with descending axons in the left connective. *E*-vector orientations (ipsilaterally descending: black; contralaterally descending: red) seem to be clustered around 154° but the distribution is not significantly different from randomness (Rao's spacing test, $p > 0.01$). *B*, Φ_{max} values from brain POL-neurons with descending axons in the right connective. Φ_{max} values are clustered around 74° but the distribution is not significantly different from randomness (Rao's spacing test, $p > 0.1$; same color-code as in *A*). *C*, Φ_{max} values of all SOG neurons (the red value is mirrored) descending through the left connective. Φ_{max} values are clustered around 42° and 116° but the distribution is not significantly different from randomness (Rao's spacing test, p > 0.1).

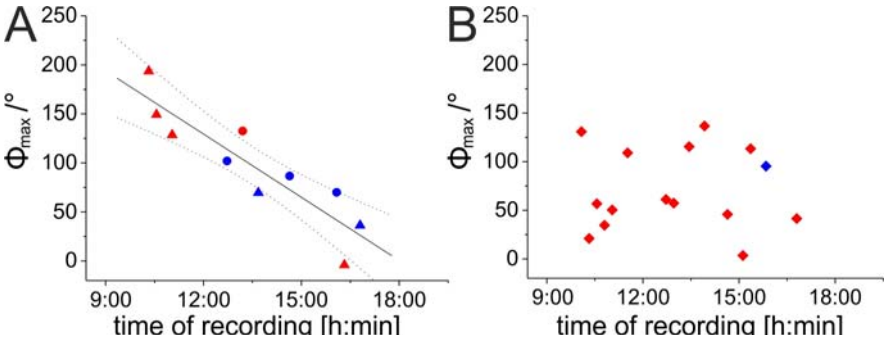

Figure 9. Daytime dependent preferred *E*-vector orientations (Φ_{max}) in descending POL-neurons. Φ_{max} values of the three descending neuron types are plotted against standard time (CET) of recording. *A*, A correlation was observed for the combined values from the two types of brain descending neuron (R_{cor} = -0.9, t test against the slope of 0, p = 0.00039; y = -515.91x + 387.37), indicated by the regression line with 95% confidence intervals. Data from ipsilaterally descending neurons (triangles) and contralaterally descending neurons (dots) are included. Neurons with axons in the left connective are shown in red and those with axons in the right connective, in blue. *B*, No correlation was observed for the descending SOG neurons (R_{corr} = 0.11, p = 0.97). Most SOG neurons were recorded from the left connective (red squares), only one recording was from the right connective (blue square).

neuron in the nervous system of the desert locust that are sensitive to the *E*-vector orientation of dorsally presented polarized light. Based on morphological similarities of the stained neurons, we suggest that the recordings were from two bilateral pairs of descending brain neurons, one with ipsilaterally and the other with contralaterally descending axon, and from two bilateral pairs of descending SOG neurons. Given the established role of dorsal eye regions in detecting the polarization pattern of the sky (Labhart and Meyer 1999), the neurons are likely to be involved in behavioral responses to sky polarization such as sky compass orientation. The ipsilaterally descending neuron and the SOG neurons responded with polarization opponency in wide receptive fields that covered the whole sky hemisphere in bilateral extension. All neurons were multisensory and responded, in addition to polarized light, to large-field motion stimuli.

POL-neurons descending from the brain

Both brain neurons responded with sinusoidal activity changes to a rotating polarizer. Whereas the ipsilaterally descending neuron showed strong variations in the responses, the contralaterally descending neuron in general had lower background activity and responded less strongly to polarized light. Both neurons showed strongest activities in response to moving bars. The ipsilaterally descending brain neuron has remarkable similarities with the descending direction-selective motion-detecting neuron (PDDSMD neuron) described by Rind (1990a). The PDDSMD neuron is sensitive to motion stimuli signaling yaw deviations with preferred direction backward across the ipsilateral eye and forward across the contralateral eye. Correspondingly, the ipsilaterally descending neuron studied here was excited by frontal horizontal motion only when movement occurred toward the ipsilateral but not toward the contralateral eye. The contralaterally descending POL-neuron was described by Williams (1975) as one of a pair of neurons with somata in the pars intercerebralis termed PI(2):5 and PI(2):6. In contrast to the PI(2):5 neuron, PI(2):6, recorded here, has no processes extending to the lateral ocellar tract and a less pronounced antero-ventral branch. Both neurons share extensive superficial arborizations in the postero-ventral brain (Williams, 1975). The PI(2):5 neuron was physiologically characterized as one of several descending deviation detector neurons in flying locusts (Hensler and Rowell, 1990; Hensler, 1988), but PI(2):6 has not been studied physiologically before.

Because of their polarization-sensitivity, we suggest that the two descending brain neurons characterized here supplement the hitherto known polarization vision pathway and are likely to bridge the gap between the brain and thoracic motor circuits. Judged by their ramifications in the posterior protocerebrum, both neurons might receive polarization-sensitive input from the LAL-pPC neuron described by Heinze and Homberg (2009). The LAL-pPC neuron receives input in the lateral accessory lobe (LAL) and gives rise to bilaterally symmetric output ramifications in the posterior protocerebrum. Therefore, the ipsi- and contralaterally descending POL-neurons might receive the same polarized-light input signals. Additionally, both neurons are highly sensitive to horizon-

tal motion. In free flight, changes in flight direction caused by lateral wind or yaw maneuvers would create both a polarization signal from the sky and a yaw motion signal from the surrounding landscape. Both signals apparently converge on the brain descending neurons studied here and might result in robust coding of changes in head orientation under various sky and ground contrasts. Testing both stimulus modalities in the same recording will show how both inputs exactly interact and complement each other.

The putative output ramifications of the descending POL-neurons are concentrated in dorsal parts of the thoracic ganglia where thoracic motor neurons receive their input (Siegler et al., 1991; Schlurmann and Hausen, 2007). Hence, the descending POL-neurons are likely to provide a direct signal to thoracic motor centers and might be the final interneurons of the polarization vision pathway from the receptor cells in the DRA and leg or wing motor neurons.

Polarization vision and time-compensation

A crucial requirement for a sky compass network that controls migratory directions is to achieve time-compensation, i.e. to continuously adjust its calculations as the sun moves across the sky during the day. Because the polarization pattern of the blue sky is generated by sunlight, it moves across the sky during the day with an average change in solar azimuth of 15° per hour. Time compensation accounting for this shift has been shown in behavioral experiments in honeybees, ants and monarch butterflies (Lindauer, 1960; Wehner, 1992; Mouritsen and Frost, 2002). Pfeiffer and Homberg (2007) suggested that a daytime dependent compensation for changes in solar elevation operates in the anterior optic tubercle of the locust, an input stage to the central-complex network. How and at what stage of the polarization vision pathway solar azimuth compensation is achieved is currently unclear. El Jundi and Homberg (2010) provided evidence for the existence of a second polarization vision pathway in the locust brain that connects the accessory medulla to the posterior optic tubercle and thus to the polarization vision network in the central complex. In the fruit fly *Drosophila melanogaster* and the cockroach *Leucophaea maderae* the accessory medulla is the site of the circadian clock controlling circadian changes in locomotion and other behaviors (Helfrich-Förster et al., 1998; Homberg et al,. 2003, Helfrich-Förster, 2004), but whether this is also true for the locust, remains to be seen.

The two descending brain neurons show *E*-vector tunings that are linearly correlated with time of day. Convergent information from the internal sky compass and the circadian clock therefore occurs in the brain at or upstream of the dendritic ramification of the descending neurons. For a compensation of solar azimuth changes, the Φ_{max} values of time-compensated POL-neurons should change by about 15° per hour which accounts for 360° azimuth changes in 24 hours. The slope of the regression curve (21.5° per hour) is close to this relation. Because all locusts used here were reared under laboratory conditions, the diurnal shift in *E*-vector tuning we see might represent a default state that is determined genetically and might require environmental cues for adjustment to local sky conditions. A peculiar aspect is that, at any given daytime, the two pairs of descending neurons have the same *E*-vector tuning. This is at present difficult to explain, but again, *E*-vector tuning and daytime dependence may be strongly influenced by environmental experience.

POL-neurons of the SOG

The descending POL-neurons of the SOG responded with polarization opponency to the rotating polarizer within a receptive field of at least 180° in bilateral expansion. The recordings did not provide evidence for a time-compensation mechanism and showed only weak unidirectional responses to moving stimuli. Based on Φ_{max} distribution (Fig. 8C) which shows two possible sub-clusters, it is possible that the SOG neurons consist of two bilateral pairs of neurons. This assumption is supported by findings from Kien et al. (1990) suggesting a pair of these neurons per SOG hemisphere.

Hensler (1989) recorded from the neuron under tethered flying conditions. The neuron responded to simulated roll deviations and was rhythmically excited during flight. Electrical stimulation of the neuron resulted in head rolling to the contralateral side (Hensler, 1989). We therefore, suggest that the SOG neurons do not take part in the polarization vision pathway used for navigation, but may be involved in the control of head orientation as suggested by Hensler (1989). The neurons might integrate sky polarization input with horizon detection to control head orientation during flight, but how both inputs interact with each other in a biological meaningful way will have to be determined in future experiments.

Comparison to head direction cells

When stimulating with a rotating polarizer, shifts in Φ_{max} would be expected to account for differences in latencies of the response during clockwise and counterclockwise rotations. As a consequence of the delayed response to the preferred orientation, Φ_{max} should have higher values for clockwise and lower values for counterclockwise rotations. Furthermore, the $\Delta\ \Phi_{max}$ value should increase with increasing numbers of intercalated neurons between photoreceptors and the neuron of interest. Interestingly, however, Φ_{max}-shifts in the opposite direction were observed. Φ_{max} values for counterclockwise rotations were higher than Φ_{max} values for clockwise rotations, and these differences were larger in the SOG than in the brain neurons. Similar shifts in directional tuning have been observed in head direction cells in the anterior dorsal thalamic nucleus and other areas involved in spatial orientation of rats (Blair and Sharp, 1995; Taube and Basset, 2003). Heinze and Homberg (2007) emphasized the similar biological roles of zenithal *E*-vector-coding neurons in locusts and head

direction cells in rats for spatial orientation. Just as proposed for tuning shifts in head direction cells during clockwise and counterclockwise rotations of rats, the *E*-vector tuning shifts in POL-neurons observed here might signal anticipatory head orientation, signaling a specific head direction in the near future (Blair and Sharp, 1995). While the neural mechanisms underlying these signaling characteristics are still unclear, anticipatory coding of celestial *E*-vectors is clearly adaptive for course corrections maintaining a chosen flight or walking direction. With recordings from identifiable neurons, the locust may be a good model to analyze the underlying cellular and synaptic mechanisms for anticipatory head direction signaling in future experiments.

References

Blair HT, Sharp PE (1995) Anticipatory head direction signals in anterior thalamus: evidence for a thalamocortical circuit that integrates angular head motion to compute head direction. J Neurosci 15:6260-6270.

Brunner D, Labhart T (1987) Behavioural evidence for polarization vision in crickets. Physiol Entomol 12:1-10.

Dacke M, Nordström P, Scholtz CH (2003) Twilight orientation to polarized light in the crepuscular dung beetle *Scarabaeus zambesianus*. J Exp Biol 206:1535-1543.

Dircksen H, Zahnow CA, Gaus G, Keller R, Rao KR, Riehm JP (1987) The ultrastructure of nerve endings containing pigment-dispersing hormone (PDH) in crustacean sinus glands: Identification by an antiserum against a synthetic PDH. Cell Tissue Res 250:377-387.

el Jundi B, Homberg U (2010) Evidence for the possible existence of a second polarization-vision pathway in the locust brain. J Insect Physiol 56:971-979.

Frye MA, Olberg RM (1995) Visual receptive field properties of feature detecting neurons in the dragonfly. J Comp Physiol A 177:569-576.

Fotowat H, Fayyazuddin A, Bellen HJ, Gabbiani F (2009) A novel neuronal pathway for visually guided escape in *Drosophila melanogaster*. J Neurophysiol 102:875-885.

Griss C, Rowell CHF (1986) Three descending interneurons reporting deviation from course in the locust. I. Anatomy. J Comp Physiol A 158:765-774.

Heinze S, Homberg U (2007) Maplike representation of celestial *E*-vector orientations in the brain of an insect. Science 315:995-997.

Heinze S, Homberg U (2008) Neuroarchitecture of the central complex of the desert locust: Intrinsic and columnar neurons. J Comp Neurol 511:454-478.

Heinze S, Homberg U (2009) Linking the input to the output: new sets of neurons complement the polarization vision network of the locust central complex. J Neurosci 29:4911-4921.

Heinze S, Gotthardt S, Homberg U (2009) Transformation of polarized light information in the central complex of the locust. J Neurosci 29:11783-11793.

Helfrich-Förster C (2004) The circadian clock in the brain: a structural and functional comparison between mammals and insects. J Comp Physiol A 190:601–613.

Helfrich-Förster C, Stengl M, Homberg U (1998) Organization of the circadian system in insects. Chronobiol Int 15:567-594.

Hensler K (1988) The pars intercerebralis neurone PI(2)5 of locusts: convergent processing of inputs reporting head movements and deviations from straight flight. J Exp Biol 140:511-533.

Hensler K (1989) Corrective flight steering in locusts: Convergence of extero- and proprioceptive inputs in descending deviation detectors. In: Neurobiology of sensory systems (Singh RN, Strausfeld NJ, eds), pp. 531-554. Plenum Press, New York and London.

Hensler K (1992) Neuronal co-processing of course deviation and head movements in locusts. I. Descending deviation detectors. J Comp Physiol A 171:257-271.

Hensler K, Rowell CHF (1990) Control of optomotor responses by descending deviation detector neurones in intact flying locusts. J Exp Biol 149:191-205.

Henze M, Labhart T (2007) Haze, clouds and limited sky visibility: polarotactic orientation of crickets under difficult stimulus conditions. J Exp Biol 210:3266-3276.

Homberg U (2004) In search of the sky compass in the insect brain. Naturwissenschaften 91:199-204.

Homberg U, Würden S, Dircksen H, Rao KR (1991) Comparative anatomy of pigment-dispersing hormone-immunoreactive neurons in the brain of orthopteroid insects. Cell Tissue Res 266:343-357.

Homberg U, Reischig T, Stengl M (2003) Neural organization of the circadian system of the cockroach *Leucophaea maderae*. Chronobiol Int 20:577-591.

Horváth G, Varjú D (2004) Polarized light in animal vision. Springer: Berlin.

Kien J (1976) Arousal changes in the locust optomotor system. J Insect Physiol 22:393-396.

Kien J, Fletcher WA, Altman JS, Ramirez J, Roth U (1990) Organization of intersegmental interneurons in the suboesophageal ganglion of *Schistocerca gregaria* (Forksal) and *Locusta migratoria migratorioides* (Reiche & Fairmaire) (Acrididae, Orthoptera). Int J Insect Morphol Embryol 19:35-60.

Labhart T (1996) How polarization-sensitive interneurones of crickets perform at low degrees of polarization. J Exp Biol 199:1467-1475.

Labhart T, Meyer EP (2002) Neural mechanisms in insect navigation: polarization compass and odometer. Curr Opin Neurobiol 12:707-714.

Lindauer M (1960) Time-compensated sun orientation in bees. Cold Spring Harbor Symp Quant Biol 25:371-377.

Mappes M, Homberg U (2004) Behavioral analysis of polarization vision in tethered flying locusts. J Comp Physiol A 190:61-68.

Marder E, Calabrese RL, Nusbaum MP, Trimmer B (1987) Distribution and partial characterization of FMRFamide-like peptides in the stomatogastric nervous systems of the rock crab, *Cancer borealis*, and the spiny lobster, *Panulirus interruptus*. J Comp Neurol 259:150-163.

Merlin C, Gegear RJ, Reppert SM (2009) Antennal circadian clocks coordinate sun compass orientation in migratory monarch butterflies. Science 325:1700-1704.

Mouritsen H, Frost BJ (2002) Virtual migration in tethered flying monarch butterflies reveals their orientation mechanisms. Proc Natl Acad Sci USA 99:10162-10166.

Okada R, Sakura M, Mizunami M (2003) Distribution of dendrites of descending neurons and its implications for the basic organization of the cockroach brain. J Comp Neurol 458:158-174.

Olberg RM (1986) Identified target-selective visual interneurons descending from the dragonfly brain. J Comp Physiol A 159:827-840.

Pfeiffer K (2006) Coding of sky-compass information in neurons of the anterior optic tubercle of the desert locust *Schistocerca gregaria*. PhD thesis, Philipps-University Marburg.

Pfeiffer K, Homberg U (2007) Coding of azimuthal directions via time-compensated combination of celestial compass cues. Curr Biol 17:960-965.

Reppert SM, Zhu H, White RH (2004) Polarized light helps monarch butterflies navigate. Curr Biol 14:155-158.

Rind FC (1990a) A directionally selective motion-detecting neurone in the brain of the locust: Physiological and morphological characterization. J Exp Biol 149:1-19.

Rind FC (1990b) Identification of directionally selective motion-detecting neurones in the locust lobula and their synaptic connections with an identified descending neurone. J Exp Biol 149:21-43.

Rind FC, Santer RD, Wright GA (2008) Arousal facilitates collision avoidance mediated by a looming sensitive visual neuron in a flying locust. J Neurophysiol 100:670-680.

Rowell CHF, Reichert H (1986) Three descending interneurons reporting deviation from course in the locust. II. Physiology. J Comp Physiol A 158:775-794.

Sakura M, Lambrinos D, Labhart T (2008) Polarized skylight navigation in insects: model and electrophysiology of e-vector coding by neurons in the central complex. J Neurophysiol 99:667-682.

Schlurmann M, Hausen K (2007) Motoneurons of the flight power muscles of the blowfly *Calliphora erythrocephala*: Structures and mutual dye coupling. J Comp Neurol 500:448-464.

Siegler MVS, Phong MP, Pousman CA (1991) Motor neurons supplying hindwing muscles of a grasshopper: Topography and distribution into anatomical groups. J Comp Neurol 310:342-355.

Sprayberry JDH (2009) Responses of descending visually-sensitive neurons in the hawkmoth, *Manduca sexta*, to three dimensional flower-like stimuli. J Insect Sci 9:7.

Strausfeld NJ, Seyan HS (1985) Convergence of visual, haltere, and prosternal inputs at neck motor neurons of *Calliphora erythrocephala*. Cell Tissue Res 240:601-615.

Taube JS, Bassett JP (2003) Persistent neural activity in head direction cells. Cereb Cortex 13:1162-1172.

Vafopoulou X, Terry KL, Steel CGH (2010) The circadian timing system in the brain of the fifth larval instar of *Rhodnius prolixus* (Hemiptera). J Comp Neurol 518:1264-1282.

Vitzthum H, Homberg U (1998) Immunocytochemical demonstration of locustatachykinin-related peptides in the central complex of the locust brain. J Comp Neurol 390:455-469.

Vitzthum H, Homberg U, Agricola H (1996) Distribution of Dip-allatostatin I-like immunoreactivity in the brain of the locust *Schistocerca gregaria* with detailed analysis of immunostaining in the central complex. J Comp Neurol 369:419-437.

Vitzthum H, Müller M, Homberg U (2002) Neurons of the central complex of the locust *Schistocerca gregaria* are sensitive to polarized light. J Neurosci 22:1114-1125.

von Philipsborn A, Labhart T (1990) A behavioural study of polarization vision in the fly, *Musca domestica*. J Comp Physiol A 167:737-743.

Wehner R (1992) Arthropods. In: Animal Homing. (Papi F, ed.), pp. 45-144. Chapman and Hall, London.

Wehner R (2003) Desert ant navigation: how miniature brains solve complex tasks. J Comp Physiol A 189:579-588.

Wehner R, Labhart T (2006) Polarisation vision. In: Invertebrate Vision (Warrant E, Nilsson DE, eds), pp 291-348. Cambridge University Press.

Wehner R, Rossel S (1985) The bee's celestial compass – a case study in behavioural neurobiology. Fortschr Zool 31:11-53.

Wertz A, Borst A, Haag J (2008) Nonlinear integration of binocular optic flow by DNOVS2, a descending neuron of the fly. J Neurosci 28:3131-3140.

Wertz A, Haag J, Borst A (2009a) Local and global motion preferences in descending neurons of the fly. J Comp Physiol A 195:1107-1120.

Wertz A, Gaub B, Plett J, Haag J, Borst A (2009b) Robust coding of ego-motion in descending neurons of the fly. J Neurosci 29:14993-15000.

Williams JLD (1975) Anatomical studies of the insect central nervous system: A ground-plan of the midbrain and an introduction to the central complex in the locust, *Schistocerca gregaria* (Orthoptera). J Zool (Lond) 176:67-86.

Yamawaki Y, Toh Y (2009) Responses of descending neurons to looming stimuli in the praying mantis *Tenodera aridifolia*. J Comp Physiol A 195:253-264.

Supporting Online Material for

Polarization Sensitive Descending Neurons in the Locust: Connecting the Brain to Thoracic Ganglia

Ulrike Träger and Uwe Homberg

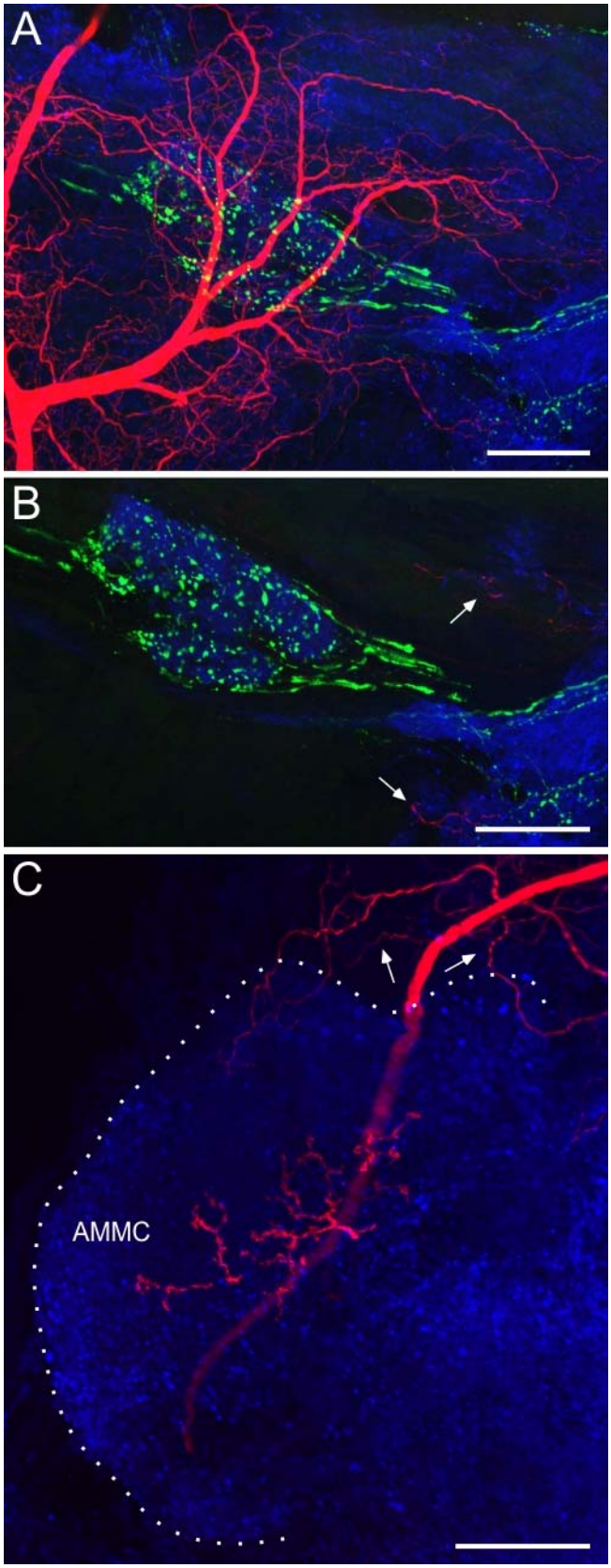

Supplemental figure 1. Morphological details of an ipsilaterally descending neuron. Maximum intensity views of optical sections (frontal plane, thickness 2 µm) from confocal image stacks showing anti-synapsin staining (blue) and anti-PDH staining (green) of distinct ramification areas of the same neuron stained with Neurobiotin (red). ***A,*** Maximum intensity projection of 78 optical sections showing ramifications around the posterior optic tubercle (POTu) which is marked with the anti-PDH antibody. ***B,*** Maximum intensity projection of optical sections from the data stack in ***A*** that show the POTu. A few arborizations from the descending neuron (red) are visible in the posterior protocerebrum around but not within the POTu (arrows). ***C,*** Maximum intensity projection of two combined stacks (76 optical sections), showing varicose arborizations in the antennal mechanosensory and motor center (AMMC). Some dendritic arborizations are visible dorsally from the AMMC. Scale bars: 40 µm.

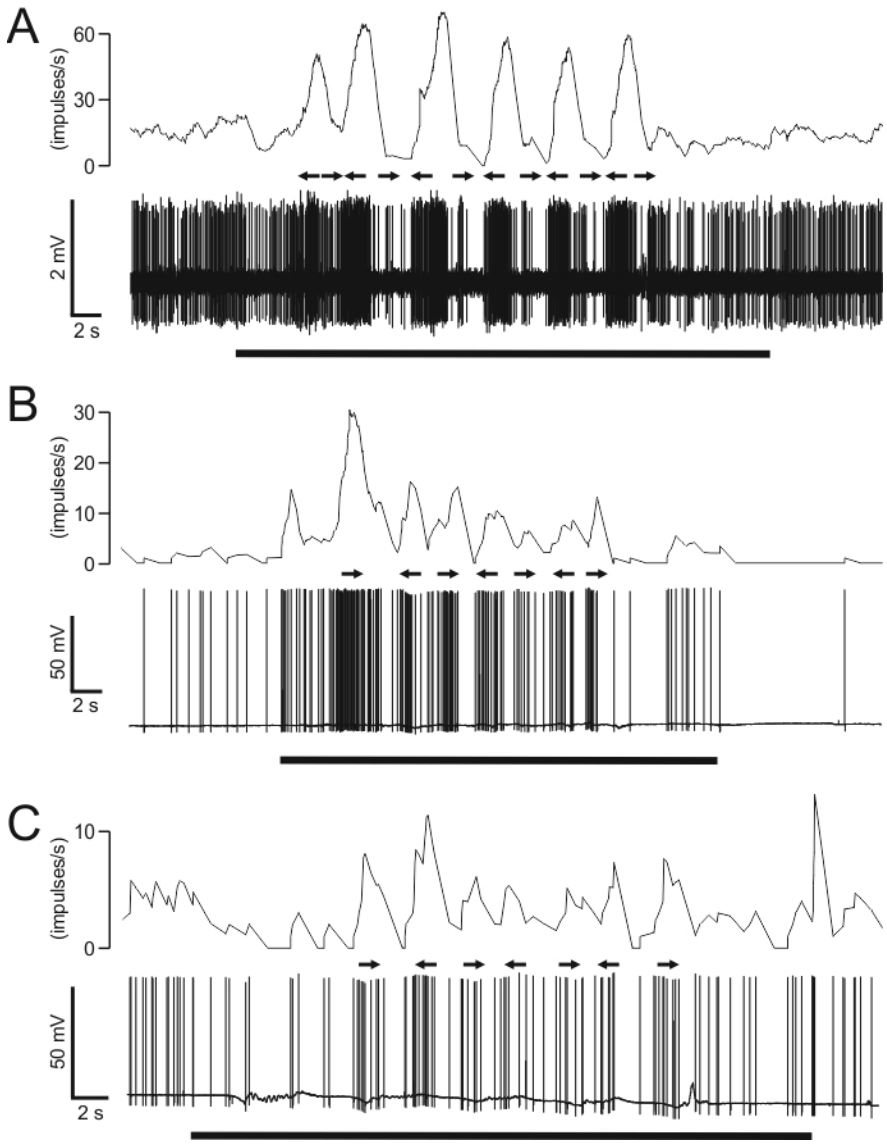

Supplemental figure 2. Responses of the descending neurons to a moving black and white grating presented in front of the animal. A small cardboard with black and white stripes was moved by hand from left to right and vice versa under unpolarized light condition (black bar). Owing to manual stimulation it was not possible to define the duration of each stimulus. Black arrows indicate movement direction of the pattern as seen by the locust. ***A,*** Recording from an ipsilaterally descending neuron in the left brain hemisphere. The neuron was excited by movement from right to left and shows inhibition to moving bars from left to right. ***B,*** Recording from a contralaterally descending brain neuron of the right brain hemisphere. The neuron was activated during movements in both directions. The response decreased with repetition of stimuli. ***C,*** Responses from a descending SOG neuron to a moving grating. The neuron showed weak activations to movements in both directions.

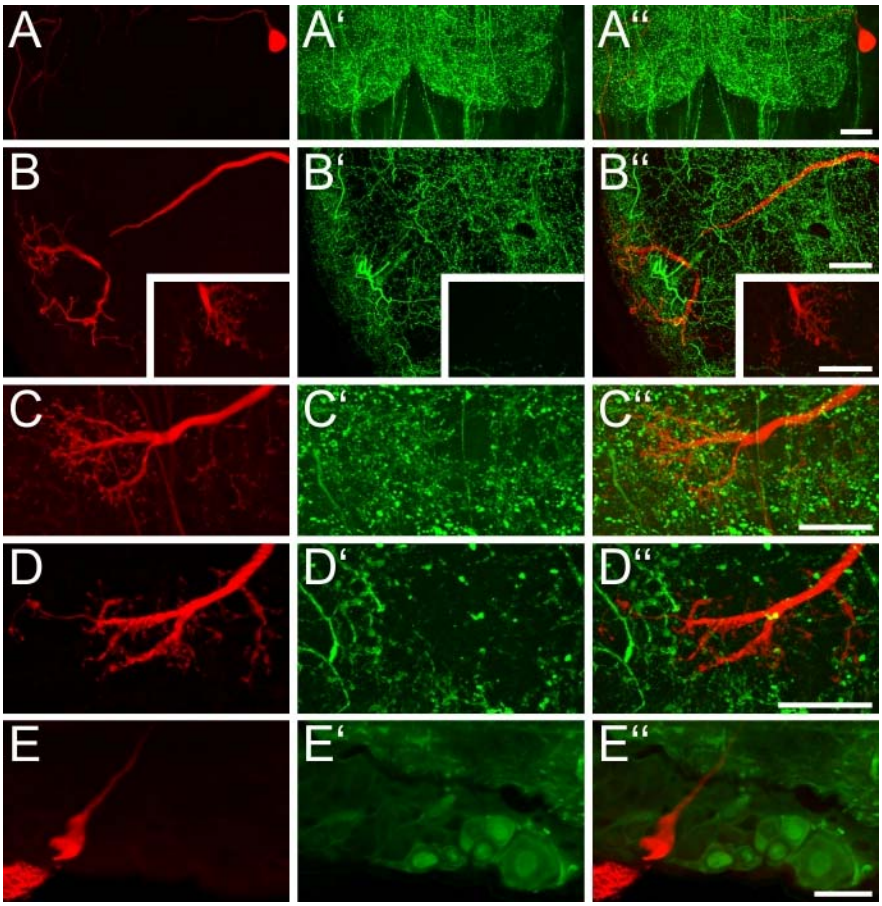

Supplemental figure 3. Confocal images of 130-µm sections showing parts of Neurobiotin stained descending SOG neurons (red) combined with immunostaining using antisera against FMRFamide, serotonin, Lom-TK II, AST-A or GABA (green). The Neurobiotin stained somata and ramifications are shown in A-E, the immunostainings are shown in ***A'-E',*** and the combined illustrations are shown in ***A''-E''***. None of the tested neuroactive substance is localized in the stained neurons. ***A,*** Soma and part of the primary neurite in the suboesophageal ganglion (SOG). FMRFamide immunostaining is not present in the soma or axon of the neuron. ***B,*** Dendritic ramifications in the SOG and presynaptic terminals from the prothoracic ganglion (Pro-TG, inset). The labeled neuron does not show serotonin immunostaining. ***C, D,*** In the Pro-TG, presynaptic terminals with bleb-like endings do not show immunostaining for Lom-TK II (***C***) or AST-A (***D***). ***E,*** The soma of the SOG neuron does not exhibit GABA immunostaining. Scale bars: 40 µm.

Behavioral and Electrophysiological Evidence for a Role of Polarized Light in Optomotor Responses of the Desert Locust *Schistocerca gregaria*

Behavioral and Electrophysiological Evidence for a Role of Polarized Light in Optomotor Responses of the Desert Locust *Schistocerca gregaria*

Ulrike Träger[1], Bianca Backasch[1], Basil el Jundi[1], Ronny Rosner[1] and Uwe Homberg[1]
[1]*Fachbereich Biologie, Tierphysiologie, Philipps-Universität Marburg, D-35032 Marburg, Germany*

Träger U, Backasch B, el Jundi B, Rosner R, Homberg U. Behavioral and electrophysiological evidence for a role of polarized light in optomotor responses of the desert locust *Schistocerca gregaria.* Animals use optomotor responses to stabilize their optic flow. In the present study, we show that tethered locusts perform an optokinetic-like response to a dorsally presented rotating polarizer. The behaviour is characterized by alternating slow pursuit responses and fast turning against the rotation direction of the polarizer. These responses are largely mediated by photoreceptors in the polarization sensitive dorsal rim area of the eye. In addition, we performed intracellular recordings and show that particular neurons in the brain and descending from the brain respond only to one rotation-direction of rotating polarized light. The behavioural as well as the electrophysiological results indicate that the locust is able to perceive the rotation-direction of rotating polarized light. The directionally selective polarization-sensitive neurons are morphologically distinct from hitherto studied polarization-sensitive neurons in the locust nervous system and appear to be identical to previously studied motion-sensitive neurons. We propose that these neurons are involved in mediating the directionally-sensitive responses to the rotating polarizer. Together with their motion-sensitivity the neurons may be involved in maintaining flight balance in a featureless environment such as in the desert or over open seawater.

INTRODUCTION

During locomotion, a continuous flow of images moves across the retina of the observer. To stabilize this optic flow animals use control mechanisms, so-called optomotor responses, like turning in the direction of motion of a pattern to maintain a straight course (Kirschfeld 1997; Srinivasan et al. 1999; Srinivasan and Zhang 2000; Egelhaaf 2006; Borst et al. 2010). In classical experiments a pattern of vertical black and white stripes is rotated around the animal. This usually elicits a turning reaction of the animal that demonstrates that the animal is able to detect the movement of the visual environment on the basis of brightness cues. The optomotor reaction of insects to black-and-white patterns has been intensively studied (in addition to the reviews cited above: Götz 1972; Kien 1974a; David 1979; Järvilehto 1985; Egelhaaf and Borst 1993; Kirschfeld 1997; Rind and Simmons 1999; Rind, 2002). While the visual subsystems detecting image motion are usually believed to be color-blind in arthropods (Schlieper 1927; Srinivasan, 1985; Yamaguchi et al. 2008; Borst et al. 2010) evidence from crabs, honeybees, flies, backswimmers and waterstriders showed that optomotor responses can also be elicited by different *E*-vector patterns depending on the orientation of the polarization-sensitive microvilli systems in the eyes of these animals (Horváth and Varjú 2004; Wehner and Labhart 2006; Glantz 2008).

Rhabdomeric photoreceptors of insects and crustaceans are inherently sensitive to the *E*-vector direction of linearly polarized light owing to the tubular arrangement of the microvillar photoreceptor membrane (reviewed in Wehner and Labhart 2006; Horváth and Varjú 2004). While in most parts of the insect eye, rhabdomeric twist or misalignment of mircovilli results in low polarization sensitivity and thus avoids the perception of polarization-induced false colors, polarization sensitivity is often high in specialized dorsal rim areas of the compound eye facing the sky or, in aquatic insects, in a ventral or lateral eye region involved in polarotactic detection of water surfaces (reviewed in Horváth and Varjú 2004). In the dorsal rim area (DRA) of all insects studied, each ommatidium consists of photoreceptors with orthogonally oriented microvilli (Labhart and Meyer 1999; Horváth and Varjú 2004). These crossed *E*-vector analysers in the DRA are not parallel to each other, but form a fan-like array, and thus have different orientations especially suited for detection of varied and dynamic *E*-vectors in the celestial field of polarization (Wehner and Labhart 2006).

The desert locust *Schistocerca gregaria* has a particularly prominent DRA visible already with the unaided eye. When presented with a rotating polarizer from above, tethered flying locusts show polarotactic yaw-torque responses in an attempt to follow the changing *E*-vector orientation (Mappes and Homberg 2004). The *E*-vector orientation is detected by photoreceptors in the DRA of the locust, and well studied polarization-sensitive neurons relay that information to higher brain areas for further processing (Homberg and Paech 2002; Homberg 2004; Pfeiffer et al. 2005; Pfeiffer and Homberg 2007; Vitzthum et al. 2002; Träger et al. 2008; Heinze and Homberg 2007, 2008, 2009; Heinze et al. 2009). Descending neurons specialized for polarized light signaling provide this information to motor circuits in the thoracic ganglia (U Träger and U Homberg, submitted).

Wehner and Labhart (2006) reviewed the problem of detecting individual *E*-vectors, based on the presence of crossed *E*-vector analyzers in each ommatidium. The successive method implies that an

Correspondence to: Uwe Homberg, Fachbereich Biologie, Tierphysiologie, Universität Marburg, D-35032 Marburg, Germany (E-mail: homberg@staff.uni-marburg.de).

animal rotates its polarization-sensitive photoreceptor and thereby changes the orientation of its microvilli relative to the *E*-vector direction. In consequence, the receptor potential would exhibit sinusoidal modulations with maximal response occurring when the microvilli and the *E*-vector are in register (Wehner and Labhart 2006). In contrast, the simultaneous method implies that at least three photoreceptors with different *E*-vector tuning cooperate by simultaneously comparing their output signals (Wehner and Labhart 2006). Horváth and Varjú (2004) reviewed another possibility for the simultaneous method, the existence of two polarization-sensitive receptors with different microvilli orientations and, in addition, independent perception of the intensity or the degree of linear polarization. At present, it is unknown whether insects use the simultaneous or the successive method for *E*-vector detection.

In the present work, we show that the polarotactic response of tethered flying locusts to a rotating polarizer is a special case of an optomotor response. We show that locusts recognize the direction of rotation of a polarizer above their head by showing *E*-vector rotation- direction specific yaw-torque responses. In addition, we have identified several neuron types that respond rotation-direction specifically to a rotating polarizer. These neurons are strong candidates to mediate the rotation direction-specific behavior. The neurons were found in the brain and descending to thoracic motor centers and are distinct from the hitherto described neuronal elements of the polarization vision pathway in the locust brain.

METHODS

Animals

Experiments were performed on desert locusts (*Schistocerca gregaria*) obtained from a crowded laboratory colony at the University of Marburg. Locusts were raised under 12L:12D photoperiod and a temperature cycle of 28°C during the night and 35°C during the day at 50% relative humidity. Adult locusts with intact wings, legs and antennae of both sexes were used 1-3 weeks after imaginal molt.

Behavioral studies

EXPERIMENTAL SETUP. Locusts, whose heads were fixed with the pronotum by a droplet of wax on both lateral sides to prevent head moving without body reactions, were tethered dorsal side up by waxing a small metal pin to their pronotum. They were flown in front of a horizontal wind tunnel (Gewecke 1975) inside a flight chamber (34 × 24.5 × 26 cm) made of matt-black plastic material. For optimal flight performance, wind speed was adjusted at 3.0 m/s. Yaw torques produced by the flying locusts were measured by a yaw-torque meter (Preiss and Gewecke 1991; Mappes and Homberg 2004, 2007). Light was produced by a fluorescent lamp (Osram Dulux EL 5 W). It passed a horizontal diffuser and evenly illuminated a circular window in the ceiling of the flight chamber. The window was fitted with a linear polarizer (HN38S Polaroid, Cambridge, MA; irradiance 10.8 $\mu W/cm^2$) and provided a wide field stimulus of 54° visual angle centered in the zenith. Rotation of the filter (speed: 15°/s) was monitored through a photodiode covered by a polarization filter (invisible to the locust).

TESTING PROCEDURE. Before starting an experiment, the locusts were adapted to darkness for at least 30 min. After mounting in the flight chamber, each locust was given at least 5 min to become accustomed to the wind tunnel. Only animals showing regular wing beat and typical flight posture were used for experiments. A single experiment consisted of three full rotations of a filter in clockwise and counterclockwise directions. Experiments with the rotating polarizer were also performed on animals that had their compound eyes painted black except the ommatidia of the DRA (Marabu Decorlack matt, water-based).

DATA ANALYSIS. Yaw-torque responses of the animal were analyzed with custom designed scripts in MatLab (MathWorks, Natrick, MA, USA). Periodic changes in yaw-torque were analyzed by fast Fourier transformation. Given the 180° periodicity of the polarization stimulus, the amplitude (*S*) of the 180° peak of the Fourier spectrum was taken as a measure of the polarotactic response. Time intervals of efforts of the locust to turn left- or rightwards were statistically analyzed with the non-parametric Wilcoxon signed-rank test for paired groups ($p < 0.05$; SPSS for windows).

Intracellular recordings

RECORDINGS FROM THE BRAIN. Adult locusts were immobilized by cooling for a minimum of 20 minutes. Legs and wings were removed and animals were waxed to a metal holder (Pfeiffer et al. 2005). A bowl of wax was prepared around the head capsule. The head capsule was opened, and the brain was exposed. The head capsule was filled with locust saline (Clements and May 1974) at all times to prevent drying. For stabilization, the esophagus was cut and the gut was pulled out from the opened abdomen. To seal the animal, the abdomen was then contracted with tightly knotted threads. To support the brain from posterior, a wire platform was inserted between the esophageal connectives and was fixed at the bowl of wax. To allow recordings from the brain, the neural sheath was treated with pronase E (from *Streptomyces griseus*; Serva Company; Heidelberg, Germany) and was partly removed with forceps. A silver wire was inserted into the hemolymph/locust saline solution and served as reference electrode.

Intracellular recordings were performed with glass microelectrodes drawn from borosilicate capillaries (0.75 mm ID, 1.5 mm OD; Hilgenberg, Malsfeld, Germany; resistance of 60-190 MΩ) using a Flaming/Brown puller (P-97, Sutter, Novato, CA). Tips were filled with 4% Neurobiotin (Vector Laboratories, Burlingame, UK) in 1M KCl. Cell signals were amplified and filtered (10×, 2 kHz low-pass) with a custom build amplifier. Spikes were monitored with a custom made audiomonitor and visualized with an oscilloscope (Hameg HM 205–3, Frankfurt/Main, Germany). After sampling at a rate of 5 kHz with a Digidata CED 1401 (Cambridge Electronic Design, UK), signals were stored on a PC using Spike2 software (Cambridge Electronic Design, UK). A drifting baseline was compensated with a high pass filter if necessary. After recording neuronal responses, Neurobiotin was iontophoretically injected with a continuous depolarizing current of 1-3 nA for 1-5 minutes.

RECORDINGS FROM THE NECK CONNECTIVES. Adult locusts were anesthetized by cooling for 15-30 min and waxed onto a metal holder in horizontal orientation. In some cases the tibiae of the hind legs were cut off. A 3×5 mm window was cut dorsally into the pronotum and, after resection of gut and removal of tracheal air sacs, fat body and the tissue membrane between gut and ventral body cavity, the neck connectives between suboesophageal- and prothoracic ganglia were exposed. The neck connectives were manipulated with a glass hook into two channels of a rectangular platform (1×2 mm) made of platinum. To prevent desiccation the connectives were submersed in locust saline (Clements and May 1974) at all times.

Glass microelectrodes (see above; resistance of 10-50 MΩ) were filled at their tips with a 3% aqueous solution of Alexa 488- or Alexa 647-conjugated dextran (10 000 MW, anionic, fixable; Invitrogen, Karlsruhe, Germany) or with 4% Neurobiotin in 1 M KCl and backed up with 1 M KCl. Intracellular signals were amplified (10×) with a custom-made amplifier and monitored with an audiomonitor and a digital oscilloscope (Hameg HM 305). After sampling at a rate of 10 kHz with a Digidata 1322A (Molecular Devices, Sunnyvale, CA, USA), signals were stored on a PC using PClamp9 software (Molecular Devices). To compensate for shifts in baseline, some recordings were digitally high pass filtered. After recording, the tracer was injected iontophoretically into the cell with constant hyperpolarizing current (4-10 nA, 9-30 min, dextran) or constant depolarizing current (2 nA, 17 min, Neurobiotin).

VISUAL STIMULATION. Light stimuli were provided by a xenon arc (XBO 150 W) connected via a light guide (Schölly, Denzlingen, Germany; spectral range 400-800 nm) to a perimeter placed around the animal. Either a linear polarizer (HN38S Polaroid, Cambridge, MA) or a neutral density filter of equal transmission was moved into the light path (irradiance/angular size: 30.8 $\mu W/cm^2/4.7°$, recordings from the brain; 105 $\mu W/cm^2/3°$, recordings from the neck connectives). The polarizer was rotated via custom build hard- and software by 360° in counterclockwise and clockwise directions at a speed of 30°/s. An *E*-vector orientation parallel to the longitudinal axis of the animal was defined as 0°. The position of the light source could be moved along the perimeter to change elevation from 0° (stimulus from lateral direction) on either side of the animal up to the zenith (90°).

DATA ANALYSIS. Sampled spike trains were stored on PC and evaluated using Spike2 software (Cambridge Electronic Design, UK) with implemented, custom designed scripts. Action potentials were detected with threshold based event detection. By using a gliding average algorithm at a bin size of 2 s, the detected events could be visualized as mean frequency. Mean background activities during darkness were obtained from counts of spikes in a defined time interval (usually 12 s) before and between visual stimuli divided by the respective time. Neuronal responses to polarized light were analyzed using Oriana 2.02a (Kovach Computing Services, Anglesey, UK) for circular statistics, and Origin 6.0 (Microcal, Northhampton, CA) was used for creating circular activity plots. Events within each 360° rotation of the polarizer were assigned a corresponding *E*-vector angle to quantify responses to polarized light. A list of these angles was exported for each *E*-vector rotation and all individual and combined rotations of each neuron were tested statistically for polarization sensitivity. If the distribution of these angles was significantly different from randomness (Rayleigh-test for axial data), a neuron was rated polarization sensitive. The mean angle of the distribution was defined as the Φ_{max}-value of that neuron.

HISTOLOGY. After recording from the neck connectives the animal was transferred to a moist chamber and kept at 4°C over night, to allow diffusion of the tracer. On the next day, the brain and ventral nerve cord, without the free abdominal ganglia were dissected out and fixed in a mixture of 4% paraformaldehyde, 0.25% glutaraldehyde and 2% saturated picric acid (in 0.1 M phosphate buffer) over night at 4°C. When recordings were made from the brain, these brains were dissected out immediately after injection and fixed in the same way as described above. Ganglia were processed as whole mounts. They were rinsed 4 × 15 min in PBS, dehydrated through an increasing ethanol series (25%, 50%, 70%, 90%, 95%, 100%; 15 min each), transferred to a 1:1 mixture of ethanol and methylsalicylate for 15 min and finally cleared in methylsalicylate for at least 45 min. When Neurobiotin was injected into the neurons, ganglia were incubated with Cy3-conjugated Streptavidin (Dianova, Hamburg, Germany; 1:1000) for three days at 4°C in PBT (PBS, including 0.5% Triton X-100) followed by rinsing with PBT (3 × 20 min) and PBS (2 × 20 min). Ganglia were finally mounted in Permount (Fisher Scientific, Pittsburgh, PA) between two coverslips. To avoid compressions, adhesive strips were used as spacers. Neurons were scanned with a confocal laser scanning microscope (CLSM; Leica TCS-SP2) at minimal pinhole size and intervals of 3-4 µm with a 10× oil immersion objective (HC PL APO 10×/0.4 Imm Corr CS; Leica, Bensheim, Germany). Reconstructions based on the data stacks were performed by using Adobe Photoshop CS2. For detailed analysis of neuronal morphologies, selected brains were rehydrated and sectioned as described by Heinze and Homberg (2008). The main step was the incubation of brain sections with a monoclonal mouse antibody against synapsin I (SYNORF1) for labeling of neuropil structures. After scanning at 1024 × 1024 pixel resolution with a CSLM (Leica TCS SP5), the further processing of the image stacks and reconstructions of the neurons were performed with the Amira 4.1.2 software (Visage Imaging, Fürth, Germany). Finally, the 3D reconstruction of the neurons were performed with the *SkeletonTree* tool. For details see el Jundi et al. (2010). Volume rendering visualization and maximum intensity projections of parts of the neurons were displayed in Amira 4.1.2.

RESULTS

Behavioral studies

We tested yaw-torque responses of tethered flying locusts that were illuminated from above through a rotating polarizer. The readiness of the locusts to fly was highly variable and did not depend on sex. For evaluation and analysis, flights were included only if locusts flew constantly without interruptions for three full rotations of the filter. As criteria for a clear polarotactic response, the amplitude (S) of the 180°-peak of the Fourier spectrum had to be at least two times higher than the mean of all other peaks of the Fourier spectrum, and, furthermore, the 180° peak was in all cases the highest peak of the Fourier spectrum within the considered range.

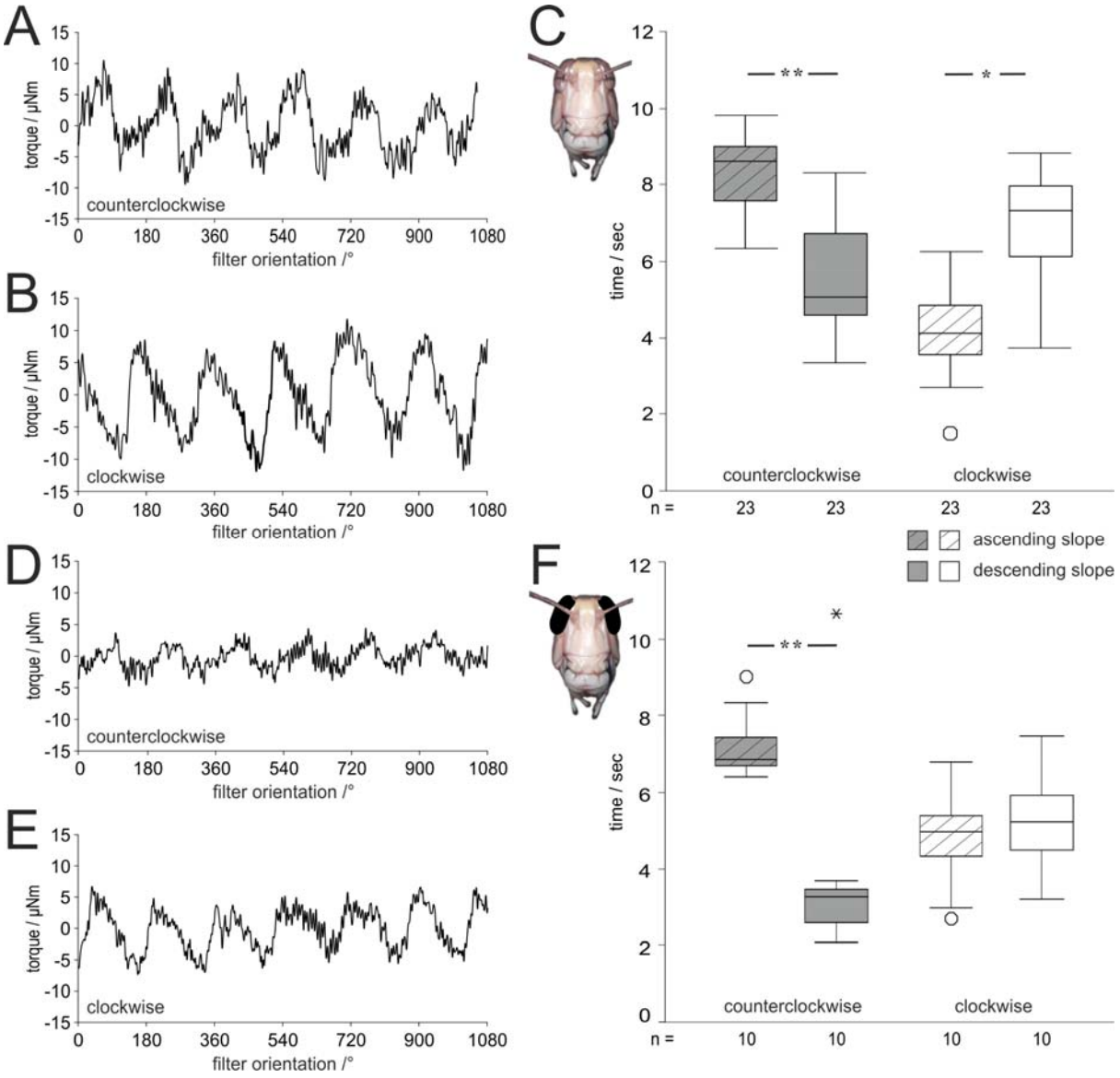

FIG. 1. Yaw torque responses of tethered flying locusts that were stimulated through a dorsally presented rotating polarization filter. **A,B,** Flight traces from a locust with unoccluded eyes during stimulation with a polarizer turning counterclockwise (**A**) or clockwise (**B**). Ascending slopes towards positive yaw torques in these and the graphs in D,E correspond to right turns (counterclockwise) of the locust and descending slopes towards negative yaw torques to left turns (clockwise). **C,** Mean time durations of ascending and descending slopes from untreated locusts during clockwise and counterclockwise rotations. The boxes include 50% of data and were bordered by the 25% and 75% quartile. The black line within the box stand for the median and the error bars for the highest and lowest value respectively. Circles indicate outliers whereas big stars stand for extreme values. Times of ascending slopes are significantly longer than times of descending slopes during counterclockwise rotations (grey boxes, n = 23, $p = 0.001$; Wilcoxon signed-rank test), while during clockwise rotations, descending slopes last longer than ascending slopes (white boxes, n = 23, $p = 0.023$). **D,E,** Flight traces from a locust during stimulation with a zenithal polarizer turning counterclockwise (**D**) and clockwise (**E**) after painting the non-DRA parts of the eyes black. **F,** For black-painted non-DRA's, time duration under counterclockwise rotations of the polarizer differ significantly between ascending and descending slopes (grey boxes, n = 10, $p = 0.007$). Under clockwise rotations (white boxes) differences were not significant.

POLAROTAXIS. For analysis of yaw-torque under the rotating polarizer, two conditions were evaluated. Animals of the first group (n = 23) flew with untreated eyes during clockwise and counterclockwise rotations of the polarizer. The locusts responded to the rotating polarizer by periodically changing yaw torque corresponding to the 180° periodicity of the rotating polarizer as shown by Mappes and Homberg (2004). Close inspection of the flight traces showed that the plotted yaw torque responses rather than being sinusoidal had a sawtooth shape resulting from alternating slow pursuit movements following the rotating polarizer and fast saccadic movements against the rotation of the polarizer (Fig. 1A,B). For quantitative evaluation of the two components, we measured the time intervals the locust spent turning in each direction, between the maximum negative and the maximum positive yaw torques (ascending slopes) and vice versa (descending slopes) and compared the mean time intervals with each other (Fig. 1C). For both rotation directions of the polarizer, the pursuit responses following the rotation direction lasted significantly longer than the saccadic responses against the rotation direction (Fig. 1C).

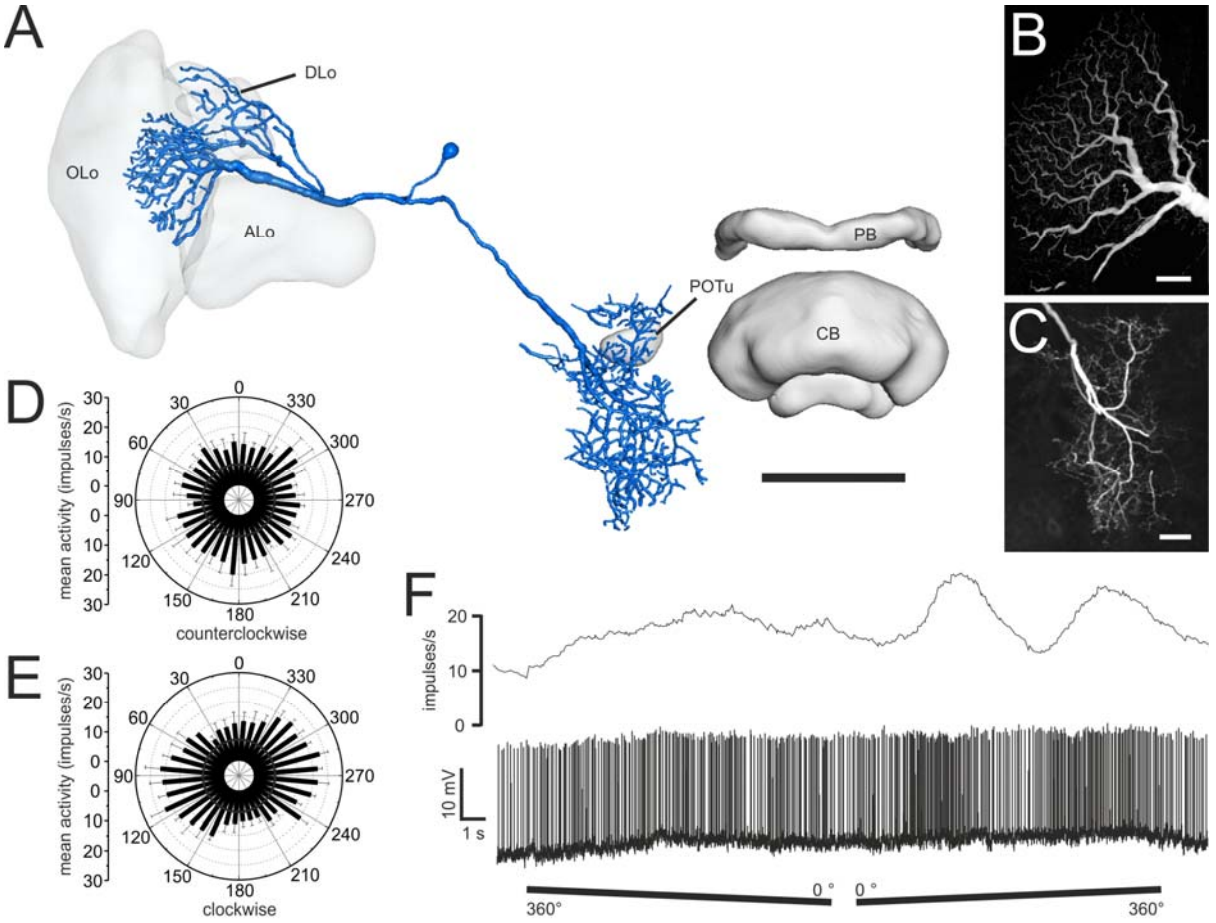

FIG. 2. Morphology and physiology of a rotation direction selective polarized light sensitive neuron in the brain of the locust. **A**, Frontal three-dimensional reconstruction of the neuron from a confocal image stack of the Neurobiotin-injected neuron. Dendritic ramifications are in the outer (OLo) and dorsal lobes (DLo) of the lobula, axonal ramifications in the posterior protocerebrum near the posterior optic tubercle (POTu). **B**,**C**, Details of arborizations of the neuron. Maximum-intensity projections of confocal image stacks reveal that arborizations in the posterior lobula are of smooth appearance (**B**) whereas endings in the posterior protocerebrum are varicose (**C**). **D,E,** Circular diagrams of mean frequencies of action potentials of the neuron plotted against *E*-vector orientation during stimulation with a rotating polarizer; counterclockwise (**D**; n = 4; error bars = SD; bin size 10°; $p = 0.445$) and clockwise (**E**; n = 4; error bars = SD; bin size 10°; $\Phi_{max} = 103°$, $p = 1.6 \times 10^{-9}$). Black circles indicate background activity of the neuron. **F,** Spike train (lower trace) and mean spiking frequency (upper trace; gliding average with bin size of 2s) of the neuron during a counterclockwise (360°-0°) and a clockwise (0°-360°) rotation of the polarizer presented at an elevation of 45° ipsilaterally. ALo, anterior lobe of the lobula; CB, central body; PB, protocerebral bridge. Scale bars: **A,** 200 µm; **B,** 25 µm; **C,** 100 µm.

Locusts from the second group flew with compound eyes black painted except the DRA (non-DRA) under the same stimulation as group one. In this second condition the willingness of the locusts to orientate was highly decreased, so that only ten locusts with flights under clockwise and counterclockwise rotations could be evaluated. These locusts showed comparable responses to the locusts with untreated eyes described above, but generally lower yaw-torque amplitude values (Fig. 1D,E). Under counterclockwise rotations of the polarizer, the ascending and descending slopes differed significantly from each other, but under clockwise rotations ascending and descending slopes were not significantly different in time duration (Fig. 1F).

Rotation direction-selective polarized light sensitive neurons

The ability of locusts to distinguish between clockwise and counterclockwise rotations of the polarizer requires that neurons in the nervous system likewise respond differently to clockwise and counterclockwise rotations of the polarizer. To date, all recordings from neurons in the polarization vision system of the locust brain showed coding for *E*-vector orientations but apart from minor differences in *E*-vector tuning, the responses to clockwise and counterclockwise rotations of the polarizer were indistinguishable (Vitzthum et al. 2002; Pfeiffer et al. 2005; Heinze and Homberg 2007, 2009; Heinze et al. 2009). Interestingly, a few types of neuron that are anatomically distinct from *E*-vector-orientation coding cells were highly sensitive to the direction of *E*-vector rotation.

BRAIN NEURONS. Neurons of three recordings showed direction dependent responses to stimulation with the rotating polarizer. All three neurons were

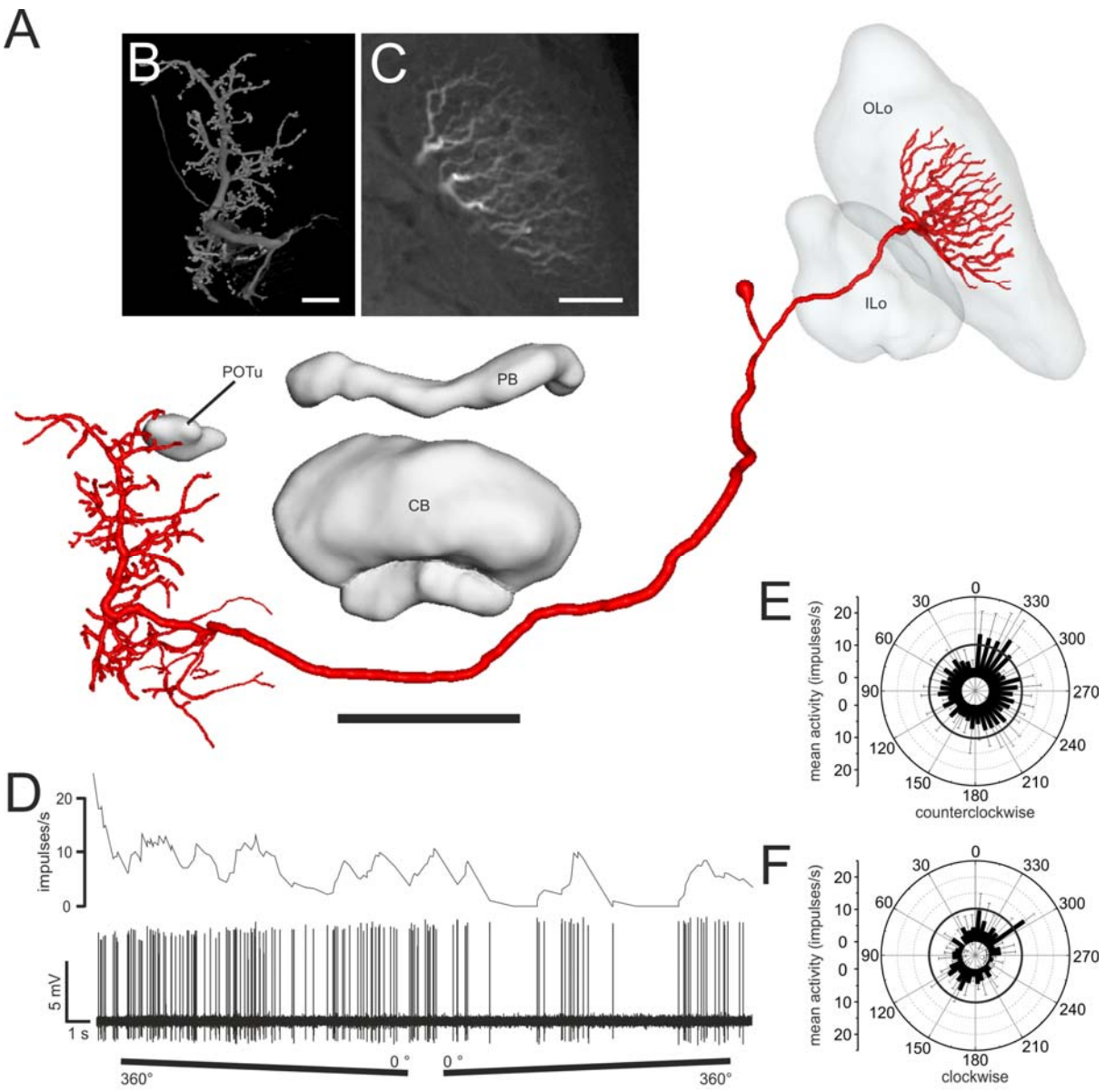

FIG. 3. Morphology and physiology of a directionally-selective polarized-light sensitive neuron that crosses the midline of the locust brain. **A**, Frontal three-dimensional reconstruction of the neuron from stacks of confocal sections. Dendritic ramifications are in the outer lobe of the lobula (OLo). The axon crosses the midline of the brain, and gives rise to axonal ramifications in the posterior protocerebrum near the posterior optic tubercle (POTu). **B**,**C**, Details of arborizations of the neuron. Maximum-intensity projections of confocal image stacks reveal varicose endings in the posterior protocerebrum (**B**) whereas the volume rendering 3D visualization show that arborizations in the posterior lobula are of smooth appearance (**C**). **D,** Spike train (lower trace) and mean spiking frequency (upper trace; gliding average with bin size of 2s) of the neuron during a counterclockwise (360°-0°) and a clockwise (0°-360°) rotation of the polarizer presented at an elevation of 60° ipsilaterally. **E,F,** Circular diagrams of mean frequencies of action potentials of the neuron plotted against *E*-vector orientation during stimulation with a rotating polarizer; counterclockwise (**E**; n = 4; error bars = SD; bin size 10°; $p = 0.424$) and clockwise (**F**; n = 4; error bars = SD; bin size 10°; $\Phi_{max} = 151°$, $p = 6.4 \times 10^{-8}$). Black circles indicate background activity of the neuron. CB, central body; ILo, inner lobe of the lobula; PB, protocerebral bridge. Scale bars: **A,** 200 µm; **B,C,** 50 µm.

recorded near their axonal projections in the central brain. One neuron resembled LDSMD cells of Rind (1990), also described as lobula protocerebrum neurons LP6 and LP7 by Gewecke and Hou (1993). Its soma was located near the optic stalk postero-lateral to the calyces. The primary neurite projected toward the optic stalk where it joined the main axonal fiber (Fig. 2A). Dendritic processes extended in a fan-like fashion throughout the inner layer of the outer lobe of the lobula (OLo; Fig. 2B); a second tree of ramifications, not described for the LDSMD/LP6/7 cells innervated the dorsal lobe of the lobula (DLo; Fig. 2A). Axonal projections of the neuron with varicose ramifications were confined to areas in the ipsilateral posterior protocerebrum near, but not within, the posterior optic tubercle (POTu; Fig. 2A,C). The neuron responded only to polarized light presented from 45° ipsilateral elevation. The background activity of this cell was 7.3 ± 3.6 impulses per second (mean frequency ± SD). Under polarized light stimulation the neuron responded with excitation above background level but did not show polarization-opponency. The

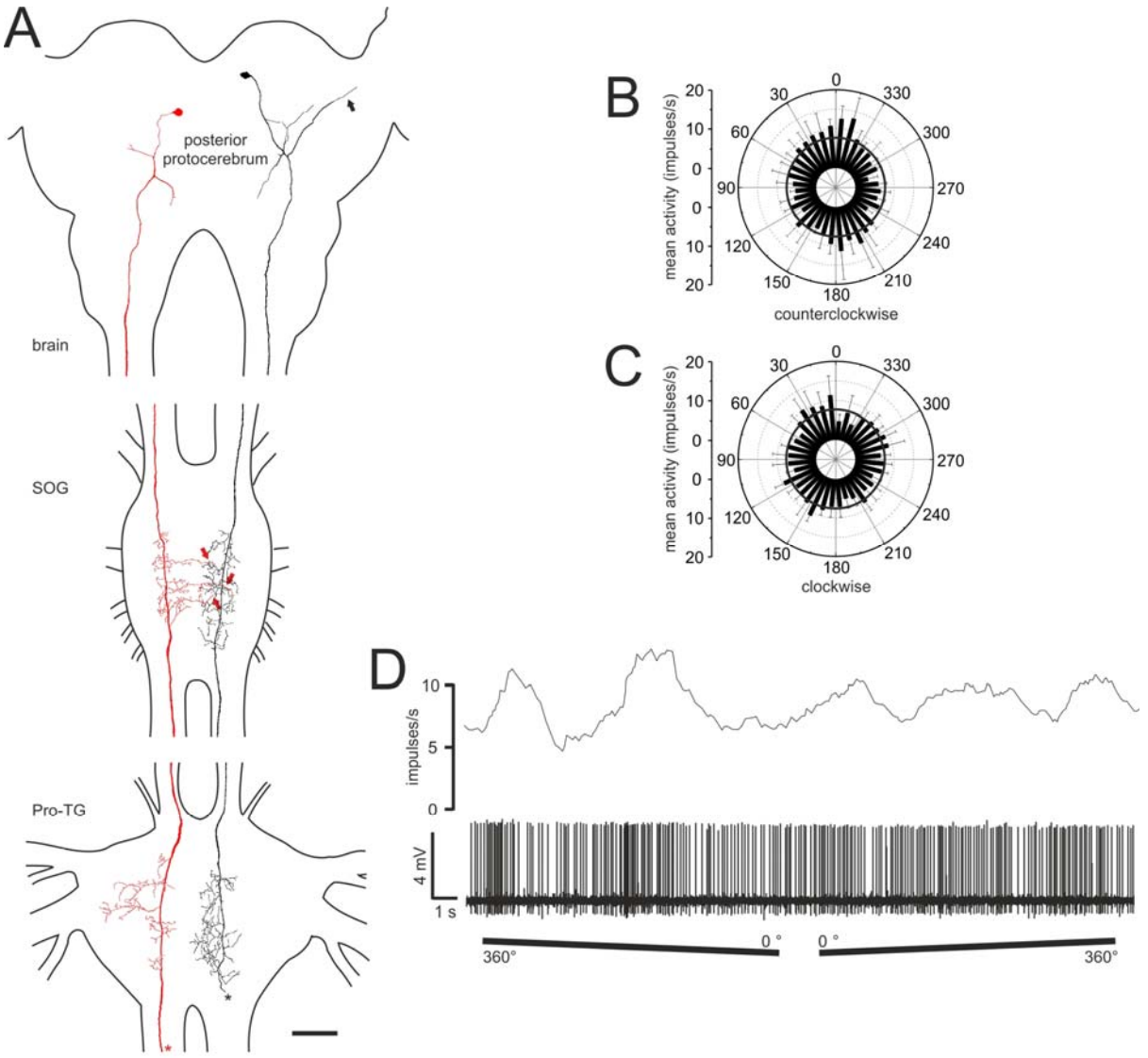

FIG. 4. Morphology and physiology of directionally-selective polarized light sensitive descending neurons. **A,** Frontal reconstructions of both neurons reveal presumably input regions in the ipsilateral posterior protocerebrum. In addition, one neuron sends a fiber toward the posterior optic lobe (black arrow). Varicose endings are present in dorsal parts of the suboesophageal (SOG) and prothoracic ganglion (Pro-TG). One neuron extends processes into the contralateral hemisphere of the SOG (red arrows). The axonal processes of both neurons could not be traced beyond the connective between pro- and mesothoracic ganglion (asterisks). **B,C,** Mean activities of another neuron during 360° rotations of the zenithal polarizer plotted against *E*-vector orientation; counterclockwise (**B**; n = 5; error bars = SD; bin size 10°; Φ_{max} = 7°, p = 3.3 × 10^{-5}) and clockwise (**C**; n = 5; error bars = SD; bin size 10°; p = 0.7). Black circles indicate background activity of the neuron. **D,** Mean activity and intracellular recording trace during counterclockwise (360°-0°) and clockwise (0°-360°) rotations of the dorsally presented polarization filter (same neuron as in B,C). Scale bar: 200 µm.

responses to clockwise and counterclockwise rotations of the polarizer differed markedly. During counterclockwise rotations of the polarizer, the neuron was excited irrespective of *E*-vector orientation (Fig. 2D,F). In contrast, the excitatory response to clockwise rotations was strongly dependent on *E*-vector orientation (Fig. 2E,F), with a preferred *E*-vector orientation (Φ_{max}) at 103° (p = 1.6 × 10^{-9}; n = 4; Fig. 2E).

Two other morphologically indistinguishable neurons had axonal projections with varicose endings exclusively in the contralateral posterior protocerebrum, near the POTu like the ipsilateral neuron (Fig. 3A,B), and resembled the lobula protocerebrum neuron LP10 of Gewecke and Hou (1993). The neurons had dendritic arborizations in the inner layer of the outer lobe of the lobula (OLo; Fig. 3A,C) but, in contrast to LP10, identified in the migratory locust, lacked additional ramifications in the inner lobe of the lobula. Illumination led to general weak reduction in background spiking activity (Fig. 3D-F). The neurons responded only to polarized light when presented in the ipsialateral hemisphere at elevations of 30°-90°. *E*-vector sensitivity was significant during clockwise rotations (Φ_{max} = 151°, p = 6.4 × 10^{-8}; n = 4; Fig. 3F) but not during counterclockwise rotations of the polarizer (p = 0.4; n = 4; Fig. 3E). The physiological properties of the other contralateral neuron are not certainly estimable because recording properties were not best suited.

DESCENDING NEURONS. Five recordings from descending neurons showed directionally sensitive responses to polarized light. Two of these neurons could be stained partly (Fig. 4A). Both neurons had their somata in the pars intercerebralis and descended through the ipsilateral connective into the suboesophageal ganglion and further into the prothoracic ganglion. Fibers continued into the connective between pro- and mesothoracic ganglion but could not be traced further. Both neurons had presumably dendritic arborizations in the posterior protocerebrum and varicose endings in dorsal parts of the suboesophageal and prothoracic ganglion. Averaged background activities in the descending neurons ranged from 0.9 ± 0.6 (red neuron in Fig. 4A) to 12.7 ± 3.3 impulses per second (not shown). Responses to polarized light were excitatory and as found in the brain neurons lacked polarization-opponency. In all neurons, the directedness in the response to the rotating polarizer corresponded with the recording side. Three neurons, recorded from the left connective, showed polarization sensitivity to clockwise rotations of the polarizer (mean $p_{clockwise} = 3.7 \times 10^{-3} \pm 0.004$, n = 3) but not to counterclockwise rotation (mean $p_{counterclockwise} = 0.649 \pm 0.199$, n = 3). In contrast, two neurons recorded from the right connective showed *E*-vector-depended responses only to counter-clockwise rotations (mean $p_{counterlockwise} = 4.5 \times 10^{-3} \pm 0.006$ and mean $p_{clockwise} = 0.48 \pm 0.371$, n = 2; Fig. 4B-D). The preferred *E*-vector orientations of the counterclockwise-sensitive descending neurons were 7° (Fig. 5A) and 115° (black neuron in Fig. 4A) whereas the clockwise-sensitive descending neurons preferred 64° (red neuron in Fig. 4A), 105° and 112° respectively. All descending neurons were stimulated with dorsally presented polarized light (90° elevation) and no other positions were tested.

DISCUSSION

Optomotor responses serve to stabilize insect flight (Horváth and Varjú 2004, Egelhaaf 2006) - here we show that, like rotations of intensity contrasts (Schlieper 1927; Varjú 1975) rotations of dorsal *E*-vector orientations elicit optomotor responses that may be useful for flight control in featureless environments like deserts or open water. Neurons tuned to a particular *E*-vector rotation direction were identified that may be involved in mediating these responses.

Behavioral study

We presented tethered flying locusts, untreated or with black-painted eyes except the DRAs, polarized light through a rotating polarizer. Under both conditions locusts showed slow pursuit responses following the rotating polarizer, alternating with fast saccadic responses against the rotation of the polarizer. The locust thus performs an optokinetic response similar to an optokinetic nystagmus during rotation of black and white stripes or a single stripe around the animal (Schlieper 1927; Varju 1975; Kien and Land 1978; Barnes and Nalbach 1993 for review). Kien and Land (1978) described that locusts either move legs, body and head to compensate for movements of a rotating striped drum, or remain stationary and attempt to compensate by head movements only. During compensation with their heads only, they show slow stimulus following reactions, alternating with fast motions in opposite direction typical for a nystagmus. Crabs also perform visually evoked compensatory optokinetic responses produced by movement of a striped drum around the animal (Barnes and Nalbach 1993). A regular sequence of slow pursuit and saccadic reset movements is elicited by rotation of such a pattern about the yaw axis. The eye of the crab follows the movement of the stripes and then flicks back at intervals to their staring position. Varjù (1975) describes the responses of the beetle *Tenebrio molitor* to a rotating striped drum, too. If plotting the angular position of the walking beetle against time, a sawtooth response pattern results comparable to the yaw torque responses of locusts to a rotating polarizer. Varjú (1975) also described the influence of angular velocity on the response. With increasing velocities the animal lags more and more behind the stripe and suddenly performs a fast turn against the direction of the drum's movement and fixates again the next stripe and follows it.

Tethered locusts tested here show similar optokinetic responses with distinct fast and slow phases of nystagmus to a dorsally rotating polarizer. We interpret the significant differences in the medians of measured time intervals as clear criteria of recognition of the rotating direction of the stimulus. Accordingly, the locust is able to distinguish between counterclockwise and clockwise rotations of the stimulus. In counterclockwise rotations, this effect was also observed when the compound eyes except the DRA (non-DRAs) were painted black. Probably because of the small sample size, the clockwise rotations were not significant. Therefore, additional experiments with black-painted non-DRAs will have to show whether the DRA mediates the nystagmus-like optomotor response to the rotating polarizer.

Rotation direction-selective polarization sensitive neurons

A variety of motion-sensitive neurons have been described in the locust brain (Kien 1974b; Hensler and Rowell 1990; Gewecke and Hou 1993; Stern and Gewecke 1993; Rind 2002 for review). These neurons are sensitive to large-field motion of intensity contrasts and are usually sensitive to particular motion directions. The neurons characterized here are novel in that they are sensitive to the direction of rotation of a rotating polarizer. We found neurons with these characteristics not only in the brain but also with descending axons to the ventral nerve cord, providing rotation-direction specific polarization information to

thoracic motor centers. Putative output regions were concentrated in dorsal parts of the thoracic ganglia where the motor neurons receive their input (Schlurmann and Hausen 2007; Siegler et al. 1991).

The rotation-direction selective neurons in the brain show a remarkable morphological similarity to directionally selective motion detectors from the lobula termed LDSMDs, described by Rind (1990a, 2002) and the lobula-protocerebrum-neurons (LP neurons) by Gewecke and Hou (1993). The neurons recorded here clearly belong to these types of motion sensitive neurons; the ipsilateral neuron is similar to the LDSMD or LP6/7 neuron whereas the contralateral neurons are similar to the LP10 neuron, but we have not tested motion stimuli like moving gratings or bars. Our results supplement the physiological properties of these motion-sensitive neurons from the lobula. Both Rind (1990a) and Gewecke and Hou (1993), distinguished two subtypes of neuron, which were directionally sensitive to motion. The LDSMD(F)/LP7 neuron is sensitive to forward movements across the ipsilateral eye, whereas the LDSMD(P)/LP6 neuron is sensitive to backward motion over the ipsilateral eye (Rind 1990a; Gewecke and Hou 1993). Both cell types showed only minor differences in branching pattern, which makes comparisons with the ipsilaterally projecting polarization-sensitive neuron in this study difficult. Gewecke and Hou (1993) showed that the LP6/LP7 and LP10 neurons respond exclusively to ipsilaterally presented stimuli. Two of our recorded brain neurons responded only to polarized light presented from 30-90° ipsilateral elevation. Hence, we suggest that these two brain neurons receive polarization information mainly from the contralateral DRA, because each DRA receives input from the contralateral celestial hemisphere (Homberg and Paech 2002). Therefore, the polarization information may be transmitted across the midline from the contralateral eye. Polarization-sensitive, but motion-insensitive neurons that cross the brain midline and that are able to provide input to the lobula or previous stations are known from the medulla (Homberg and Würden 1997; Loesel and Homberg 2001). In summary, we suggest that the directionally selective motion detectors from the lobula are additionally able to differentiate between the rotation direction of polarized light presented through a linear polarizer. Furthermore, the similar output region within the posterior protocerebrum suggests that these neurons could provide information from both lobulae to the same downstream neurons.

Because of incomplete labeling of the descending neurons, comparisons with known descending neurons have to be preliminary. Rind (1990b) described a descending neuron, the protocerebral, descending direction-selective motion-detecting neuron (PDDSMD neuron) that shows direction-selective responses. The PDDSMD neuron has a preferred direction backward across the ipsilateral eye and forward across the contralateral eye. At least one of the neurons studied here, the black neuron in Fig. 4A, shares some morphological features with the PDDSMD neuron. Both neurons have arborizations towards the optic lobe, share a characteristic double-s-shaped course of the primary neurite, have a descending axon, and exclusively ipsilateral ramifications in the SOG and Pro-TG. The PDDSMD neuron descending through the left connective responds to a clockwise rotating stimulus around the yaw axis as viewed by the locust. The descending neurons in our study recorded from the left connective likewise only responded to clockwise rotations of the polarizer while the neurons recorded from the right connective only responded to counterclockwise rotations. Kien (1974b) also described directionally selective descending neurons that respond exclusively to one direction of horizontally rotating stripes, but because she performed some recordings on upright locusts and others on locusts with their ventral side up, it is hard to follow the explanation about defining the rotation-direction. Kien (1974b) described two descending neurons (B1, B2) per connective with the same directedness per connective, but opposite direction-sensitivities between the two connectives. Based on the different branching patterns of descending neurons in our study (Fig. 4A), we suggest that we recorded at least from two different types of descending neurons. That is comparable with the findings of Kien (1974b).

Role of polarized light in optomotor responses

Probably all types of directionally-selective polarization-sensitive neurons described in this study were mentioned in previous studies as directionally selective movement detector neurons related to black and white patterns (Kien 1974b; Rind 1990a; Gewecke and Hou 1993). This suggests that these neurons process congruent changes in the orientation of celestial *E*-vectors and movement of the environment during particular flight maneuvers and use these for maintaining flight balance. The ipsi- and contralaterally projecting lobula output neuron share overlapping projections in the posterior protocerebrum that, furthermore, appear to overlap with the dendritic ramifications of the descending neurons. These common projection areas suggest direct connections between these neurons that would be required for fast behavioral responses for maintaining flight balance. Correspondingly, Rind (1990a,b) demonstrated a monosynaptic connection between one of the LDSMD neurons and the PDDSMD neuron. In summary, we discovered a new physiological property of these directionally selective motion-detecting neurons: The detection of directionally selective polarization-sensitive stimuli.

E-vector detection in the locust

Our study, finally, provides some progress to the problem of detecting individual *E*-vectors discussed by Wehner and Labhart (2006) or Horváth and Varjú (2004). Single photoreceptor cells in the DRA or the

rest of the compound eye only detect differences in brightness or darkness. Motion sensitivity requires downstream neurons receiving input from neighboring photoreceptors or ommatidia with one of the two inputs delayed. The Reichardt elementary movement detector is the cardinal model mechanism underlying motion detection (reviews: Egelhaaf, 2006; Borst et al., 2010). Because locusts are not only able to detect the orientation of polarized light, but also the rotation direction of a dorsally rotating polarizer, a Reichardt-type elementary movement detector might not only operate for detecting moving intensity contrasts but, in the DRA, also for detecting moving *E*-vectors. Interestingly, in the locust and all other insects studied so far, ommatidia in the DRA are arranged in a fan-like orientation. Wehner (1989) has interpreted this arrangement as a peripheral sensory filter matching the arrangement of celestial *E*-vectors in the sky. As an alternative hypothesis, lateral interactions between adjacent ommatidial channels in a fan-like arrangement would be ideally suited to generate sensitivity to rotational movements of *E*-vector orientations above the animal as they occur during yaw movements. With rotational sensitivity, the polarization-vision system of the locust is clearly superior to a successive mechanism of *E*-vector detection as outlined by Wehner and Labhart (2006). The successive model of *E*-vector orientation assumes a global pooling of the light signal provided by all DRA photoreceptors and thus requires permanent screening movements of the animal to detect the *E*-vector orientation based on brightness differences. It would not allow the animal to determine the direction of rotation of a rotating polarizer. Our data therefore add indirect evidence to a simultaneous mechanism of *E*-vector detection through the instantaneous comparison of at least three independent channels of *E*-vector analysers as proposed by (Kirschfeld 1972).

ACKNOWLEDGEMENTS

We are grateful to Dr. Keram Pfeiffer for providing Spike2-scripts. We thank Christoph Busche for reconstruction of the brain neurons with AMIRA, Sebastian Richter and Manfred Peil for constructing the stimulation devices and control equipment, and Karl Heinz Herklotz and Martina Kern for raising desert locusts.

GRANTS

This work was supported by the Deutsche Forschungsgemeinschaft, Grant number: HO 950/18-1 and the Air Force Office of Scientific Research (AFOSR).

REFERENCES

Barnes W, Nalbach H. Eye movements in freely moving crabs: Their sensory basis and possible role in flow-field analysis. *Comp Biochem Physiol* 104A: 675-693, 1993.

Bartsch K. Polarization-sensitive photoreceptors of different spectral types in the compound eye of waterstriders. *Naturwissenschaften* 82: 292-293, 1995.

Borst A, Haag J, Reiff DF. Fly motion vision. *Annu Rev Neurosci* 33: 49-70, 2010.

Brunner D, Labhart T. Behavioural evidence for polarization vision in crickets. *Physiol Entomol* 12: 1-10, 1987.

Clements A, May TE. Studies on locust neuromuscular physiology in relation to glutamic acid. *J Exp Biol* 60: 673-705, 1974.

David CT. Optomotor control of speed and height by free-flying *Drosophila*. *J Exp Biol* 82: 389-392, 1979.

Egelhaaf M. The neural computation of visual motion information. In: *Invertebrate Vision*, edited by Warrant E, Nilsson D-E. Cambridge University Press, 2006, p. 399-461.

Egelhaaf M, Borst A. A look into the cockpit of the fly: visual orientation, algorithms, and identified neurons. *J Neurosci* 13: 4563-4574, 1993.

el Jundi B, Homberg U. Evidence for the possible existence of a second polarization-vision pathway in the locust brain. *J Insect Physiol* 56: 971-979, 2010.

Gewecke M. The influence of the air-current sense organs on the flight behaviour of *Locusta migratoria*. *J Comp Physiol* 103: 79-95, 1975.

Gewecke M, Hou T. Visual brain neurons in *Locusta migratoria*. In: *Sensory systems of arthropods*, edited by Wiese K, Gribakin FG, Popov AV, Renninger G. Basel: Birkhäuser, 1993, p. 119–144.

Glantz RM. Polarization vision in crayfish motion detectors. *J Comp Physiol A* 194: 565-575, 2008.

Götz KG. Processing of cues from the moving environment in the *Drosophila* navigation system. In: *Information Processing in the Visual Systems of Arthropods*, edited by Wehner R. Berlin; Springer-Verlag, 1972, p. 255-263.

Hassenstein B, Reichardt W. Systemtheoretische Analyse der Zeit, Reihenfolgen- und Vorzeichenauswertung bei der Bewegungsperzeption des Rüsselkäfers *Chlorophanus*. *Z Naturforsch* 11b: 513-524, 1956.

Heinze S, Homberg U. Maplike representation of celestial *E*-vector orientations in the brain of an insect. *Science* 315: 995-997, 2007.

Heinze S, Homberg U. Neuroarchitecture of the central complex of the desert locust: Intrinsic and columnar neurons. *J Comp Neurol* 511: 454-478, 2008.

Heinze S, Homberg U. Linking the input to the output: new sets of neurons complement the polarization vision network of the locust central complex. *J Neurosci* 29: 4911-4921, 2009.

Heinze S, Gotthardt S, Homberg U. Transformation of polarized light information in the central complex of the locust. *J Neurosci* 29: 11783-11793, 2009.

Hensler K, Rowell CHF. Control of optomotor responses by descending deviation detector neurons in intact flying locusts. *J Exp Biol* 149: 191-205, 1990.

Homberg U. In search of the sky compass in the insect brain. *Naturwissenschaften* 91: 199-208, 2004.

Homberg U, Paech A. Ultrastructure and orientation of ommatidia in the dorsal rim area of the locust compound eye. *Arthropod Struct Dev* 30: 271-280, 2002.

Homberg U, Würden S. Movement-sensitive, polarization-sensitive, and light-sensitive neurons of the medulla and accessory medulla of the locust, *Schistocerca gregaria*. *J Comp Neurol* 386: 329-346, 1997.

Horváth G, Varjú D. *Polarized light in animal vision*. Springer: Berlin, 2004.

Järvilehto M. The eye: Vision and perception. In: *Comprehensive Insect Physiology Biochemistry and Pharmacology. Volume 6 Nervous System: Sensory*, edited by Kerkut GA, Gilbert LI. Pergamon Press Ltd., 1985, p 355-429.

Kien J. Sensory integration in the locust optomotor system-I: Behavioural analysis. *Vision Res* 14: 1245-1254, 1974a.

Kien J. Sensory integration in the locust optomotor system-II: Direction selective neurons in the circumoesophageal connectives and the optic lobe. *Vision Res* 14: 1255-1268, 1974b.

Kien J, Land M. The fast phase of optokinetic nystagmus in the locust. *Physiol Entomol* 3: 53-57, 1978.

Kirschfeld K. Die notwendige Anzahl von Rezeptoren zur Bestimmung der Richtung des elektrischen Vektors linear polarisierten Lichtes. *Z Naturforsch* 27: 578-579, 1972.

Kirschfeld K. Course control and tracking: orientation through image stabilization. *EXS* 84: 67-93, 1997.

Labhart T, Meyer EP. Detectors for polarized skylight in insects: a survey of ommatidial specializations in the dorsal rim area

of the compound eye. *Microsc Res Tech* 47: 368-379, 1999.

Loesel R, Homberg U. Anatomy and physiology of neurons with processes in the accessory medulla of the cockroach *Leucophaea maderae*. *J Comp Neurol* 439: 193-207, 2001.

Mappes M, Homberg U. Behavioral analysis of polarization vision in tethered flying locusts. *J Comp Physiol A* 190: 61-68, 2004.

Mappes M, Homberg U. Surgical lesion of the anterior optic tract abolishes polarotaxis in tethered flying locusts, *Schistocerca gregaria*. *J Comp Physiol A* 193: 43-50, 2007.

Pfeiffer K, Homberg U. Coding of azimuthal directions via time-compensated combination of celestial compass cues. *Curr Biol* 17: 960-965, 2007.

Pfeiffer K, Kinoshita M, Homberg U. Polarization-sensitive and light-sensitive neurons in two parallel pathways passing through the anterior optic tubercle in the locust brain. *J Neurophysiol* 94: 3903-3915, 2005.

Preiss R, Gewecke M. Compensation of visually simulated wind drift in the swarming flight of the desert locust (*Schistocerca gregaria*). *J Exp Biol* 157: 461–481, 1991.

Rind FC. Identification of directionally selective motion-detecting neurones in the locust lobula and their synaptic connections with an identified descending neurone. *J Exp Biol* 149: 21-43, 1990a.

Rind FC. A directionally selective motion-detecting neurone in the brain of the locust: Physiological and morphological characterization. *J Exp Biol* 149: 1-19, 1990b.

Rind FC. Motion detectors in the locust visual system: From biology to robot sensors. *Micros Res Tech* 56: 256-269, 2002.

Rind FC, Simmons PJ. Seeing what is coming: building collision-sensitive neurones. *Trends Neurosci* 22: 215-220, 1999.

Schlieper C. Farbensinn der Tiere und optomotorische Reaktionen. *Z Vgl Physiol* 6: 453-472, 1927.

Schlurmann M, Hausen K. Motoneurons of the flight power muscles of the blowfly *Calliphora erythrocephala*: Structures and mutual dye coupling. *J Comp Neurol* 500: 448-464, 2007.

Schneider L, Langer H. Die Struktur des Rhabdoms im "Doppelauge" des Wasserläufers *Gerris lacustris*. *Z Zellforsch* 99: 538-559, 1969.

Schwind R. Sehen unter und über Wasser, Sehen von Wasser. Das Sehen eines Wasserinsektes. *Naturwissenschaften* 72: 343-352, 1985.

Siegler MVS, Phong MP, Pousman CA. Motor neurons supplying hindwing muscles of a grasshopper: Topography and distribution into anatomical groups. *J Comp Neurol* 310: 342-355, 1991.

Srinivasan MV. Shouldn't directional movement detection necessarily be "colour-blind"? *Vision Res* 25: 997-1000, 1985.

Srinivasan MV, Poteser M, Kral K. Motion detection in insect orientation and navigation. *Vision Res* 39: 2749-2766, 1999.

Srinivasan MV, Zhang SW. Visual navigation in flying insects. *Int Rev Neurobiol* 44: 67-92, 2000.

Srinivasan MV, Zhang S. Visual motor computations in insects. *Annu Rev Neurosci* 27: 679-696, 2004.

Stern M, Gewecke M. Spatial sensitivity profiles of motion sensitive neurons in the locust brain. In: *Sensory Systems of Arthropods*, edited by Wiese K, Gribakin FG, Popov AV, Renninger G. Basel: Birkhäuser, 1993, p. 184–195.

Träger U, Wagner R, Bausenwein B, Homberg U. A novel type of microglomerular synaptic complex in the polarization vision pathway of the locust brain. *J Comp Neurol* 506: 288-300, 2008.

Varjú D. Stationary and dynamic responses during visual edge fixation by walking insects. *Nature* 255: 330-332, 1975.

Vitzthum H, Müller M, Homberg U. Neurons of the central complex of the locust *Schistocerca gregaria* are sensitive to polarized light. *J Neurosci* 22: 1114-1125, 2002.

Wehner R. The hymenopteran skylight compass: Matched filtering and parallel coding. *J Exp Biol* 146: 62-85, 1989.

Wehner R, Labhart T. Polarisation vision. In: *Invertebrate Vision*, edited by Warrant E, Nilsson D-E. Cambridge University Press, 2006, p. 291-348.

Yamaguchi S, Wolf R, Desplan C, Heisenberg M. Motion vision is independent of color in *Drosophila*. *Proc Natl Acad Sci U S A* 105: 4910-4915, 2008.

Danksagung

Mein ganz besonderer Dank gebührt Herrn Prof. Dr. Uwe Homberg für die Bereitstellung des reizvollen Themas, der großen Freiheiten und Möglichkeiten zum selbstständigen Arbeiten, der steten Unterstützung durch zahlreiche motivierende Gespräche und unermüdliches Korrigieren von Manuskripten sowie ein ausgesprochen gutes Arbeitsklima. Ebenso danke ich Herrn Prof. Dr. Roland Brandl für die wie selbstverständliche Bereitschaft zur Zweitkorrektur dieser Arbeit. Frau Prof. Dr. Monika Hassel danke ich herzlich für ihre Bereitwilligkeit, als Drittprüfer zum erfolgreichen Abschluss meiner Promotion beizutragen. Zuletzt möchte ich mich auch bei Herrn Prof. Dr. Joachim Schachtner für die Komplettierung der Prüfungskommission und für die unzähligen Ratschläge bedanken, die - wenn nötig - immer zur Stelle waren.

Bei allen (ehemaligen) Mitglieder der AGs Homberg, Schachtner, Wegener und Stengl (HoSchaWeSte) möchte ich mich für die unvoreingenommene Integration, die ausgezeichnete Arbeitsatmosphäre sowie stete Bereitschaft zu helfen wann immer Hilfe benötigt wurde, bedanken. Ganz besonders danke ich Tini, die mir nicht nur uneingeschränkt im Labor zur Seite stand, sondern auch privat zu einer festen Freundin geworden ist. Jutta, Sabine und Torsten danke ich ebenfalls ganz herzlich für ihre Unterstützung, die den Laboralltag erleichterte. Auch Conny gilt ein besonderer Dank, sie stand mir nicht nur unterstützend im Labor zur Seite - was oft auch gegenseitig galt☺- denn wir teilten auch so manche schweißtreibende Stunde im Fitnessstudio, wo ich nicht zuletzt durch sie meinen Schatz kennenlernte. Weiterhin danke ich Karl-Heinz Herklotz für langjährige gute Aufzucht unserer Heuschrecken und allen (ehemaligen) Mitgliedern der E-Werkstatt und Fein-/Mechanik für ihre Mithilfe u. a. beim Aufbau meines Setups und für die Zusatzausrüstung meines Afrika-Einsatzes.

Ebenfalls gebührender Dank gilt Dr. Stanley Heinze, der mich äußerst geduldig mit der Elektrophysiologie vertraut machte und mir auch so manche Tücken am KLSM erklärte. Die Auswertung meiner elektrophysiologischen Daten wäre ohne die von Dr. Keram Pfeiffer verfassten Spike2-Skripte nicht so effizient gewesen. Dafür und auch für die zahllosen hilfreichen Diskussionen möchte ich auch ihm danken. Basil el Jundi danke ich für die schöne gemeinsame "elektrophysiologische" Zeit mit unzähligen wertvollen Diskussionen, Dr. Martina Mappes für die Einführung in den immunhistochemischen Laboralltag, Dr. Sandra Söhler für die Unterweisung mit der Druckinjektionsapparatur, Dr. Angela Kurylas für das Anlernen der 3D-Software AMIRA, Bianca Backasch für die Einführung in die "Verhaltenswelt", um mich für meinen Forschungsauftritt in Südafrika inklusive Flugtonne und Co. fit zu machen, für hilfreiche Tipps im Umgang mit statistischen Methoden sowie für manche schöne Stunde abseits des Labors und Dr. Wolf Hütteroth für seine unentwegte positive Stimmung und so manchen guten Hinweis. Meinen verbliebenen "Bürokollegen" Martin Kollmann, Fabian Schmeling und Christoph Busche möchte ich ebenfalls für die stets gute Atmosphäre und auch so manche "dienstliche" wie private Hilfe danken. Auch bei Dr. Sandra Utz bedanke ich mich ganz herzlich für die Überlassung ihres Aquariums, welches heute mit neubelebter Pracht mein "Heimbüro" verschönert.

Meiner mittlerweile langjährigen ehemaligen Studienkollegin und jetzt besten Freundin Anja Tippmann danke ich tausendfach für zahlreiche Gespräche, die der Ablenkung vom Laboralltag oder aber der Aufarbeitung dieser galten☺. Anja ist einfach immer für mich da, wenn ich sie brauche! Genauso danke ich meinen treuen Freunden Kristin Hofmann und den "Mutzschener Mädels", vor allem Doreen Kluge und Anke Schmidt, für "ein Leben außerhalb des Labors". Bei Lynn B. Johnson bedanke ich mich für die spontane Bereitschaft der Korrektur der englischsprachigen Einleitung.

Meinen "Schwiegereltern" in Stuttgart danke ich für ihre uneingeschränkte und herzliche Aufnahme in ihre Familie sowie die unentwegte Unterstützung.

An dieser Stelle möchte ich erneut meinen lieben Eltern und meinem Bruder Thomas für ihren grenzenlosen Beistand in allen Lebenslagen danken, ohne welchen weder mein Studium noch die Promotion möglich gewesen wäre!

Zuletzt danke ich mit unendlicher Liebe meinem Verlobten Frank, der mein Leben ungemein bereichert hat, für seine Liebe und unaufhörliche Motivation, die mir besonders in der Endphase meiner Promotion die nötige Kraft zum Durchhalten gab. Ich bin dankbar für jeden Tag, den ich bisher an seiner Seite verbringen durfte und freue mich auf eine unendliche gemeinsame Zukunft!

Curriculum Vitae

Ulrike Annelies Träger

Diplom-Biologin

geb. 15. März 1982 in Grimma

Lindenstraße 15b
35094 Lahntal
Tel.: 06423/541279
Mobil: 0174/2196904
E-Mail: u.traeger@web.de

Familienstand
ledig, keine Kinder

Promotion

12/2005 – 2010 „Ein- und Ausgang des Zentralkomplexes in Bezug auf polarisiertes Licht im Nervensystem der Wüstenheuschrecke (*Schistocerca gregaria)*" wiss. Mitarbeiterin an der Philipps-Universität Marburg in der Arbeitsgruppe von Prof. Dr. Uwe Homberg (Vertragsende 03/2010)

11/2008 Feldforschung in Südafrika (Pofadder und Johannesburg) in Kooperation mit Prof. Shirley Hanrahan

Publikationen

2008 Träger U, Wagner R, Bausenwein B, Homberg U. A novel type of microglomerular synaptic complex in the polarization vision pathway of the locust brain. *J Comp Neurol, 506*(2):288-300.

eingereicht Träger U, Homberg U. Polarization sensitive descending neurons in the locust: connecting the brain to thoracic ganglia. *J Neurosci.*

in prep. Träger U, Backasch B, el Jundi B, Rosner R, Homberg U. Behavioral and electrophysiological evidence for a role of polarized light in optomotor responses of the desert locust *Schistocerca gregaria. J Neurophysiol.*

Konferenzbeiträge

09/2009	Konferenzbeitrag, 102. Jahrestagung der DZG in Regensburg, O NB. 6 (englischer Fachvortrag) Träger U and Homberg U 2009. Descending neurons sensitive to polarized light in the locust *Schistocerca gregaria*.
05/2009	Rauischholzhausen Seminar: Entwicklung und Plastizität des Insektennervensystems mit deutschem Kurzvortrag
03/2009	Konferenzbeitrag, 8. NWG Treffen in Göttingen, T14-1A Träger U and Homberg U 2009. Do descending neurons of the locust *Schistocerca gregaria* respond to polarized light?
09/2008	Konferenzbeitrag, 101. Jahrestagung der DZG in Jena, P NB.26 Träger U and Homberg U 2008. Polarization-sensitive descending neurons in the nervous system of the locust *Schistocerca gregaria*.
10/2007	Beitrag auf der Kleinsthirnkonferenz: Insect Brain and Control of Behaviour in Tutzing Träger U, Wagner R, Bausenwein B, Homberg U 2007. A novel type of microglomerular synaptic complex in the polarization vision pathway of the locust brain.
05/2007	Rauischholzhausen Seminar: Entwicklung und Plastizität des Insektennervensystems mit deutschem Kurzvortrag
03-04/2007	Konferenzbeitrag, 7. NWG Treffen in Göttingen, T6-7C Träger U, Wagner R, Bausenwein B, Homberg U 2007. Specialized synaptic contacts in the polarization vision pathway of the locust brain.
10/2006	Teilnahme am 14-tägigen Kurs „Sensory Ecology“ in Lund/Schweden mit Kurzvortrag in Englisch
09/2006	englischer Fachvortrag auf dem Arthropodenseminar in Schwandalpe

Mitwirkung an der Lehre

2006 – 2009	Betreuung des Tierphysiologischen Praktikums Kursteil: Sinnesphysiologie am Insektenauge
10-11/2006	Betreuung des Blockpraktikums für Fortgeschrittene in der Neurobiologie

Studium

10/2000 – 08/2005 Biologiestudium (Diplom) an der Universität Leipzig

Biologische Hauptfächer:	Spezielle Zoologie
	Neurobiologie
	Verhaltensphysiologie
Nicht-biologisches Hauptfach:	Psychologie

Abschluss des Diplom – Studiengangs Biologie

Prüfung & Anfertigung der Diplomarbeit „Lokale Interneurone des *vfa*-Neuropils der Grille *Gryllus bimaculatus* de Geer“ (Note: 1,3)

Nebentätigkeit während des Studiums

09/2004 – 12/2004 studentische Hilfskraft an der Universität Leipzig (zehn Stunden/Woche); Betreuung des Tierphysiologischen Kurses

Schulbildung

09/1994 – 07/2000 Gymnasium St. Augustin zu Grimma
Abschluss mit der allgemeinen Hochschulreife (Note: 1,9)

09/1988 – 09/1994 Besuch der allgemein bildenden polytechnischen Oberschule Mutzschen (ab 1993 Mittelschule Mutzschen)

Lahntal, im September 2010

_____

(Ulrike Träger)

Erklärung

Ich versichere, dass ich meine Dissertation mit dem Titel

"Input and output of the central complex related to polarized light in the nervous system of the desert locust *Schistocerca gregaria*"

("Ein- und Ausgang des Zentralkomplexes in Bezug auf polarisiertes Licht im Nervensystem der Wüstenheuschrecke *Schistocerca gregaria*")

selbstständig, ohne unerlaubte Hilfe angefertigt und mich dabei keiner anderen als der von mir ausdrücklich bezeichneten Quellen und Hilfen bedient habe.

Die Dissertation wurde in der jetzigen oder einer ähnlichen Form noch bei keiner anderen Hochschule eingereicht und hat noch keinen sonstigen Prüfungszwecken gedient.

Lahntal, den 27.09.2010

(Ulrike Träger)